DOE/NASA/1011-78/24
NASA TM-78884

A STIRLING ENGINE COMPUTER MODEL FOR PERFORMANCE CALCULATIONS

Roy Tew, Kent Jefferies, and David Miao
National Aeronautics and Space Administration
Lewis Research Center

JULY 1978

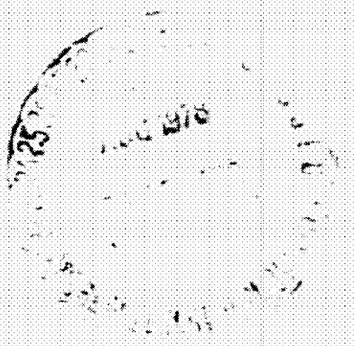

Prepared for
U.S. DEPARTMENT OF ENERGY
Office of Conservation and Solar Applications
Division of Transportation Energy Conservation

DOE/NASA/1011-78/24
NASA TM-78884

A STIRLING ENGINE COMPUTER MODEL FOR PERFORMANCE CALCULATIONS

Roy Tew, Kent Jefferies, and David Miao
National Aeronautics and Space Administration
Lewis Research Center
Cleveland, Ohio 44135

July 1978

Prepared for
U. S. Department of Energy
Office of Conservation and Solar Applications
Division of Transportation Energy Conservation
Washington, D. C. 20545
Under Interagency Agreement EC-77-A-31-1011

A STIRLING ENGINE COMPUTER MODEL FOR PERFORMANCE CALCULATIONS

by Roy Tew, Kent Jefferies, and David Miao

Lewis Research Center

SUMMARY

To support the development of the Stirling engine as a possible alternative to the automobile spark-ignition engine, the thermodynamic characteristics of the Stirling engine were analyzed and modeled on a computer. The modeling techniques used are presented. The performance of an existing rhombic-drive Stirling engine was simulated by use of this computer program, and some typical results are presented. Engine tests are planned in order to evaluate this theoretical model.

INTRODUCTION

The Department of Energy (DOE) has established programs whose purpose is to reduce fuel consumption and emissions of highway vehicles. The Stirling Engine Highway Vehicle Systems Program is one such program. Its purpose is to develop the Stirling engine as a possible alternative to the spark-ignition engine. It will be implemented through government participation with industry. NASA Lewis Research Center has project management responsibility for the program.

At NASA Lewis a Stirling-engine digital-computer model is being developed for predicting engine performance. This report documents the present modeling techniques and shows some preliminary predictions of one version of the model, which is configured to represent a particular single-cylinder rhombic-drive engine.

Analysis of the ideal Stirling cycle is straightforward (ref. 1), but this analysis is useful only as a reference against which to compare real cycles. Schmidt developed a somewhat more realistic analysis that considers the effect of dead volume and assumes sinusoidal piston motion (ref. 1). The basic power and efficiency (the Carnot efficiency) calculated by the Schmidt analysis can be multiplied by experience factors to estimate performance in the initial stages of engine sizing. (Ranges of experience factors are discussed in refs. 2 and 3.) Rios (ref. 4), Qvale (ref. 5), and Martini (ref. 2) have each developed models that first calculate a basic power and efficiency and then correct these basic values with separate, independent loss calculations. The most detailed performance models so far reported simulate real-time variations in gas temperatures, pressures, and flow rates at various control volumes within the working space. Some or all of the loss calculations are an integral part of the model and can thus interact with the basic thermodynamic calculations and with each other. Detailed models that have been reported in the open literature are those of Urieli (refs. 6 and 7), Finkelstein (ref. 8), and Finegold and Vanderbrug (ref. 3). A listing of Urieli's computer model is given in reference 8 and a listing of the Finegold-Vanderbrug model, in reference 3. Allan Shock of Fairchild Industries is also developing a detailed model (ref. 9). The more detailed models should be of value in studying the effects on performance of engine details not considered in the simpler models, in refining the loss calculations of the simpler models, and in investigating the significance of physical effects such as gas inertia and pressure dynamics on engine performance. However, these models appear to require too much computer time for use in a design optimization program: One run with such an optimization program might investigate hundreds of designs, or even several thousand. Since the less detailed models such as those of Qvale, Rios, and Martini require much less computer time, they would seem to be more appropriate for use in a design optimization program. Unfortunately, the models that have been published in the open literature have not been adequately validated.

N. V. Philips and its licensees have both a design-optimization program and detailed performance prediction models, which have been developed over the years with the aid of extensive test data. However, these programs and the test data are proprietary and are presently available only under license.

The model being developed by NASA Lewis differs from the Urieli and Finegold models essentially in that the Lewis model assumes that gas inertia and pressure-wave dynamics can be neglected in predicting Stirling engine performance. The Lewis model also uses an integration technique that avoids instability caused by excessive heat transfer between gas and metal when large time increments are used. Thus, the Lewis type model should be inherently more efficient in terms of computing time, than the more general Urieli and Finegold models.

The Lewis model differs from the Rios and Martini models essentially in that it more closely represents the distributed-parameter nature of the working space by dividing each heat exchanger into several control volumes and, also, by making the heat-exchanger inefficiencies an integral part of the cycle calculations. The Lewis model is thus more general in nature but less efficient in terms of computing time than the models of Rios and Martini.

Two versions of the computer performance model have been developed. One version is configured to model a rhombic-drive ground power unit (GPU) designed and built for the U.S. Army by General Motors. This unit was designed to produce 3 kilowatts of electric power (or about 6 kW of brake power). The other version is configured to model a free-piston engine. This document contains a description and program listing of the GPU version of the model. The GPU engine parameters are given in reference 2. The model is also briefly described in reference 2, along with some performance prediction comparisons between it and the Martini model.

The GPU-3 engine has been run through initial checkout tests at NASA Lewis; engine accessories were powered by the engine and instrumentation

was minimal (ref. 10). Testing with accessories run independently of the engine and with more instrumentation is now getting under way; these tests will provide basic engine data for evaluation and refinement of the computer model.

GENERAL DESCRIPTION OF MODEL

The GPU engine, for which this model predicts performance, is shown schematically in figure 1. There are actually eight separate flowpaths through each of eight regenerators and coolers with five heater tubes serving each regenerator. In the model, however, it is assumed that the same flow conditions exist in each of the eight flowpaths so that it is necessary to model only one path. The model represents the working space by a series of subdivisions called control volumes; this type of model is sometimes called a nodal model.

The model calculates indicated power and efficiency for given engine speed, mean pressure, and fixed heater and cooler metal temperatures. The indicated efficiency is based on heat into the gas plus conduction losses. The model also simulates temperature, pressure, and flow variations over the cycle at various stations in the working space. The working space consists of the expansion space, the heater, the regenerator, the cooler, and the compression space.

The engine working space is represented by 13 control volumes, as shown in figure 2; the adjacent metal walls are represented by 13 corresponding control volumes. The metal temperatures, except for those in the regenerator, are assumed to be constant. This is a reasonable assumption for any given run since the heater and cooler metal temperatures are essentially boundary temperatures that are controlled by the combustor and the cooling water flow, respectively; these temperatures vary little over a cycle because the metal heat capacity is much greater than that of the gas.

The calculation procedure used in the model is outlined in figure 3; the equations used in the calculations are discussed in the section EQUATIONS AND ASSUMPTIONS USED IN DEVELOPING THE MODEL. Each set of calculations shown in figure 3 within the inner loop is made at each integration time step during each engine cycle except that it is necessary to use the pressure-drop equations only during the last cycle. Also, the conduction and shuttle heat-transfer losses are calculated just once, during the last engine cycle. (Shuttle heat transfer is heat transfer by heating of the displacer at the hot end of the stroke and cooling of the displacer at the cold end (ref. 2).) Between cycles, corrections to the regenerator metal temperatures are made to speed up convergence to steady operation. Typically it takes about 10 cycles with regenerator temperature correction to adjust the regenerator metal temperatures to their steady operating values. (The model predicts that these temperatures vary with an amplitude of about 6° C or less over a cycle.) In addition, a number of cycles are required for the leakage between the working and buffer spaces to adjust the mass distribution. The smaller the leakage rate, the longer the time required for the mass distribution to reach steady state. For the range of leakage rates considered thus far, it takes longer for the mass distribution to steady out than for the regenerator metal temperatures to settle out. Current procedure is to turn the metal temperature convergence scheme on at the fifth cycle and off at the 15th cycle. The model is then allowed to run for 15 to 25 more cycles to allow the mass distribution to settle out. When a sufficient number of cycles have been completed for steady-state operation to be achieved, the run is terminated.

Current computing time is about 5 minutes for 50 cycles on a UNIVAC 1100, or 0.1 minute per cycle. This is based on 1000 iterations per cycle, or a time increment of 2×10^{-5} second when the engine frequency is 50 hertz.

The computing time can be decreased by decreasing the number of iterations per cycle; the corresponding effect on predicted indicated power and efficiency is shown in figures 4 and 5 for one series of runs. These figures show that some error is introduced by reducing from 1000 to 500 iterations per cycle and that the error becomes more significant if only 200 iterations per cycle are used.

The computer program is written in FORTRAN V and, in card format, is about 1300 cards long (including plotting subroutines). The program was designed to be an engineering tool for use in establishing the validity of the modeling techniques. It could be used rather easily by others but has not been designed or extensively documented for that purpose. A listing, not including the plotting subroutines, is presented in appendix E.

EQUATIONS AND ASSUMPTIONS USED IN DEVELOPING THE MODEL

First, the basic equations and assumptions used in making the thermodynamic calculations in the working space are stated. Then a relatively complete presentation of the equations used in the model is made that corresponds very closely to the steps shown in the outline of calculation procedure (fig. 3).

WORKING-SPACE THERMODYNAMIC CALCULATIONS

Each of the 13 gas control volumes shown in figure 2 is a special case of the generalized control volume shown in figure 6. The generalized control volume includes flow across two surfaces, heat transfer across a surface, and work interchange between the gas and a piston. Each of the three heater, five regenerator, and three cooler control volumes has flow across two surfaces and heat transfer across one surface but is of fixed volume; therefore, no work is done by the gas in these volumes. The expansion- and compression-space control volumes each have flow across one surface and heat transfer across one surface and are of variable volume; therefore, the gas in these two volumes is responsible for the work output of the engine.

The three basic equations used to model the thermodynamics of the gas in each control volume are conservation of energy, conservation of mass, and equation of state. These equations are used to determine the temperature and mass distributions and the pressure level within the working space at a particular time. A fourth basic equation, the momentum equation, in steady-state form, is used to calculate pressure drop across each control volume in order to evaluate its effect on indicated power and efficiency. However, this pressure-drop calculation is decoupled from the thermodynamic calculations; it has no effect on the temperature and mass distributions. This assumption simplifies the model and should be reasonable when the pressure drop is sufficiently small in relation to the pressure level.

The energy, mass, and state equations, as written for the generalized control volume shown in figure 6, are as follows, where three formulations of the equation of state are shown:

Conservation of energy (for negligible change in kinetic energy across the control volume):

$$\frac{d}{dt}(MC_vT) = hA(T_w - T) + C_p(w_iT_i - w_oT_o) - P\frac{dV}{dt} \qquad (1)$$

Rate of change of internal energy of control volume	Rate of heat transfer across boundary of control volume	Rate of enthalpy flow across boundary of control volume	Rate of work done by gas in control volume

Conservation of mass:

$$\frac{dM}{dt} = w_i - w_o \qquad (2)$$

Equation of state:

$$\left.\begin{aligned} PV &= MRT \qquad \text{for ideal gas} \\ PV &= MR\left[T + \left(0.02358\ \frac{^{\circ}R}{psi}\right)P\right] \qquad \text{for hydrogen - real gas} \\ PV &= MR\left[T + \left(0.01613\ \frac{^{\circ}R}{psi}\right)P\right] \qquad \text{for helium - real gas} \end{aligned}\right\} \tag{8}$$

where

A	heat-transfer area of control volume
C_p, C_v	heat capacities at constant pressure and volume
h	heat-transfer coefficient
M	mass of gas in volume
P	pressure
R	gas constant
T	bulk or average temperature of gas in volume
T_i, T_o	temperatures of gas flowing across surfaces i and o, respectively (in fig. 6)
T_w	temperature of metal wall adjacent to heat-transfer area A
t	time
V	volume
w_i, w_o	flow rate across surfaces i and o, respectively

(The real-gas equations of state were developed from data in ref. 11.)

Several assumptions are inherent in the use of these equations:

(1) Flow is one dimensional.

(2) Heat conduction through the gas and the regenerator matrix along the flow axis is neglected. The thermal conductivity of the regenerator

matrix is assumed to be infinite in calculating the overall gas-to-matrix heat-transfer coefficient.

(3) Kinetic energy can be neglected in the energy equation.

(4) The pressure-drop calculation (based on the conservation-of-momentum equation) can be decoupled from the other three basic equations. This implies use of a uniform pressure level throughout the working space at a given time in applying these equations.

(5) The time derivative term in the momentum equation is neglected (see appendix D).

(The last three assumptions are not made in the generalized models of Urieli (refs. 6 and 7) and Shock (ref. 9).) Thus these two models provide a means of checking the validity of these assumptions.)

In appendix A it is shown that equations (1) and (2) and the ideal-gas equation of state can be used to derive the following differential equation:

$$MC_p \frac{dT}{dt} = hA(T_w - T) + C_p w_i (T_i - T) - C_p w_o (T_o - T) + V \frac{dP}{dt} \tag{4}$$

The same result is obtained if either of the real-gas equations of state are used in the derivation. This equation says that the bulk or average gas temperature of a control volume is a function of the following three processes:

(1) Heat transfer across the boundary from the wall

(2) Gas flow across the boundary

(3) Pressure level

One approach to numerically integrating equation (4) is to solve for the temperature derivative

$$\frac{dT}{dt} = \frac{hA}{MC_p}(T_w - T) + \frac{w_i}{M}(T_i - T) - \frac{w_o}{M}(T_o - T) + \frac{V}{MC_p}\frac{dP}{dt} \tag{5}$$

and then set

$$T^{t+\Delta t} = T^{t} + \frac{dT}{dt}\,\Delta t$$

where

$T^{t+\Delta t}$ new gas temperature (at time $t + \Delta t$)

T^{t} old gas temperature (at time t)

Δt time increment

This is a first-order numerical integration. A similar but higher order technique (Runge-Kutta fourth order, for example) could also be used on equation (5). This type of approach was not used.

The approach used (which helps to avoid numerical instability problems) was to decouple the three processes that contribute to the temperature change and solve for the temperature change due to each process separately. This second approach allows a trade-off between computing time and accuracy of solution (as indicated in figs. 4 and 5) with much less concern for numerical instabilities. The approach is suggested by representation of equation (5) in the following form:

$$\left.\frac{dT}{dt}\right|_{\text{total}} = \left.\frac{dT}{dt}\right|_{\substack{\text{due to}\\ \text{heat transfer}}} + \left.\frac{dT}{dt}\right|_{\substack{\text{due to}\\ \text{mixing}}} + \left.\frac{dT}{dt}\right|_{\substack{\text{due to change}\\ \text{in pressure}}}$$

where

$$\left.\frac{dT}{dt}\right|_{\substack{\text{due to change}\\ \text{in pressure}}} = \frac{V}{MC_p}\frac{dP}{dt} \tag{5a}$$

$$\left.\frac{dT}{dt}\right|_{\substack{\text{due to}\\ \text{mixing}}} = \frac{w_i(T_i - T) - w_o(T_o - T)}{M} \tag{5b}$$

$$\left.\frac{dT}{dt}\right|_{\substack{\text{due to}\\ \text{heat transfer}}} = \frac{hA}{MC_p}(T_w - T) \tag{5c}$$

In appendix B it is shown that equations (5a) and (5c) can be integrated in closed form and that equation (5b) can be numerically integrated. When the results of appendix B are modified slightly to show just how they are used in the model, the resulting expressions are

$$T_P^{t+\Delta t} = T^t \left(\frac{P^{t+\Delta t}}{P^t}\right)^{(\gamma-1)/\gamma} \tag{5a'}$$

$$T_{PM}^{t+\Delta t} = \frac{M^t T_P^{t+\Delta t} + \left(w_i^{t+\Delta t} T_i^{t+\Delta t} - w_o^{t+\Delta t} T_o^{t+\Delta t}\right)\Delta t}{M^{t+\Delta t}} \tag{5b'}$$

$$T^{t+\Delta t} = T_{PM}^{t+\Delta t} + \left(T_w^t - T_{PM}^{t+\Delta t}\right)\left(1 - e^{-\left(h^{t+\Delta t} A / M^{t+\Delta t} C_p\right)\Delta t}\right) \tag{5c'}$$

where the superscripts t and t+Δt denote values of the variables at times t and t + Δt. The subscript P denotes the value of the temperature after it has been updated for the effect of change in pressure. The subscript PM denotes the value of the temperature after it has been updated for the effects of change in pressure and mixing. No subscript (as

on the left side of equation (5c') denotes the value of the temperature after it has been updated for all three effects - change in pressure, mixing, and heat transfer to or from the metal.

PRESENTATION OF EQUATIONS IN ORDER OF CALCULATION PROCEDURE

The equations considered so far have been derived and discussed with reference to the generalized control volume of figure 6. In the computer model these equations are applied to each of the 13 control volumes shown in figure 2. Thus temperatures, masses, heat-transfer coefficients, flow rates, etc., are all subscripted with an index. The index varies from 1 to 13 for variables that are averages of the control volumes and from 1 to 12 for values at the interfaces between control volumes. The numbering procedure used for control volume and interface indexes is defined in figure 2. The equations discussed in this section include these indexes. The presentation of the equations follows the steps shown in the outline of calculation procedure in figure 3.

Pressure (step 2 in fig. 3). - The pressure P is calculated by

$$p^{t+\Delta t} = R \frac{\sum_{l=1}^{13} M_l^t r_l^t}{\sum_{l=1}^{13} V_l^t} \tag{6}$$

where

P pressure

R gas constant

M_I mass in I^{th} volume

T_I average temperature in I^{th} volume

V_I I^{th} volume

I an index denoting which control volume is under consideration

Equation (6) is obtained by summing the ideal-gas equation

$$PV_I = M_I R T_I \qquad I = 1, 13$$

over each of the 13 control volumes (remembering that pressure is assumed to be the same in all control volumes) and then solving for P. If the real-gas equation of state for hydrogen is used then and the same procedure is followed, the result is

$$p^{t+\Delta t} = R \frac{\sum_{I=1}^{13} M_I^t T_I^t}{\sum_{I=1}^{13} V_I^t - 0.02358\, R \sum_{I=1}^{13} M_I^t} \tag{7}$$

Equations (6) and (7) are both included in the program. Also an equivalent real-gas equation for helium is included. An index in the input data specifies whether a real or ideal equation is to be used.

Update temperatures for effect of change in pressure (step 3 in fig. 3). - It was not necessary to use the subscripts P and PM of equations (5a'), (5b'), and (5c') in the computer model. Applying the three equations in sequence without the subscripts produced the same effect as if the subscripts had been used. Therefore, if the subscript P is dropped from equation (5a') and the control volume index I is introduced, the result is

$$T_I^{t+\Delta t} = T_I^t \left(\frac{P^{t+\Delta t}}{P^t} \right)^{(\gamma-1)/\gamma} \tag{8}$$

This equation is commonly used to relate temperature and pressure for an adiabatic fixed-mass process.

Mass distribution (step 4 in fig. 3). - The equations for mass distribution are derived by assuming that the mass redistributes itself in accordance with the new volumes and temperatures in such a way that pressure is uniform throughout the working space. This assumption, of course, introduces inaccuracies in the solution, but the inaccuracies are relatively small because the pressure drop in Stirling engines is usually a small portion of the total pressure of the fluid. The pressure P throughout the working space is derived from the perfect-gas law as follows: The perfect-gas law for the I^{th} control volume can be written

$$M_I = \frac{PV_I}{RT_I}$$

Summing over the 13 control volumes

$$\sum M_I = M_{total} = \frac{P}{R} \sum_{I=1}^{13} \frac{V_I}{T_I}$$

and solving for P/R gives

$$\frac{P}{R} = \frac{M_{total}}{\sum_{I=1}^{13} \frac{V_I}{T_I}}$$

Now substituting for P/R into the perfect-gas equation for the I^{th} control volume gives

$$M_I = \frac{M_{total}\,\dfrac{V_I}{T_I}}{\sum_{I=1}^{13}\dfrac{V_I}{T_I}}$$

The form of this equation used in the model is

$$M_I^{t+\Delta t} = M_{total}\,\frac{\dfrac{V_I^t}{T_{I,P}^{t+\Delta t}}}{\sum_{I=1}^{13}\left[\dfrac{V_I^t}{T_{I,P}^{t+\Delta t}}\right]} \qquad I = 1, 13 \qquad (9)$$

(where $T_{I,P}^{t+\Delta t}$ represents T_I updated for pressure but not for mixing and heat transfer).

The preceding equation calculates the new mass distribution for the case of a perfect gas. The following equation, which can be derived in the same manner, is used to approximate the real properties of hydrogen:

$$M_I^{t+\Delta t} = M_{total}\,\frac{\dfrac{V_I^t}{\left(T_{I,P}^{t+\Delta t} + 0.02358\ p^{t+\Delta t}\right)}}{\sum_{I=1}^{13}\left[\dfrac{V_I^t}{\left(T_{I,P}^{t+\Delta t} + 0.02358\ p^{t+\Delta t}\right)}\right]} \qquad I = 1, 13 \qquad (10)$$

A similar equation that approximates the real properties of helium is included in the model.

Flow rates (step 5 in fig. 3). - Once the new mass distribution is known, the new flow rates are calculated from the old and new mass distributions according to

$$\left.\begin{aligned} w_1 &= \frac{M_1^t - M_1^{t+\Delta t}}{\Delta t} \\ \text{and} \\ w_I &= \frac{M_I^t - M_I^{t+\Delta t}}{\Delta t} + w_{I-1} \qquad \text{for } I = 2, 12 \end{aligned}\right\} \tag{11}$$

where w_I is the flow rate at the I^{th} interface between control volumes.

Update temperatures in each control volume for effect of gas flow between control volumes (step 6 in fig. 3). - The following equations (modifications of equation (5b') in the section WORKING-SPACE THERMODYNAMIC CALCULATIONS) were used to update temperature for the mixing effect following gas flow between control volumes:

$$\left.\begin{aligned} T_{1,PM}^{t+\Delta t} &= \frac{M_1^t T_{1,P}^{t+\Delta t} + \left(-w_1^{t+\Delta t}\theta_1^{t+\Delta t}\right)\Delta t}{M_1^{t+\Delta t}} \\ T_{I,PM}^{t+\Delta t} &= \frac{M_I^t T_{I,P}^{t+\Delta t} + \left(w_{I-1}^{t+\Delta t}\theta_{I-1}^{t+\Delta t} - w_I^{t+\Delta t}\theta_I^{t+\Delta t}\right)\Delta t}{M_I^{t+\Delta t}} \quad \text{for } I = 2, 12 \\ T_{13,PM}^{t+\Delta t} &= \frac{M_{13}^t T_{13,P}^{t+\Delta t} + \left(w_{12}^{t+\Delta t}\theta_{12}^{t+\Delta t}\right)\Delta t}{M_{13}^{t+\Delta t}} \end{aligned}\right\} \tag{12}$$

(where the subscript PM indicates the temperature has been updated for pressure change and mixing).

The equations for the first and thirteenth control volumes (expansion and compression spaces, respectively) are simpler in form than those for the other control volumes because there is flow across only one surface in each of these volumes. (The leakage flow between compression and buffer spaces is handled independently; it does not appear in eq. (12).) The temperature of the fluid flowing across the interface has been given a new variable name θ to better distinguish it from the average control volume temperature T and to keep the subscripts as simple as possible. The procedure used to update the temperature θ for each interface is now defined.

The temperature of the fluid flowing across a control volume boundary is just the bulk temperature of the control volume from which the fluid came - for flow from the expansion-space, heater, cooler, or compression-space control volumes. This is a reasonable assumption for these volumes since the actual temperature gradient across each is expected to be relatively small. In the five-control-volume regenerator, however, the temperature gradient is not small. One option would be to increase the number of control volumes in the regenerator. However, to save computing time, an alternative approach was used. It was assumed that a temperature gradient existed across each volume in the regenerator. The magnitude of the gradient was assumed to be equal to the corresponding regenerator metal gradient.

A schematic of a regenerator control volume is shown in figure 7(a). Flow across both interfaces is, for now, assumed to be in the direction shown (which is defined to be the positive flow direction). The cross-hatched area represents the portion of the fluid that will flow across interface I during the time increment Δt. The assumed temperature profile of the control volume is characterized in figure 7(b). The vertical dashed line in figure 7(b) defines the temperature at the left boundary of the fluid that will flow across interface I during Δt. If T_I is defined as the average temperature of control volume I and ΔT_I equals

one-half the change in temperature across the control volume, then $T_I - \Delta T_I$ is the temperature of the fluid at interface I and

$$T_I - \Delta T_I + \frac{w_I \Delta t}{M_I} 2 \Delta T_I$$

is the temperature of fluid at the vertical dashed line. (Figure 3 shows the numbering schemes used for the control volumes and the interfaces between control volumes.)

Now the temperature of the fluid that flows across an interface during Δt is assumed to be equal to the average temperature of that fluid before it crosses the interface. The average temperature of the fluid in the crosshatched area of figure 7(a) is then

$$\frac{1}{2}\left[\left(T_I - \Delta T_I + \frac{w_I \Delta t}{M_I} 2 \Delta T_I\right) + \left(T_I - \Delta T_I\right)\right] = T_I - \Delta T_I + \frac{w_I \Delta t}{M_I} \Delta T_I$$

Therefore, for the flow directions shown in figure 7(a), the updated temperatures of the fluid that crosses the interfaces during Δt are

$$\left.\begin{aligned} \theta_I^{t+\Delta t} &= T_{I,P}^{t+\Delta t} - \Delta T_I + \frac{w_I^{t+\Delta t} \Delta t}{M_I^t} \Delta T_I \qquad w_I^{t+\Delta t} > 0 \\ \theta_{I-1}^{t+\Delta t} &= T_{I-1,P}^{t+\Delta t} - \Delta T_{I-1} + \frac{w_{I-1}^{t+\Delta t} \Delta t}{M_{I-1}^t} \Delta T_{I-1} \qquad w_{I-1}^{t+\Delta t} < 0 \end{aligned}\right\} \tag{13}$$

If the flow direction is reversed at both interfaces, then

$$\left.\begin{aligned}\theta_I^{t+\Delta t} &= T_{I+1}^{t+\Delta t} + \Delta T_{I+1} + \frac{w_I^{t+\Delta t}\,\Delta t}{M_{I+1}^t}\,\Delta T_{I+1} \qquad w_I^{t+\Delta t} < 0 \\ \theta_{I-1}^{t+\Delta t} &= T_I^{t+\Delta t} + \Delta T_I + \frac{w_{I-1}^{t+\Delta t}\,\Delta t}{M_I^t}\,\Delta T_I \qquad w_{I-1}^{t+\Delta t} < 0\end{aligned}\right\} \tag{14}$$

Heat-transfer coefficients (step 7 in fig. 3). - The assumptions and equations used in calculating heat-transfer coefficients are discussed in appendix C. The heater and cooler equations are based on well-established, steady-flow correlations for tubes. The regenerator equation is based on an extrapolation of a steady-flow correlation. There is a need for additional steady-flow heat-transfer data for Stirling engine heat-exchanger components, especially regenerators. In addition, data are needed to determine how to modify steady-flow correlations for the periodic-flow conditions that exist in Stirling engines.

Update temperature in each gas control volume for effect of heat transfer between gas and metal (and determine heat transfer between gas and metal) (step 8 in fig. 3). - This temperature update is accomplished by using the following equation (a modification of eq. (5c')):

$$T_I^{t+\Delta t} = T_{I,PM}^{t+\Delta t}\left(T_{w,I}^t - T_{I,PM}^{t+\Delta t}\right)\left[1 - e^{\left(-h_I^{t+\Delta t}A_I/M_I^{t+\Delta t}C_p\right)\Delta t}\right] \qquad I = 1, 13$$

where $T_{w,I}$ is the wall temperature of I^{th} control volume. Note that, no matter how large the heat-transfer coefficient, the gas temperature cannot change more than the ΔT between the wall and the gas. Thus this calculation cannot cause the solution to become unstable, but it can lead to significant inaccuracies if the time increment Δt is made too large.

The heat transferred between gas and metal is then calculated from

$$Q_I^{t+\Delta t} = -\left(T_I^{t+\Delta t} - T_{I,PM}^{t+\Delta t}\right) M_I^{t+\Delta t} C_p \qquad I = 1, 13 \tag{15}$$

so that heat transfer from gas to metal is defined to be positive.

Regenerator metal temperature (step 9 in fig. 3). - The equation used to update the metal temperatures in the five regenerator control volumes is

$$M_I C \frac{dT_{w,I}}{dt} = Q_I \qquad I = 5, 9 \tag{16}$$

where Q_I is the rate of heat transfer between gas and metal. This is integrated numerically by setting

$$T_{w,I}^{t+\Delta t} = T_{w,I}^{t} + \frac{Q_I^{t+\Delta t}}{M_I C} \Delta t \tag{17}$$

where

M_I mass of metal in I^{th} volume

C thermal capacitance of metal

Δt time increment

For most regenerators the thermal capacitance of the metal is so much larger than the thermal capacitance of the adjacent gas volume that an excessive number of engines cycles (from the point of view of computing time) are required for the metal temperatures to reach steady state. Therefore, it is necessary to apply a correction to the metal temperatures after each cycle to speed up convergence. The method used is discussed in the section Convergence scheme for regenerator metal temperatures (step 19 in fig. 3).

Pressure-drop calculations (step 10 in fig. 3). - Since the pressure-drop calculations have been decoupled from the heat- and mass-transfer calculations, pressure drop needs to be calculated only over the last cycle. The indicated work calculation can then be corrected for pressure-drop loss.

A general form of the conservation of momentum equation for one-dimensional flow is

$$\frac{\partial}{\partial t}(\rho v) = -\frac{\partial}{\partial x}(\rho v^2) - \frac{f}{D_h}\frac{1}{2}\rho v^2 - \frac{\partial P}{\partial x} \qquad (18)$$

Rate of accumulation of momentum per unit volume	Rate of momentum gain by convection per unit volume	Rate of momentum gain by viscous transport (frictional forces) per unit volume	Rate of momentum gain due to pressure force per unit volume

where

ρ density

v velocity of flow

f friction factor

D_h hydraulic diameter

P pressure

t time

x distance

In appendix D it is shown that by combining the continuity and momentum equations and then neglecting the time derivative term in the resulting equation, the following equation results:

$$v\,dv + \frac{fv^2}{2D_h}\,dx + \frac{dP}{\rho} = 0 \qquad (19)$$

This equation can be integrated over a length L for the special cases of adiabatic or isothermal flow processes (the two extremes). When the resulting adiabatic and isothermal expressions are applied to the GPU regenerator, the contribution of the v dv term is negligible for the two extremes. Since the effect of the term is more significant in the regenerator than in the heater and cooler, the expression for pressure drop can be reduced to

$$\frac{f}{2}\frac{v^2}{D_h}\,dx + \frac{dP}{\rho} = 0 \tag{20}$$

or applying the differential equation (20) over a finite length L

$$\Delta P = \frac{f}{D_h}\,\frac{1}{2}\rho v^2 L \tag{21}$$

where ΔP is the pressure drop over length L.

A modification of this equation can also be used to ccount for the effect of expansions and contractions in flow area. The form of the modified equation is

$$\Delta P = K\,\frac{1}{2}\rho v^2 \tag{22}$$

It is applied at each area change in the flowpath between the expansion and compression spaces. At a particular point where an area change occurs, K is a function of the two areas and the direction of flow (since an expansion for one flow direction is a contraction when the flow reverses). The term K is calculated in accordance with the procedure given in references 12 and 13.

For the heater and cooler control volumes the friction factor f is determined from

$$\left.\begin{aligned} f_I &= \frac{16}{N_{Re_I}} \qquad N_{Re_I} < 1500 \\ f_I &= \frac{0.046}{N_{Re_I}^{0.2}} \qquad N_{Re_I} \geq 1500 \end{aligned}\right\} \tag{23}$$

where N_{Re_I} is the Reynolds number (based on plots of smooth-tube friction factors in ref. 14).

For the regenerator control volumes

$$f_I = 0.96\, e^{-0.0190 N_{Re_I}} + 0.54 \qquad I = 5,9 \tag{24}$$

which is a fit of the curve shown in figure 8. This curve was derived from the experimental steady-flow air data taken on the regenerator cooler unit of the GPU-3 engine and was extrapolated to the low Reynolds number range (below 50). Since the sample runs for this report were made, this curve has been compared with other wire-screen data from Kays and London (ref. 13). This comparison suggests that the curve should be somewhat higher in the below-50 Reynolds number range. (This range is important in the regenerator.)

There is a need for additional pressure drop data for Stirling engine heat-exchanger components, especially for regenerators. Also additional data are needed to determine how to modify the steady-flow pressure drop correlations for periodic-flow conditions. With the pressure level P known (which is now assumed to be the pressure at the center of the regenerator) and the ΔP's across each of the control volumes in the heater, regenerator, and cooler known, the pressures needed in the work calculations, P_e and P_c, can be calculated as follows:

$$P_e = \sum_{I=2}^{6} \Delta P_I + \frac{\Delta P_7}{2} + P$$

$$P_c = P - \frac{\Delta P_7}{2} - \sum_{I=8}^{12} \Delta P_I$$

Heat conduction from hot end to cold end of engine and shuttle loss (step 11 in fig. 3). - Three separate paths were considered in the calculation of heat-conduction losses from the hot end to the cold end of the engine:

(1) Through each of the eight regenerators

(2) Through the cylinder walls

(3) Through the walls of the displacer from the hot space to the cold space

The effect of temperature on conductivity was considered. A calculation of the conduction loss through the gas inside the displacer suggested that the loss along this path was small enough to be neglected. The dimensions used in calculating these conduction losses and the locations where the temperature measurements will be made are shown in figure 9.

The displacer picks up heat from the cylinder at the hot end of its stroke and loses heat to the cylinder at the cold end of its stroke. This shuttle loss is calculated by using the following equation from reference 2:

$$Q_{shuttle} = \frac{K\pi DS^2 \Delta T}{8CL} \tag{26}$$

where

K thermal conductivity of gas

D displacer diameter

S stroke

ΔT temperature difference across displacer length

C clearance between displacer and cylinder

L displacer length

Conduction and shuttle calculations are made just once after steady operation has been achieved.

Sum up heat transfers between gas and metal for each component (step 12 in fig. 3). - The basic heat into the working space per cycle is the sum of the net heat transfer from metal to gas in the heater and expansion-space control volumes over the cycle. The basic heat out of the working space per cycle is the sum of the net heat transfer from the gas to the metal in cooler and compression-space control volumes per cycle. Since it is assumed that there are no losses from the regenerator matrix, the net heat transferred between gas and metal in the regenerator over a cycle should be zero. This net heat transfer in the regenerator over the cycle appears to be the most convenient single criterion for judging when convergence of regenerator metal temperatures has been achieved. However, for small leakage rates, using this criterion to judge convergence to steady operation can lead to significant errors. That is, even though the regenerator metal temperatures have converged so that the net heat transfer in the regenerator per cycle is small, small changes in the mass distribution between working and buffer spaces from one cycle to the next can cause a significant change in performance over many cycles.

Leakage flow between working and buffer spaces (step 13 in fig. 3). - A leakage flow between working and buffer spaces can be calculated according to

$$w = C\sqrt{|P_c - P_{buff}|} \tag{27}$$

where

C constant (0.0001 was assumed for sample run)

P_c, P_{buff} compression- and buffer-space pressures

where flow is from compression space to buffer space if $P_c > P_{buff}$, and the reverse if $P_{buff} > P_c$. This equation was used to investigate the sensitivity of performance to leakage. This procedure for calculating loss due to leakage will have to be updated when more information about leakage flow becomes available. Relatively small leakage flows will increase the number of cycles required for the mass distribution between the working and buffer spaces to reach steady operating values.

Compression-, expansion-, and buffer-space volumes (step 14 in fig. 3). - The crankshaft angle is defined in the schematic shown in figure 10. Compression-, expansion-, and buffer-space volumes are calculated from the crankshaft angle by the following set of equations (as derived from fig. 10):

$$\left.\begin{aligned}
&L_y = \sqrt{L^2 - (e - r\cos x)^2} \equiv \text{Projection of rod length L on vertical axis.}\\
&Y_1 = r\sin x + L_y \equiv \text{Position of displacer yoke}\\
&Y_2 = r\sin x - L_y \equiv \text{Position of power-piston yoke}\\
&Y_{1,min} = \sqrt{(L - r)^2 - e^2}\\
&L_{y,max} = \sqrt{L^2 - (e - r)^2}\\
&V_e = A_d(Y_1 - Y_{1,min}) + V_{e,clearance} \equiv \text{Expansion-space volume}\\
&V_e = 2(A_d - A_{rod})(L_{y,max} - L_y) + V_{c,clearance} \equiv \text{Compression-space volume}\\
&V_{buff} = A_{pr}(-Y_2 - Y_{1,min}) + V_{buff,clearance} \equiv \text{Buffer-space volume}
\end{aligned}\right\} \tag{28}$$

where

e eccentricity

r crank radius

x crank angle

A_d displacer cross-sectional area

A_{pr} piston cross-sectional area minus piston rod cross-sectional area

A_{rod} displacer rod cross-sectional area

and V_e and V_c are the two volumes needed to calculate the indicated power.

Work, power, and efficiency calculations (step 16 in fig. 3). - The indicated work is calculated according to

$$W = \oint P(dV_e + dV_c) \tag{29}$$

over all but the last cycle. Since heat-exchanger ineffectivenesses, dead volumes, and leakage from working space to buffer space are all an integral part of the calculations, the work calculated in equation (29) includes the effect of these losses. Over the last cycle, after steady operation has been achieved, pressure-drop losses are calculated. To include this loss, the indicated work calculation was revised to

$$W = \oint \left[P_e\, dV_e + P_c\, dV_c\right] \tag{30}$$

The indicated power is just the indicated work per cycle times the engine frequency.

The conduction and shuttle transfer losses are calculated only once after steady operation has been achieved. These losses increase the heat input and heat output by the same amount. Since it is assumed that they do not interact with the working space, they affect the efficiency but not the power calculations.

The net heat into the engine per cycle is defined to be the basic heat input (from step 12) plus conduction and shuttle losses minus one-half the total windage (pressure drop) loss. (It would probably be more accurate to use the heater windage loss plus one-half the regenerator windage loss for windage credit in calculating the net heat input (as in ref. 2). However, if the regenerator loss is considerably larger than the heater and cooler losses, it is a reasonable assumption to use one-half the total loss for windage credit.)

Indicated efficiency is defined to be the indicated work per cycle divided by the net heat into the engine per cycle (as defined in the previous paragraph).

Convergence scheme for regenerator metal temperatures (step 19 in fig. 3). - The scheme used to correct regenerator metal temperatures between cycles was arrived at through trial and error. The correction is made as follows:

$$\Delta T_I = \frac{\sum_{\text{Time}=0}^{\text{Time}=N\,\Delta t} (T_{w,I} - T_I)\left[1 - e^{\left(-h_I A_I / M_I C_p\right)\Delta t}\right] M_I}{\sum_{\text{Time}=0}^{\text{Time}=N\,\Delta t} \left[1 - e^{\left(-h_I A_I / M_I C_p\right)\Delta t}\right] M_I} \qquad I = 5,9 \qquad (31)$$

where

N	number of iterations per cycle
ΔT_I	weighted average change in gas temperature over cycle for I^{th} regenerator control volume
T_I	I^{th} average gas temperature
$T_{w,I}$	I^{th} wall temperature

Then let

$$\Delta T_I = \Delta T_{I,old} \times F_1 + \Delta T_I \times F_2 \qquad I = 5,9 \tag{32}$$

where $F_1 = 0.4$ and $F_2 = 10.0$ are the factors that seem to work best. The final step in the correction is

$$\left.\begin{aligned}
T_{w,5,new} &= T_{w,5,old} - \left(\frac{5\,\Delta T_5 + 4\,\Delta T_6 + 3\,\Delta T_7 + 2\,\Delta T_8 + \Delta T_9}{3}\right) \\
T_{w,6,new} &= T_{w,6,old} - \left(\frac{4\,\Delta T_5 + 8\,\Delta T_6 + 6\,\Delta T_7 + 4\,\Delta T_8 + 2\,\Delta T_9}{3}\right) \\
T_{w,7,new} &= T_{w,7,old} - \left(\frac{\Delta T_5 + 2\,\Delta T_6 + 3\,\Delta T_7 + 2\,\Delta T_8 + \Delta T_9}{1}\right) \\
T_{w,8,new} &= T_{w,8,old} - \left(\frac{2\,\Delta T_5 + 4\,\Delta T_6 + 6\,\Delta T_7 + 8\,\Delta T_8 + 4\,\Delta T_9}{3}\right) \\
T_{w,9,new} &= T_{w,9,old} - \left(\frac{\Delta T_5 + 2\,\Delta T_6 + 3\,\Delta T_7 + 4\,\Delta T_8 + 5\,\Delta T_9}{3}\right)
\end{aligned}\right\} \tag{33}$$

In an attempt to improve upon the rate of convergence, the scheme used by Urieli (ref. 7) was tried. This is a correction of the form

$$T_{w,I,new} = T_{w,I,old} - F_I \times Q_I \qquad I = 5,9 \tag{34}$$

where Q_I is the net heat transferred from the I^{th} metal node to the I^{th} gas node over the previous cycle. An attempt was made, by trial and error, to pick the optimum combination of factors F_I (I - 5,9) to speed

up convergence. This procedure worked in the Lewis model but not as well as the previously described approach.

RESULTS GENERATED WITH MODEL

Some sample performance predictions and plots of engine variables over a cycle are shown for the GPU simulation run characterized in table I. The assumed metal boundary temperatures are shown in figure 11. Performance predictions for this run are shown in table II.

The ratio of "dead volume" to the change in total working-space volume over the cycle is a very important factor in Stirling engine performance. Dead volume is the volume of the heat-exchanger components plus clearances in the expansion and compression spaces. It decreases the ratio of maximum to minimum pressure that can be achieved over the cycle. Better definitions of GPU engine dead volume by refined calculations and gas displacement measurements, since these sample runs were made, indicate a larger dead volume than used in the model for the sample runs. Using the larger dead volume would result in lower predicted power than shown here.

Expansion- and compression-space volumes are shown in figure 12 as a function of time. Zero time corresponds to minimum compression-space volume. The cycle is complete at 0.02 second. One and one-half cycles are shown on this and the following plots. These volumes, together with the plot of total volume in figure 13, are keys to the behavior of the engine variables shown in later figures.

Expansion- and compression-space pressures are plotted in figure 14. These plots correlate closely with the plot of total volume in figure 13: Minimum pressure corresponds closely to maximum total volume. The pressure drop between expansion and compression spaces is a small percentage of the pressure level (<3 percent).

A plot of this pressure drop as a function of time in figure 15 shows that the maximum positive ΔP (where $\Delta P = P_e - P_c$) occurs a little

before 0.008 second. The corresponding flow rates into and out of the heat exchangers are shown in figures 16 to 18. (Additional flow rates calculated at the control-volume interfaces within the heat exchangers are not shown here). The maximum positive flow rates just before 0.008 second correspond to the region of the volume plots in figure 12, where the compression-space volume is increasing at its maximum rate and the expansion-space volume is decreasing at its maximum rate (to give the maximum rate of volume displacement from the hot to the cold space). Similarly, the maximum negative flow rates and pressure drop occur just before 0.016 second, where the maximum rate of volume displacement from the cold to the hot space occurs. Pressure drop is greater for positive than for negative flow primarily because of the lower average pressures and, therefore, higher velocities when flow is from the hot toward the cold space. Pressure is lower because positive flow occurs when working-space volume is at and near its maximum.

The differences in inlet and outlet flows for each of the heat-exchanger components divide each cycle into two regions - a region where net mass is removed from the component, and a region where net mass is stored in the component. These regions are labeled in the plots of flow rates for the heater in figure 16. Similar flow-rate plots for the regenerator and cooler are shown in figures 17 and 18.

Pressure-volume diagrams for the expansion and compression spaces are shown in figures 19 and 20. Since the expansion-space work is positive and the compression-space work is negative, the net indicated work per cycle is the difference of the areas within these two diagrams (219 joules (162 ft-lbf) in this case). The area within the pressure-volume diagram of figure 21 represents net indicated work uncorrected for pressure-drop loss (231 joules, or 170 ft-lbf).

Expansion- and compression-space temperatures are shown in figures 22 and 23. The temperature variations correlate well with the pressure variations of figure 14. In both the expansion and compression spaces the temperature variations are about 23 percent of the peak temperature in the space.

Plots of indicated power and efficiency are shown in figures 24 and 25 as a function of engine speed for three average working-space pressures. Other run conditions are as specified in table I, except that for the runs at the two lower pressure levels the cooler temperature was 5.6 K (10° R) lower than specified in table I.

A number of runs were made to compare predicted performance for hydrogen and helium. Indicated power for both fluids is shown as a function of frequency in figure 26. The power was larger for hydrogen except for frequencies below about 17 hertz. (For a series of runs made with no leakage, power was greater for hydrogen for all frequencies above 5 Hz.)

Indicated efficiency for both fluids is shown as a function of frequency in figure 27. The efficiency for hydrogen was greater than that for helium above about 13.5 hertz, at which point the curves cross over. (For the series of runs made with no leakage, there was no crossover; however, the curves did get closer together as the frequency was decreased to 5 hertz. At 5 hertz, the efficiencies were 35.7 percent for hydrogen and 34.8 percent for helium.)

The data from figures 26 and 27 are replotted in figure 28 in a form used by several other authors. The hydrogen and helium curves cross over so that below about 12 hertz the model predicts higher efficiencies for helium than for hydrogen at a given pressure level. When the runs were repeated with no leakage calculation, the curves did not cross over but became quite close at 5 hertz, the lowest frequency considered. Similar curves predicted by Urieli's model indicated a crossover of the helium and hydrogen curves in the 30- to 40-hertz range (ref. 7) for no leakage and a significantly different engine. In the same reference, Urieli also shows curves for a Philips engine (a heat-pipe-operated swashplate type) which indicate that, in an efficiency-versus-power plot, the helium and hydrogen curves would cross over in the 40- to 45-hertz range. (It is not known whether or not the Philips' curves include the effect of a leakage calculation).

In figure 28, in the low-frequency range, the efficiency drops off rapidly due to the increasing significance of static conduction and shuttle heat-transfer losses as the power level drops.

CONCLUDING REMARKS

As shown above, the Stirling engine performance model discussed herein tracks engine cyclical performance. Testing of the ground-power-unit engine now under way at NASA Lewis will provide the basic engine performance data necessary for a quantitative evaluation of the modeling process for mechanically linked engines. The data resulting from these tests and comparisons of the model predictions with the data are subjects for future reports.

There is little information in the literature applicable to the periodic-flow processes occurring in Stirling engines. An expanded base on both periodic-flow and steady-flow heat-transfer and pressure-drop data for Stirling engine heat-exchanger components is needed to improve the level of confidence in predicting engine heat-transfer and pressure-drop characteristics.

It is expected that better definition of the actual engine dead volumes, modifications to the presently incorporated heat-transfer and pressure-drop correlations, and, perhaps, tightening of some of the simplifying assumptions may be required before the model predicts real-engine performance with a high degree of quantitative accuracy. However, the model's qualitative ability to predict variations in the state of the working gas over a cycle and to predict performance trends has already been useful in helping to understand operation of the engine, to plan the experimental program, and to study sensitivity to various engine and working-gas parameters.

APPENDIX A

DERIVATION OF GAS TEMPERATURE DIFFERENTIAL EQUATION

The basic gas-volume equations are used in the derivation. For convenience they are listed again here:

$$\frac{d}{dt}(MC_vT) = hA(T_w - T) + C_p(w_iT_i - w_oT_o) - P\frac{dV}{dt} \tag{1}$$

$$\frac{dM}{dt} = w_i - w_o \tag{2}$$

$$PV = MRT \tag{3}$$

Expanding the first term of equation (1) gives

$$MC_v\frac{dT}{dt} + C_vT\frac{dM}{dt} = hA(T_w - T) + C_p(w_iT_i - w_oT_o) - P\frac{dV}{dt} \tag{A1}$$

Differentiating equation (3) gives

$$MR\frac{dT}{dt} + RT\frac{dM}{dt} = P\frac{dV}{dt} + V\frac{dP}{dt} \tag{A2}$$

Letting $R = C_p - C_v$ in the first and second terms of equation (A2) and solving for

$$C_vT\frac{dM}{dt}$$

yields

$$C_v T \frac{dM}{dt} = M(C_p - C_v) \frac{dT}{dt} + C_p T \frac{dM}{dt} - P \frac{dV}{dt} - V \frac{dP}{dt} \qquad \text{(A3)}$$

Substituting the right side of equation (A3) for the second term of equation (A1) yields

$$M\cancel{C_v} \frac{dT}{dt} + M(C_p - \cancel{C_v}) \frac{dT}{dt} + C_p T \frac{dM}{dt} - P \cancel{\frac{dV}{dt}} - V \frac{dP}{dt}$$

$$= hA(T_w - T) + C_p(w_i T_i - w_o T_o) - P \cancel{\frac{dV}{dt}}$$

or

$$MC_p \frac{dT}{dt} + C_p T \frac{dM}{dt} - V \frac{dP}{dt} = hA(T_w - T) + C_p(w_i T_i - w_o T_o) \qquad \text{(A4)}$$

Using equation (2) to substitute for dM/dt in equation (A4) gives

$$MC_p \frac{dT}{dt} = hA(T_w - T) + C_p(w_i T_i - w_o T_o) - C_p T(w_i - w_o) + V \frac{dP}{dt}$$

or

$$MC_p \frac{dT}{dt} = hA(T_w - T) + C_p w_i(T_i - T) - C_p w_o(T_o - T) + V \frac{dP}{dt} \qquad (4)$$

which is the equation used in the model to solve for gas temperature.

APPENDIX B

INTEGRATION OF DECOUPLED TEMPERATURE EQUATIONS

The equation

$$\left.\frac{dT}{dt}\right|_{\substack{\text{due to}\\ \text{change in}\\ \text{pressure}}} = \frac{V}{MC_p}\frac{dP}{dt} \tag{5a}$$

can be integrated in closed form by solving the equation of state for V/M and substituting in equation (5a).

$$PV = MRT \rightarrow \frac{V}{M} = \frac{RT}{P}$$

Substituting

$$\frac{dT}{dt} = \frac{RT}{PC_p}\frac{dP}{dt}$$

$$\therefore \frac{dT}{T} = \frac{R}{C_p}\frac{dP}{P} = \frac{C_p - C_v}{C_p}\frac{dP}{P} = \frac{\gamma - 1}{\gamma}\frac{dP}{P}$$

$$\therefore \ln T\Big|_t^{t+\Delta t} = \frac{\gamma - 1}{\gamma}\ln P\Big|_t^{t+\Delta t}$$

$$\frac{T^{t+\Delta t}}{T^t} = \left(\frac{P^{t+\Delta t}}{P^t}\right)^{(\gamma-1)/\gamma}$$

$$\therefore\ T^{t+\Delta t} = T^t \left(\frac{p^{t+\Delta t}}{p^t} \right)^{(\gamma-1)/\gamma}$$

$$\left.\frac{dT}{dt}\right|_{\substack{\text{due to} \\ \text{mixing}}} = \frac{w_i(T_i - T) - w_o(T_o - T)}{M} \tag{5b}$$

By using numerical integration let

$$T^{t+\Delta t} = T^t + \frac{dT}{dt}\Delta t$$

$$= T^t + \frac{w_i^{t+\Delta t}\left(T_i^{t+\Delta t} - T^t\right) - w_o^{t+\Delta t}\left(T_o^{t+\Delta t} - T^t\right)}{M^{t+\Delta t}}\Delta t$$

$$= T^t + \frac{\left(w_o^{t+\Delta t} - w_i^{t+\Delta t}\right)T^t}{M^{t+\Delta t}}\Delta t + \frac{w_i^{t+\Delta t}T_i^{t+\Delta t} - w_o^{t+\Delta t}T_o^{t+\Delta t}}{M^{t+\Delta t}}\Delta t$$

Since

$$w_i = \frac{M^{t+\Delta t} - M^t}{\Delta t} + w_o^{t+\Delta t} \rightarrow \left(w_i^{t+\Delta t} - w_o^{t+\Delta t}\right)\Delta t = M^{t+\Delta t} - M^t$$

have

$$T^{t+\Delta t} = \cancel{T^t} + \frac{(M^t - \cancel{M^{t+\Delta t}})}{M^{t+\Delta t}} T^t + \frac{\left(w_i^{t+\Delta t}T_i^{t+\Delta t} - w_o^{t+\Delta t}T_o^{t+\Delta t}\right)}{M^{t+\Delta t}}\Delta t$$

$$\therefore T^{t+\Delta t} = \frac{M^t T^t + \left(w_i^{t+\Delta t} T_i^{t+\Delta t} - w_o^{t+\Delta t} T_o^{t+\Delta t}\right)\Delta t}{M^{t+\Delta t}}$$

$$\left.\frac{dT}{dt}\right|_{\substack{\text{due to} \\ \text{heat transfer}}} = \frac{hA}{MC_p}(T_w - T) \rightarrow \frac{dT}{T_w - T} = \frac{hA}{MC_p}\,dt \qquad (5c)$$

Assume T_w is constant over the time increment for the purpose of integrating the left side with respect to time. This is a reasonable assumption since T_w changes much more slowly than T due to the relatively large heat capacity of the metal. It was also assumed that h and M were constant over the time increment to allow integration of the right side of the equation.

$$\therefore -\ln(T_w - T)\Big|_t^{t+\Delta t} = \frac{hA}{MC_p}\,t\Big|_t^{t+\Delta t}$$

$$\ln \frac{(T_w - T)^{t+\Delta t}}{(T_w - T)^t} = -\frac{hA}{MC_p}\,\Delta t$$

$$\therefore (T_w - T)^{t+\Delta t} = (T_w - T)^t\, e^{-(hA/MC_p)\Delta t}$$

$$\therefore T^{t+\Delta t} = T_w - (T_w - T)^t\, e^{-(hA/MC_p)\Delta t}$$

or

$$T^{t+\Delta t} = T^{t} + \left(T_w - T^{t}\right)\left(1 - e^{-(hA/MC_p)\Delta t}\right)$$

This equation says that, as the time increment is made larger, the gas temperature approaches the wall temperature asymptotically. Thus using large time increments cannot cause instabilities because of excessive change in gas temperature.

APPENDIX C

HEAT-TRANSFER-COEFFICIENT EQUATIONS

HEATER AND COOLER

The heat-transfer equation used in the heater and cooler is

$$h_I = \frac{k_I}{D_I}\left(0.001871\,\frac{D_I \bar{w}_I}{\mu_I A_{cs,I}} + 15\right) \tag{C1}$$

which was derived by linearizing

$$\underset{\text{Nusselt number}}{\frac{hD}{k}} = 0.023\underbrace{\left(\frac{Dw}{\mu A_{cs}}\right)^{0.8}}_{\text{Reynolds number}} \times \underbrace{\left(\frac{C_p \mu}{k}\right)^{0.4}}_{\text{Prandtl number}} \tag{C2}$$

where

h heat-transfer coefficient

D hydraulic diameter

k thermal conductivity

w flow rate

u viscosity

A_{cs} cross-sectional flow area

C_p specific heat

This equation is reportedly valid (ref. 14) for turbulent flow of gases when $0.7 \leq$ Prandtl number ≤ 120, $10\,000 \leq$ Reynolds number $\leq 120\,000$, and ΔT is moderate. The Prandtl number was essentially constant over the temperature range of interest at 0.68 to 0.69. With the assumption that

$$\left(\frac{C_p \mu}{k}\right)^{0.4} = (0.688)^{0.4} = 0.861$$

equation (C2) reduces to

$$\frac{hD}{k} = 0.0198 \left(\frac{Dw}{\mu A_{cs}}\right)^{0.8} \tag{C3}$$

Heater and cooler Reynolds numbers were calculated in the model range from 0 to 25 000 but are mostly above 10 000. When equation (C3) was linearized, the result was

$$\frac{hD}{k} = 0.001871 \left(\frac{Dw}{\mu A_{cs}}\right) + 15 \tag{C4}$$

which is equivalent to equation (C1). Plots of equations (C3) to (C4) are compared in figure 29.

REGENERATOR

In reference 15, heat-transfer data for a 79 × 79-wire/cm (200 × 200-wire/in.), 0.051-cm- (0.002-in.-) diameter wire screen are given. The data were extrapolated to 400 layers with the result shown as a solid curve in figure 12.

A linear approximation to this curve

$$\frac{hD}{k} = 0.06071 \left(\frac{Dw}{\mu A_{cs}}\right) + 3.7 \tag{C5}$$

is also shown in figure 30. This equation was used to calculate heat-transfer coefficients in the regenerator.

EXPANSION SPACE

This analysis assumes perfect insulation between the combustion gas and the expansion-space wall. Heat transfer between metal and gas is a combination of radiation and convection. For radiation

$$\frac{Q}{A} = \sigma F \left(T_w^4 - T^4 \right) \tag{C6}$$

and

$$h_{rad} = \frac{\frac{Q}{A}}{T_w - T}$$

where

σ Boltzmann constant

F emissivity times view factor

T_w wall temperature

T gas temperature

Q rate of heat flow

A heat-transfer area

h_{rad} radiation heat-transfer coefficient

The overall F is assumed to be 0.7.

The convection heat-transfer coefficient is

$$h_{conv} = 0.023 \, (Re)^{0.8} (Pr)^{0.4} \frac{k}{D_h} \qquad Re > 10\,000 \tag{C7a}$$

$$h_{conv} = 0.023\,(Re)^{0.8}(Pr)^{0.4}\,\frac{k}{D_h}\left[1+\left(\frac{D_h}{L}\right)^{0.07}\right] \qquad 2100 < Re \leq 10\,000$$

where L is the maximum distance from the cylinder head to the displacer, and

$$h_{conv} = 1.86\,(\text{Graetz number})^{0.333}\,\frac{k}{D_h} \qquad \text{Graetz number} > 10;\ Re \leq 2100 \qquad \text{(C7b)}$$

or

$$h_{conv} = 5.0\ \text{Btu/hr-ft}^2\text{-}^{\circ}\text{R} \qquad \text{Graetz number} \leq 10;\ Re \leq 2100 \qquad \text{(C7c)}$$

where Graetz number = $Re \times Pr \times D_h/L$. The value in equation (C7c) is an assumed cutoff point (close to the natural convection coefficient). For the combined heat-transfer coefficient the values obtained from equations (C6) and (C7) are added.

The volume of the insulated part of the heater tubes adjacent to the expansion space is lumped with the expansion space. (It is treated as an expansion-space clearance volume.) However, the heat-transfer rates between the insulated tubes and the gas are calculated separately before they are combined with the rate for the expansion space. The same equations, (C6) and (C7), are used, but in this case the convection strongly dominates the combined value.

COMPRESSION SPACE

Since the radiation effect is small in the compression space, only convection heat transfer is considered. Equation (C7) is used for the calculation. It is assumed that the wall temperature is known. Without detailed analysis or test data to identify this wall temperature, it seems reasonable to assume that it is about equal to the average compression-space gas temperature over the cycle. The net result is that very little heat transfer takes place in the compression space and the compression-space process is essentially adiabatic.

APPENDIX D

MOMENTUM EQUATION

A general form of the conservation-of-momentum equation for one-dimensional flow is

$$\frac{\partial}{\partial t}(\rho v) + \frac{\partial}{\partial x}(\rho v^2) + \frac{f}{2D_h}\rho v^2 + \frac{\partial P}{\partial x} = 0 \qquad \text{(D1)}$$

Rate of accumulation of momentum per unit volume	Rate of momentum gain by convection per unit volume	Rate of momentum gain by viscous transport per unit volume	Rate of momentum gain by pressure force per unit volume

Expanding the first and second terms of equation (D1) yields

$$\rho \frac{\partial v}{\partial t} + v \frac{\partial \rho}{\partial t} + v \frac{\partial(\rho v)}{\partial x} + \rho v \frac{\partial v}{\partial x} + \frac{f}{2D_h}\rho v^2 + \frac{\partial P}{\partial x} = 0 \qquad \text{(D2)}$$

By the continuity equation

$$\frac{\partial \rho}{\partial t} + \frac{\partial}{\partial x}(\rho v) = 0$$

and second and third terms of equation (D2) can be eliminated to yield

$$\rho \frac{\partial v}{\partial t} + \rho v \frac{\partial v}{\partial x} + \frac{f}{2D_h}\rho v^2 + \frac{\partial P}{\partial x} = 0 \qquad \text{(D3)}$$

The first term in equation (D3) is neglected in the model. Neglecting this term and multiply the resulting equation by $\partial x/\rho$ yields

$$v\,\partial v + \frac{f}{D_h} v^2\,\partial x + \frac{\partial P}{\rho} = 0 \qquad \text{(D4)}$$

Note that at zero flow and second and third terms of equation (D3) are zero, so that it reduces to

$$\rho \frac{\partial v}{\partial t} + \frac{\partial P}{\partial x} = 0$$

in which case the time derivative term is responsible for any pressure drop. The significance of this time derivative term could be investigated by the use of a comprehensive model such as that of Urieli (ref. 7).

APPENDIX E

PROGRAM LISTING AND DEFINITION OF VARIABLES

This appendix includes

(1) A listing of the computer program with the short form of the printed output for a sample run. (The Calcomp plotting subroutines are not included in the listing.)

(2) Definitions of the variables that are read into the main program using a NAMELIST format

(3) Definitions of the variables shown in the printed output

Other key variables used in the program are defined with comment statements that are used throughout the program.

The program consists of a main program and four subroutines. It is programmed in FORTRAN V and has been run on a UNIVAC 1110. All input data are either contained within the program or are read into the main program via the 20 NAMELIST parameters. Values of the NAMELIST parameters used in the sample run were printed out and are shown as part of the output.

LISTING OF COMPUTER PROGRAM

Main Program

```
C MAIN PROGRAM
C DOES INITIALIZATION. UPDATES PISTON POSITIONS--EXPANSION, COMPRESSION
C AND BUFFER SPACE VOLUMES.  INTEGRATES P*DELTA(V) TO DETERMINE WORK.
C DETERMINES WHEN CYCLES IS COMPLETE.
      DIMENSION X(2),V(13),REYNO(13),          QR(5),TMAX(12)
      DIMENSION TG(12),TGA(13),TM(13),TMAVG(13),DTM(13)
      COMMON DTIME,F(12),WB(13),DELP(13),P,PE,PC
      COMMON /CYC/ QEXP,QHEATR,QREGEN,QCOOLR,QCOMP,ENFRTH,ENFHTR,
     1ENFCTR,ENFRTC,WRKP,WRKEXP,
     2WRKCMP,WRKLEX,WRKLCM,WRKLP,WRKH,SUMNUM(13),SUMDEN(13),ENTH,
     3WDISP,WPIST,WTPIST,QEXPN,QEXPP,QHEATN,QHEATP,
     4QCOOLN,QCOOLP,QCOMPN,QCOMPP,QREGN,QREGP,WDISPP,WDISPN,WPISTP,
     5WPISTN,QCNDRI,QCNDRO,QCNDCL,QCNDD,QCNDCN, QSHTL,TGEXPA,TGCMPA
      COMMON /DELTAP/AD,AP,                    HA(13)
      COMMON  /TAVCYC/TGCYC(12),TGACYC(13),TMCYC(13)
      COMMON/CTIT/NCURV,ISET1,ISET2,ISET3
      COMMON /JNDEX/JIP,NOCYC
      NAMELIST /STRLNG/P,REALGS,FIPCYC,IPRINT,ITMPS,COEFF,T3,P3,OMEGA,
     *FACT1,FACT2,NOCYC,NSTRT,NOEND,MWGAS,TG,TGA,TM,RHCFAC,JIP
      DATA                    AD ,  AP ,  AR , APISTR /
     1                    6.0,6.0,0.11,0.60/
      DATA RCRANK,E,RODL,V3CL,DIAMD,DIAMP,DIAMDR,DIAMPR/
     13.543,0.82,1.91,29.84,2.75,2.75,0.375,0.875/
      DATA   V/0.0,2*1.5948,.933,5*0.624,3*0.249,0.0/
   10 CONTINUE
C READ IN INITIAL PRESSURES, TEMPERATURES AND OTHER PARAMETERS WHICH
C DEFINE THE NATURE OF THE RUN TO BE MADE
      READ (5,STRLNG,END=1000)
      DTIME=1./(OMEGA*FIPCYC)
      WRITE (6,STRLNG)
C     INITIALIZATION
      FMULT=1.
      ITER=0
      TIME=0.0
      PSI=0.0
      PSIDEG=0.0
      SAVET=0.0
      IPLOT=0
      PRSUM=0.0
      NOITPC=0
      DO 11 I=1,13
      IF(I.EQ.13)  GO TO 12
      TGCYC(I)=TG(I)
   12 TGACYC(I)=TGA(I)
   11 TMCYC(I)=TM(I)
      CPCYC=1./(OMEGA*DTIME)
C R,CP,CV IN UNITS OF IN-LBF/ LBM-DEG. R
      GAMMA=1.396
      R=9197.
      CP=32557.
      CV=23360.
      B=.02758
      IF (MWGAS.NE.4) GO TO 15
      B=.01613
```

```
      GAMMA=1.667
      R=96.32.
      CP=11980.
      CV=8998.
   15 CONTINUE
      IP=IPRINT
      IPRNT2=IPRINT/25
      ADR=AD-AR
      APR=AP-APISTR
      RINMIN=SQRT((RODL-RCRANK)**2-E**2)
      RODYMX=SQRT((RODL**2-(E-RCRANK)**2)
      RODYMN=SQRT((RODL**2-(E+RCRANK)**2)
      STROKE=2.*(RODYMX-RODYMN)
      RODY=RODYMX
      R(1)=RODYMX
      R(2)=-RODYMX
      V(1)=ADR*(R(1)-RIMIN)*3.965
      V(13)=2.*ADR*(RODYMX-RODY)*0.353
      V3=APR*(-R(2)-RIMIN)*V3CL
      V3STAR=V3
      VOVRT=0.3
      DO 33 I=1,13
   30 VOVRT=VOVRT+V(I)/(TBA(I)*R*PR*REALGS)
      W3=P3*V3ST_R/(R*(3*R*P3*REALGS))
      ALPHA=W3*R/VOVRT
      SIB3=ALPHA/(P+ALPHA)
      W=W3/SIB3
      PE=P
      PC=P
      DO 50 I=1,13
   50 WB(I)=P*V(I)/(R*(TBA(I)*R*PR*REALGS))
      ISTART=1
      J=1
  100 CONTINUE
      IF (J .LT. ISTART) GO TO 140
  125 IF (JIP.GT.0) GO TO 140
      IF (J.LT.(NOCYC-1)) WRITE (6,133)
  130 FORMAT (' TIME   ANGLE   R(1)   V(2)   T0',7X,'T9',7X,'T11',9X,'T2
     1',5X,'  PE      PC      PRIN   PROUT ',3X,'F(8)',5X,'F(9) ')
      IF (J.EQ.(NOCYC-1)) WRITE (6,132)
  132 FORMAT (' TIME    ANGLE    RE1      RE2      RE3      RE4      RE5'
     1'      RE6      RE7      RE8      RE9      RE10      RE11      RE12
     2'RE13 ')
      IF (J.EQ.NOCYC) WRITE (6,133)
  133 FORMAT (' TIME    ANGLE      F1       F2       F3       F4       F5'
     1'       F6       F7       F8       F9       F10       F11       F12')
C     BEGINNING OF LOOP
  140 TIER=TIER+1
      IF(J.GE.(NOCYC-9)) IPRINT=IPRNT2
      IF ((TIME+SAVET).GT.5.0) GO TO 700
      IP=IP+1
      VTOTL=0.0
      DO 142 IJK=1,13
  142 VTOTL=VTOTL+V(IJK)
      IF (JIP.GT.0) GO TO 170
      IF (IP .LT. IPRINT) GO TO 165
      IF (J .LT. ISTART) GO TO 170
      IF (J.LT.(NOCYC-1)) WRITE (6,160) TIME,PSIDEG,R,TBA(1),TBA(9),
     1TBA(11),TBA(13),PE,PC,PRIN,PROUT,F(8),F(9)
  160 FORMAT (1X,F7.4,F8.1,2F8.2,1X,2F8.2,F8.0,F8.0,1X,4F8.2,2F8.5)
      IF (J.EQ.(NOCYC-1)) WRITE (6,162) TIME,PSIDEG,REYNO
  162 FORMAT (1X,F7.4,F8.1,13F8.0)
      IF (J.EQ.NOCYC) WRITE (6,163) TIME,PSIDEG,F
  163 FORMAT (1X,F7.4,F8.1,12F8.5)
      IF (ITMPS.EQ.1) WRITE (6,660) T0,TBA,TM
  660 FORMAT (' T0=',4X,12F8.0/,' TBA=',13F8.0/,'  TM=',13F8.0/)
```

```
  170 IP=0
  180 TIME=DTIME*FLOAT(ITER)
      IF(ITER.EQ.IFIX(.3/DTIME) .AND. J.LT.6) GO TO 700
C CALL HEAT EXCHANGER SUBROUTINE TO UPDATE GAS LUMP MASSES, FLOW RATES,
C TEMPERATURES, PRESSURE + REGENERATOR METAL TEMPERATURES.
      CALL HEATX (TIME,TG,TGA,TM,REYNO,OR,X,RODY,J,DIAND,XIMIN,
     1RODYMX,V,SI63,W,MWGAS,RMCFAC,REALGS,CONDID,NOCYC)
      PRSUM=PRSUM+P
      NOITPC=NOITPC+1
C UPDATE EXPANSION AND COMPRESSION SPACE PRESSURES. (LBF/IN2)
      PEOLD=PE
      PCOLD=PC
      POLD=P
      IF (J.LT.(NOCYC-5)) GO TO 240
      PRIN=(DELP(5)+DELP(6)+0.5*DELP(7))*FMULT+P
      PROUT=P-(0.5*DELP(7)+DELP(8)+DELP(9))*FMULT
      PE=(DELP(2)+DELP(3)+DELP(4))*FMULT+PRIN
      PC=PROUT-(DELP(10)+DELP(11)+DELP(12))*FMULT
      GO TO 245
  240 PE=P
      PC=P
      PRIN=P
      PROUT=P
  245 CONTINUE
      AE=(PE+PEOLD)/2.
      AC=(PC+PCOLD)/2.
      A=(P+POLD)/2.
      DELPRG=PRIN-PROUT
      DELPHT=PE-PRIN
      DELPCL=PROUT-PC
C CALCULATE INTERNAL ENERGY OF WORKING SPACE GAS. (FT-LBF)
      UTOTAL=0.0
      DO 250 I=1,13
  250 UTOTAL=WG(I)*CV*TGA(I)/12.+UTOTAL
  260 CONTINUE
C BUFFER SPACE BLEED FLOW,FLOTOB (LBM/SEC)
      IF ((PC-P3) .GE. 0.) GO TO 270
      SI63P=-COEFF*(P3-PC)**.5/W
      GO TO 280
  270 SI63P=COEFF*(PC-P3)**.5/W
  280 CONTINUE
      FLOTOB=SI63P*W
      IF (FLOTOB.GE.0) ENTHWB=CP*TGA(13)*FLOTOB*DTIME/12.
      IF (FLOTOB.LT.0) ENTHWB=CP*T3*FLOTOB*DTIME/12.
      ENTH=ENTH+ENTHWB
      SI63=SI63+SI63P*DTIME
      WG(13)=WG(13)-FLOTOB*DTIME
      IF (FLOTOB.LT.0.0) TGA(13)=TGA(13)-FLOTOB*DTIME*
     1(T3-TGA(13))/WG(13)
  520 P3OLD=P3
      P3=T3/(V3/(SI63*R*R)-B*REALGS)
      A3=(P3OLD+P3)/2.
C UPDATE CRANK ANGLE,  PSI(RADIANS), PSIDEG(DEGREES)
      PSIOLD=PSI
      PSI=PSI+OMEGA*DTIME*6.28318
      IF (PSI.GE.6.28318) PSI=PSI-6.28318
      PSIDEG=PSI*360./6.28318
C UPDATE PISTON POSITIONS (IN)
      RODY=SQRT(RODL**2-(E-RCRANK*COS(PSI))**2)
      X1OLD=X(1)
      X2OLD=X(2)
      X(1)=RCRANK*SIN(PSI)+RODY
      X(2)=RCRANK*SIN(PSI)-RODY
C UPDATE EXPANSION, COMPRESSION, AND BUFFER SPACE VOLUMES. (IN3)
      V1OLD=V(1)
      V13OLD=V(13)
```

```
      V(1)=AD*(X(1)-XIMIN)+0.965
      V(13)=2.*ADR*(RODYNX-RODY)+0.353
      V3=APR*(1-X(2)-XIMIN)+V3CL
C CALCULATE WORK (FT-LBF)--EXPANSION SPACE WORK,WRKEXP; COMPRESSION
C SPACE WORK,WRKCMP; TOTAL WORK, WRKN; DISPLACER WORK,WDISP; POWER PISTON
C WORK,WPIST; PRESSURE DROP WORK LOSS IN EXPANSION AND COMPRESSION
C SPACES, WRKLEX AND WRKLCN
      WRKP=WRKP+AC*(V(13)-V130LD)/12.
      DWEXP=AE*(V(1)-V10LD)/12.
      WRKEXP=WRKEXP+DWEXP
      IF (DWEXP.GT.0.0) WEXPP=WEXPP+DWEXP
      IF (DWEXP.LT.0.0) WEXPN=WEXPN+DWEXP
      DWCMP=AC*(V(13)-V130LD)/12.
      WRKCMP=WRKCMP+DWCMP
      IF (DWCMP.GT.0.0) WCMPP=WCMPP+DWCMP
      IF (DWCMP.LT.0.0) WCMPN=WCMPN+DWCMP
      WRKLEX=WRKLEX+(A-AE)*(V(1)-V10LD)/12.
      WRKLCN=WRKLCN+(A-AC)*(V(13)-V130LD)/12.
      WRKLP=WRKLP+(A-AC)*(V(13)-V130LD)/12.
      WRKN=WRKN+(AE*(V(1)-V10LD)+AC*(V(13)-V130LD))/12.
      DWDISP=(AE*AD-AC*ADR)*(X(1)-X10LD)/12.
      WDISP=WDISP+DWDISP
      IF (DWDISP.GT.0.0) WDISPP=WDISPP+DWDISP
      IF (DWDISP.LT.0.0) WDISPN=WDISPN+DWDISP
      DWPIST=AC*ADR*(X(2)-X20LD)/12.
      WPIST=WPIST+DWPIST
      IF (DWPIST.GT.0.0) WPISTP=WPISTP+DWPIST
      IF (DWPIST.LT.0.0) WPISTN=WPISTN+DWPIST
      WTPIST=WTPIST+AC*ADR*(X(2)-X20LD)/12.
      DO 533 I=1,13
      IF(I.EQ.13)  GO TO 531
      TGCYC(I)=TGCYC(I)+TG(I)
  531 TGACYC(I)=TGACYC(I)+TGA(I)
  530 TMCYC(I)=TMCYC(I)+TM(I)
      IF (PSIOLD.GT.3.14159      .AND. PSI.LT.3.14159       ) GO TO 650
      GO TO 140
C     END OF LOOP
  650 CONTINUE
C CALCULATE AVERAGE GAS TEMPERATURES OVER THE CYCLE FOR EACH CONTROL VOLUME
      DO 533 I=1,13
      IF(I.EQ.13)  GO TO 534
      TGCYC(I)=TGCYC(I)/CPCYC
  534 TGACYC(I)=TGACYC(I)/CPCYC
  533 TMCYC(I)=TMCYC(I)/CPCYC
      TGEXPA=TGACYC(1)
      TGCMPA=TGACYC(13)
      DO 667 II=1,6
      JJ=II+6
      TMAX(II)=0.0
  667 TMAX(JJ)=5000.
      IF (JIP.GT.0.AND.J.NE.(NOCYC-1)) GO TO 668
      IF (J.LT.(NOCYC-1)) WRITE (6,163) TIME,PSIDEG,X,P,P3,TGA(1),
     1TGA(13),PE,PC,PRIN,PROUT,V(1),V(13)
      IF (JIP.EQ.0) WRITE (6,663) TG,TGA,TM
  668 CONTINUE
      IF(J.LT.NSTRT  .OR.  J.GT.NOEND) GO TO 675
C CONVERGENCE SCHEME FOR REGENERATOR METAL TEMPERATURES.
      DO 670 JI=5,9
  670 DTM(JI)=FACT1*DTM(JI)+FACT2*SUMNUM(JI)/SUMDEN(JI)
      TM(5)=TM(5)-(5.*DTM(5)+4.*DTM(6)+3.*DTM(7)+2.*DTM(8)+DTM(9))/3.
      TM(6)=TM(6)-(4.*DTM(5)+8.*DTM(6)+6.*DTM(7)+4.*DTM(8)+2.*DTM(9))/3.
      TM(7)=TM(7)-(3.*DTM(5)+2.*DTM(6)+3.*DTM(7)+2.*DTM(8)+DTM(9))
      TM(8)=TM(8)-(2.*DTM(5)+4.*DTM(6)+6.*DTM(7)+8.*DTM(8)+4.*DTM(9))/3.
      TM(9)=TM(9)-(DTM(5)+2.*DTM(6)+3.*DTM(7)+4.*DTM(8)+5.*DTM(9))/3.
      GO TO 675
  675 CONTINUE
```

```
      DO 673 I=1,5
  673 DR(I)=0.0
      AVGWSP=PRSUM/FLOAT(NOITPC)
      CALL CYCL (TIME,UTOTAL,STROKV,AVGWSP)
      DO 532 I=1,13
      IF (I.EQ.13) GO TO 535
      TGCYC(I)=0.0
  535 TGACYC(I)=0.0
  532 TMCYC(I)=0.0
      PRSUM=0.0
      NOITPC=0
      J=J+1
      IF(J.NE.(NOCYC-1)) GO TO 680
      IPLOT=0
      ITER=0
      SAVET=TIME
      TIME=0.
  680 IF(J.LE.NOCYC) GO TO 125
  700 CONTINUE
      GO TO 10
 1000 CONTINUE
      STOP
      END
```

Subroutine HEATEX

```
C THIS SUBROUTINE CALCULATES HEAT TRANSFER AND UPDATES TEMPERATURES AND
C PRESSURE
      SUBROUTINE HEATX (TIME,TG,TGA,TMA,REYNO,QR,X,RODY,JCYCLE,DIAND,
     1XININ,RODYNX,V,SIGS,W,MWGAS,RHCFAC,REALGS,CONDID,NOCYC)
      COMMON DTIME,F(12),WG(13),DELP(13),P,PE,PC
      COMMON /CYC/ QEXP,QHEATR,QREGEN,QCOOLR,QCOMP,ENFRTH,ENFHTR,
     1ENFCTR,ENFRTC,WRKP,WRKEXP,
     2WRKCMP,WRKLEX,WRKLCH,WRKLP,WRKH,SUMNUM(13),SUMDEN(13),ENTH,
     3WDISP,WPIST,WTPIST,QEXPN,QEXPP,QHEATN,QHEAT ,
     4QCOOLN,QCOOLP,QCOMPN,QCOMPP,QREGN,QREGP,WDISPP,WDISPN,WPISTP,
     5WPISTN,QCNDRI,QCNDRO,QCNDCL,QCNDD,QCNDCN, QSHTL,TGEXPA,TGCMPA
      COMMON /DELTAP/AD,AP,                    HA(13)
      DIMENSION COEFX(40),DPX(40)
      DIMENSION TGA(13),        TMA(13),TGAO(13),TMAO(13), X(2)
      DIMENSION CPH(13),        Q(13),TMIX(13),TG(12),DH(13),ACS(13),
     1AHT(13),COND(13),VIS(13),REYNO(13),                    QR(5)
      DIMENSION V(13),WGOLD(13),XL(13),FAVG(13),DNSTY(13),FRICT(13)
      DATA DH/1.937,3*0.1190,5*0.003800,3*0.0439,1.487/,
     1     ACS/3.250,3*0.05561,5*0.4380,3*0.05120,3.150/,
     1     AHT/3.0,2*5.72 ...922,5*82.56,3*2.288,0.0/,
     1      CPH/4*10.0,5*.011,              4*10.0/,
     1      XL/0.0,2*3.06,2.098,5*0.178,3*0.187,0.0/,
     1 IDEX/1/
C DH(I)=HYDRAULIC DIAMETER,IN.; ACS(I)=FLOW AREA, IN2; AHT=HEAT TRANSFER,IN2;
C CPH(I)=METAL HEAT CAPACITY, BTU/LBM-DEG.R; XL(I)=LENGTHS FOR CALCULATING
C PRESSURE DROP,IN
C CP,CV ARE IN BTU/LBM-DEG.R;GAS CONSTANT, R, IS
C IN IN-LBF/(LBM-DEG R)
      R=.02358
      CP=3.484
      GAMMA=1.394
```

```
      R=9197.
      IF (NWGAS.NE.4) GO TO 5
      B=.01613
      CP=1.239
      R=4632.
      GAMMA=1.667
    5 CONTINUE
      CV=CP/GAMMA
      DO 10 I=1,13
      IF (NWGAS.EQ.4) GO TO 6
C CONDUCTIVITY, COND(I) HAS UNITS BTU/IN-SEC-DEG.R
C VISCOSITY,VIS(I) HAS UNITS LBM/IN-SEC
      COND(I)=2.481E-9*TGA(I)+1.263E-6
      VIS(I)=4.683E-10*TGA(I)+2.619E-7
      GO TO 8
    6 COND(I)=1.962E-9*TGA(I)+1.115E-6
      VIS(I)=1.058E-9*TGA(I)+5.919E-7
    8 TMAO(I)=TMA(I)
   10 TGAO(I)=TGA(I)
      POLD=P
C CALCULATE PRESSURE,LBF/IN2
      SUMWT=0.0
      SUMV=0.0
      DO 14 I=1,13
      SUMWT=SUMWT+WG(I)*TGA(I)
   14 SUMV=SUMV+V(I)
      P=R*SUMWT/(SUMV-B*R*W*(1.-SIG3)*REALGS)
      FGAMMA=(P/POLD)**((GAMMA-1.)/GAMMA)
      DO 20 J=1,13
      TGAO(J)=TGAO(J)*FGAMMA
   20 TMIX(J)=TGAO(J)
C CALCULATE MASSES, WG(I), IN EACH GAS LUMP. ,LBM
      SUM=0.0
      DO 200 I=1,13
  200 SUM=SUM+P*V(I)/(R*(TMIX(I)+B*P*REALGS))
      DO 220 I=1,13
  220 WGOLD(I)=WG(I)
      DO 240 I=1,13
  240 WG(I)=W*(1.-SIG3)*P*V(I)/(R*SUM*(TMIX(I)+B*P*REALGS))
      IF (NDEX.EQ.2) GO TO 243
      DO 242 I=1,13
  242 WGOLD(I)=WG(I)
C CALCULATE FLOW RATES, F(I) [illegible]LBM/SEC, BETWEEN GAS LUMPS
  243 NDEX=2
      F(1)=(WGOLD(1)-WG(1))/DTIME
      DO 300 I=2,12
  300 F(I)=(WGOLD(I)-WG(I))/DTIME+F(I-1)
      DO 24 I=1,12
      IF(F(I).LT.0.) GO TO 22
      TG(I)=TGAO(I)
      IF(I.GT.4 .AND. I.LT.10) TG(I)=TGAO(I)-(TMA(5)-TMA(9))/F.*
     1F(I)*DTIME*(TMA(5)-TMA(9))/8./WGOLD(I)
      GO TO 24
   22 TG(I)=TGAO(I+1)
      IF(I.GT.3 .AND. I.LT.9) TG(I)=TGAO(I+1)+(TMA(5)-TMA(9))/8.*
     1F(I)*DTIME*(TMA(5)-TMA(9))/8./WGOLD(I+1)
   24 CONTINUE
C CALCULATE AVERAGE FLOW RATES FOR EACH GAS LUMP.
      FAVG(1)=F(1)
      DO 30 I=2,12
   30 FAVG(I)=(F(I-1)+F(I))/2.
      FAVG(13)=F(13)
C REVISE GAS TEMPERATURES TO ACCOUNT FOR MIXING.
      IF (F(1).LT.0.0) TMIX(1)=(WGOLD(1)*TMIX(1)-F(1)*DTIME*
     1TG(1))/WG(1)
      DO 100 I=2,12
```

```
  100 TMIX(I)=(WBOLD(I)*TMIX(I)*(F(I-1)*TG(I-1)-F(I)*TG(I))*
     ;DTIME)/WG(I)
      IF (F(12).ST.0.0) TMIX(13)=(WBOLD(13)*TMIX(13)*F(12)*
     1DTIME*TG(12))/WG(13)
  110 CONTINUE
C CALCULATE REYNOLDS NO S, REYNO(I); HEAT TRANSFER AREAS, AHT(I);
C HEAT TRANSFER COEFFICIENTS, HA(I) BETWEEN GAS + METAL LUMPS.
C HA(I) HAS UNITS BTU/SEC-DEG.R
      REYNO(1)=DH(1)*ABS(F(1))/(VIS(1)*ACS(1))+.3331
      AHT(1)=3.1416*DIAMD*(X(1)-X1MIN)*16.6
      HA(1)=COND(1)/DH(1)*(1.871E-3*DH(1)*ABS(F(1))/(VIS(1)*
     *    1))*15.)*AHT(1)
C TO M  : EXPANSION SPACE PROCESS ADIABATIC SET HA 1 =0.0
C     HA(1)=  3.3
C
C  QUENCHING IN EXP. SPACE--RADIATION .7D EFFECTIVE--HCONV=5/3600/144 HI
      I=1
      XL(1)=X(1)-X1MIN+.01
      XL(13)=V(13)/AP+.01
      FOA=0.7
      IF(ABS(TMIX(1)-TWA(1)).LE.1.3)  GO TO 42
      QRAD=0.173*FOA*((TMIX(1)/100.)**4-(TWA(1)/100.)**4)
      HRAD=QRAD/(TMIX(1)-TWA(1))/36J)./144.
      GO TO 43
   42 HRAD=0.0
   43 CONTINUE
      PR=CP*VIS(I)/COND(I)
      HCONV=0.023* REYNO(I)**0.8*PR**0.4*COND(I)/DH(I)
      IF(REYNO(I).GT.2100.0.AND.REYNO(I).LT.10000.) HCONV=HCONV*(1.+(DH(
     1I)/XL(I))**0.7)
      GRAETZ=REYNO(I)*PR*DH(I)/XL(I)
      IF(REYNO(I).LE.21JJ.J.AND.GRAETZ.GT.10.) HCONV=1.86*GRAETZ**J.333*
     1COND(I)/DH(I)
      IF(REYNO(I).LE.21JJ.J.AND.GRAETZ.LE.10.)  HCONV=5.J/36JJ./144.
      IF(I.EQ.13)  GO TO 44
C ACCOUNT FOR HEAT TRANSFER TO INSULATED PORTION OF HEATER TUBES
C (ADJACENT TO EXPANSION SPACE) ALONG WITH HEAT TRANSFER TO EXPANSION
C SPACE WALL
      XL1=1.321
      REYNO1=DH(2)*ABS(F(1))/8.D/(VIS(1)*ACS(2))+.0001
      AHT1=14.955*XL1
      HCONV1=0.023*REYNO1**0.8*PR**0.4*COND(1)/DH(2)
      HA1=(HRAD+HCONV1)*AHT1
      HA(1)=(HRAD+HCONV)*AHT(1)+HA1
C
      DO 40 I=2,12
      REYNO(I)=DH(I)*ABS(F(I-1)+F(I))/2./8./(VIS(I)*ACS(I))+.0001
      IF (I.LT.5.OR.I.GT.9) HA(I)=COND(I)/DH(I)*(1.871E-3*
     1DH(I)*ABS((F(I-1)+F(I))/2.)/8./
     2(VIS(I)*ACS(I))*15.)*AHT(I)*8.
      IF (I.GE.5.AND.I.LE.9) HA(I)=COND(I)/DH(I)*(3.06371*
     1DH(I)*ABS((F(I-1)+F(I))/2.)/8./
     2(VIS(I)*ACS(I))*3.7)*AHT(I)*8.
   40 CONTINUE
      HA(9)=0.J
      DO 41 I=5,9
   41 HA(I)=RHCFAC*HA(I)
      REYNO(13)=DH(13)*ABS(F(12))/(VIS(13)*ACS(13))+.0331
      AHT(13)=6.2832*DIAMD*(RODYMX-RODY)*5.5
      HA(13)=COND(13)/DH(13)*(1.871E-3*DH(13)*ABS(F(12))/
     1(VIS(13)*ACS(13))*15.)*AHT(13)
C TO MAKE COMPRESSION SPACE PROCESS ADIABATIC SET HA 13 =3.0
C     HA(13)=  0.J
      I=13
      IF(I.EQ.13) GO TO 42
   44 HA(13)=HCONV*AHT(13)
C
```

```
C CALCULATE RATES OF HEAT TRANSFER BETWEEN GAS AND METAL AND REVISE
C GAS TEMPERATURES TO ACCOUNT FOR HEAT TRANSFER TO OR FROM METAL.
      DO 120 N=1,13
      HAWC=-DTIME*HA(N)/(WB(N)*CP)
      FCTR=1.-EXP(HAWC)
      DTGA=(TMAO(N)-TMIX(N))*FCTR
      DTM(N)=-DTGA*WB(N)*CP/DTIME
      WFCTR=FCTR*WB(N)
      WDTGA=DTGA*WB(N)
      SUMNUM(N)=SUMNUM(N)+WDTGA
      SUMDEN(N)=SUMDEN(N)+WFCTR
  120 TGA(N)=TMIX(N)+DTGA
      IF (JCYCLE.LT.(NOCYC-5)) GO TO 64
C CALCULATE DENSITY,FRICTION FACTORS, AND DELTA PRESSURES
C FOR EACH LUMP.
      DO 130 I=1,13
  130 DNSTY(I)=P/(R*(TGA(I)+B*P*REALGS))
      DO 140 I=2,12
      IF (REYNO(I).LT.1500.AND.I.LT.5.OR.I.GT.9) FRICT(I)=16./REYNO(I)
      IF (REYNO(I).GE.1500..AND.I.LT.5.OR.I.GT.9) FRICT(I)=0.046/
     1REYNO(I)**0.2
      IF (I.GE.5.AND.I.LE.9) FRICT(I)=3.96*EXP(-0.0190*REYNO(I))+0.54
  140 DELP(I)=FRICT(I)*FAVG(I)*ABS(FAVG(I))*XL(I)/
     1(32.2*DH(I)*DNSTY(I)*ACS(I)**2*6.944.)
C PRESSURE DROP CALCULATIONS
      DO 141 I=1,40
  141 DPR(I)=GAMMA
      ACSEXP=V(1)/AD*3.141592.75/8.
      ACSCOM=V(13)/AP*3.141592.75/8.
      J=1
      IF(F(1).LE.0.0)  J=2
      P=P
      F01=F(1)
      F02=F(2)
      F09=F(9)
      F10=F(10)
      F12=F(12)
      CALL XDELP(J,ACSEXP, ACS(02),DH(02),XL(02),DNSTY(02),VIS(02),F01
     X,2,COEFR(01),DPR(01),1)
C
      CALL XDELP(3,ACS(02),ACS(02),DH(02),XL(02),DNSTY(02),VIS(02),F01
     X,2,COEFR(02),DPR(02),2)
      CALL XDELP(4,ACS(02),ACS(02),DH(02),XL(02),DNSTY(03),VIS(03),F02
     X,2,COEFR(03),DPR(03),3)
C
      DPFRIC=0.0
      XL2=XL(2)
      DO 142 I=2,12
      IF(I.EQ.2)  XL(2)=XL2*1.321
      IF(I.LT.5.OR.I.GT.9)  NTYPE=10
      IF(I.GE.5.AND.I.LE.9)  NTYPE=11
      CALL XDELP(NTYPE,ACS(I),ACS(I1),DH(I),XL(I),DNSTY(I),VIS(I),FAVG(I
     X,2,COEFR(I*2),DPR(I*2),(I*2))
      XL(2)=XL2
      DELP(I)=DPR(1*2)
      DPFRIC=DPFRIC+DELP(I)
  142 CONTINUE
C
      IF(F(9).GT.0.0)  GO TO 61
      CALL XDELP(1,ACS(09),.622000,DH(09),XL(09),DNSTY(09),VIS(09),F09
     X,2,COEFR(15),DPR(15),15)
      GO TO 62
   61 CONTINUE
      CALL XDELP(1,.62.000,ACS(10),DH(10),XL(10),DNSTY(10),VIS(10),F09
     X,2,COEFR(16),DPR(16),16)
   62 CONTINUE
```

```
      CALL XDELP(5,ACS(12),.043370,DM(12),XL(12),DNSTY(12),VIS(12),F12
     X,Z,COEFX(17),DPX(17),17)
      J=2
      IF(F(12).LE.0.0)  J=1
      CALL XDELP(J,ACS(12),ACSCON, DM(12),XL(12),DNSTY(12),VIS(12),F12
     X,Z,COEFX(18),DPX(18),18)
      DPSUM=0.0
      DO 63 I=1,17
      DPSUM=DPSUM+DPX(I)
   63 CONTINUE
      DELP(11)=DPFRIC
      DELP(13)=DPSUM
C
      DELP(02)=DELP(02)+DPX(01)+DPX(02)
      DELP(03)=DELP(03)+DPX(03)
      DELP(04)=DELP(04)+DPX(15)
      DELP(10)=DELP(10)+DPX(16)
      DELP(12)=DELP(12)+DPX(17)+DPX(18)
  174 CONTINUE
C CALCULATE HEAT CONDUCTION (CALL HEAT CONDUCTION SUBROUTINE)
      IF (NCOND.NE.3) CALL CNDCT (TMA,QCREG ,QCYL,QCOND0,QCAN,QSHTTL,
     1WGAS)
      NCOND=3
   64 CONTINUE
C REVISE REGENERATOR METAL TEMPERATURES.
      DO 177 J=5,9
  177 TMA(J)=TMA(J)+Q(J)*DTIME/CPM(J)
C  CONVERT Q(J)'S TO FT-LBF & SUM UP FOR EACH COMPONENT.
      QTOT=0.0
      QEX=0.0
      QHEAT=0.0
      QHETN=0.0
      QHETP=0.0
      QREGE=0.0
      QR6P=0.0
      QR6N=0.0
      QCOOL=0.0
      QCOLP=0.0
      QCOLN=0.0
      QCON=0.0
      DO 179 J=1,13
      QADD=Q(J)*DTIME*777.3
      IF (J.EQ.1) QEX=QEX+QADD
      IF (J.GE.2.AND.J.LE.4) QHEAT=QHEAT+QADD
      IF (J.GE.2.AND.J.LE.4.AND.QADD.LT.0.0) QHETN=QHETN+QADD
      IF (J.GE.2.AND.J.LE.4.AND.QADD.GT.0.0) QHETP=QHETP+QADD
      IF (J.GE.5.AND.J.LE.9) QREGE=QREGE+QADD
      IF (J.GE.5.AND.J.LE.9.AND.QADD.GT.0.0) QR6P=QR6P+QADD
      IF (J.GE.5.AND.J.LE.9.AND.QADD.LT.0.0) QR6N=QR6N+QADD
      IF (J.GE.10.AND.J.LE.12) QCOOL=QCOOL+QADD
      IF (J.GE.10.AND.J.LE.12.AND.QADD.LT.0.0) QCOLN=QCOLN+QADD
      IF (J.GE.10.AND.J.LE.12.AND.QADD.GT.0.0) QCOLP=QCOLP+QADD
      IF (J.EQ.13) QCON=QCON+QADD
  179 QTOT=QTOT+QADD
      DO 185 J=1,5
  185 QR(J)=QR(J)+Q(J)*DTIME/CPM(J)
      QEXP=QEXP+QEX
      IF (QEX .LT.0.0) QEXPN=QEXPN+QEX
      IF (QEX .GT.0.0) QEXPP=QEXPP+QEX
      QHEATR=QHEATR+QHEAT
      QHEATN=QHEATN+QHETN
      QHEATP=QHEATP+QHETP
      QREGEN=QRTGEN+QREGE
      QREGN=QREGN+QR6N
      QREGP=QREGP+QR6P
      QCOOLR=QCOOLR+QCOOL
```

```
      QCOOLP=QCOOLP+QCOLP
      QCOOLN=QCOOLN+QCOLN
      QCONP=QCONP+QCON
      IF (QCON.GT.0.0) QCONPP=QCONPP+QCON
      IF (QCON.LT.0.0) QCONPN=QCONPN+QCON
      QCNDRI=QCNDRI+QCREG     *DTIME*777.3
      QCNDRO=QCNDRO+QCREG     *DTIME*777.3
      QCNDCL=QCNDCL+QCYL*DTIME*777.3
      QCNDD=QCNDD+QCONDD*DTIME*777.3
      QCNDCN=QCNDCN+QCAN*DTIME*777.3
      QSHTL=QSHTTL*DTIME*777.3+QSHTL
  350 CONTINUE
      ENFRTN=ENFRTN-AMIN1(F(10)*CP,0.0)*T6(10)*DTIME
      ENFNTR=ENFNTR+AMAX1(F(10)*CP,0.0)*T6(10)*DTIME
      ENFCTR=ENFCTR-AMIN1(F(9)*CP,0.0)*T6(9)*DTIME
      ENFRTC=ENFRTC+AMAX1(F(9)*CP,0.0)*T6(9)*DTIME
      RETURN
      END
```

Subroutine CYCL

```
C THIS SUBROUTINE IS CALLED JUST ONCE PER CYCLE--WHEN THE CYCLE IS COMPLETE.
C IT CALCULATES--NET HEAT IN AND OUT, NET WORK PER CYCLE, INDICATED POWERS
C AND EFFICIENCY, ETC.  HEAT AND WORK QUANTITIES ARE STORED FOR CALCULATION
C OF AVERAGES OVER 5 CYCLES.  AFTER STORING, INTEGRATED HEAT AND WORK
C QUANTITIES ARE RESET TO ZERO IN PREPARATION FOR NEXT CYCLE.
      SUBROUTINE CYCL (TIME,UTOTAL,STROKV,AVGUSP)
      DIMENSION VAR(1006),STORE(11,86)
      COMMON DTIME,P(121),WS(13),DELP(13),P,PL,PC
      DATA J,K,STORE,OLDTIM/2*0,9670.0,/
      DATA  JIP1/0/
      COMMON /CYC/ QEXP,QHEATR,QREGEN,QCOOLR,QCONP,ENFRTN,ENFNTR,
     1ENFCTR,ENFRTC,WNRP,WNREXP,
     2WRACMP,WRALER,WRALCM,WRALP,WRKN,SUMNUM(13),SUMDEN(13),ENTN,
     3WDISP,WPIST,WIPIST,QEXPN,QEXPP,QHEATN,QHEATP,
     4QCOOLN,QCOOLP,QCONPN,QCONPP,QREGN,QREGP,WDISPP,WDISPN,WPISTP,
     5WPISTN,QCNDRI,QCNDRO,QCNDCL,QCNDD,QCNDCN, QSHTL,TQEXPA,TQCMPA
      COMMON  /TAVCYC/TQCYC(12),TQACYC(13),TMCYC(13)
      COMMON /UNDER/JIP,NOCYC
      EQUIVALENCE (VAR(1),QEXP)
      J=J+1
      K=K+1
      JIP1=JIP1+1
      IF(OLDTIM.GT.TIME) OLDTIM=0.
      DELTIM=TIME-OLDTIM
      OLDTIM=TIME
      QIN=-QEXP-QHEATR+QCNDRI+QCNDCL+QCNDD+QCNDCN+QSHTL-WRKLT/2.
      QIND=-QEXP-QHEATR
      QOUT=QCOOLR+QCONP+QCNDRO+QCNDCL+QCNDD+QCNDCN+QSHTL
      WRKTOT=WRKEXP+WRACMP
      WRKLT=WRALER+WRALCM
      WRKBAS=WRKTOT+WRKLT
      EFFTOT=WRKTOT/QIN
      EFFP=WRKP/QIN
      QEFF1=ENFRTN/ENFNTR
      QEFF2=ENFCTR/ENFRTC
      PWRMP=WRKN/(550.*DELTIM)
```

```
      PWRKW=PWRHP*.7457
      FREQ=1./DELTIN
      EN3PH=STROKV*FREQ*6J.
C STORE VARIABLES FOR CALCULATION OF AVERAGES OVER 5 CYCLES.
      STORE(K,1)=QIN
      STORE(K,2)=QOUT
      STORE(K,3)=WRKEXP
      STORE(K,4)=WRKCMP
      STORE(K,5)=WRKTOT
      STORE(K,6)=EFFTOT
      STORE(K,7)=REFF1
      STORE(K,8)=REFF2
      STORE(K,9)=QREGEN
      STORE(K,10)=PWRHP
      STORE(K,11)=FREQ
      STORE(K,12)=WRKLT
      STORE(K,13)=ENTH
      STORE(K,14)=UTOTAL
      STORE(K,15)=EN3PH
      STORE(K,16)=AVGWSP
      STORE(K,17)=WDISP
      STORE(K,18)=WPIST
      STORE(K,19)=WTPIST
      STORE(K,20)=WRKLP
      STORE(K,21)=QEXPN
      STORE(K,22)=QEXPP
      STORE(K,23)=QHEATN
      STORE(K,24)=QHEATP
      STORE(K,25)=QCOOLN
      STORE(K,26)=QCOOLP
      STORE(K,27)=QCOMPN
      STORE(K,28)=QCOMPP
      STORE(K,29)=QREGN
      STORE(K,30)=QREGP
      STORE(K,31)=WDISPP
      STORE(K,32)=WDISPN
      STORE(K,33)=WPISTP
      STORE(K,34)=WPISTN
      STORE(K,35)=QCNDRI
      STORE(K,36)=QCNDRO
      STORE(K,37)=QCNDCL
      STORE(K,38)=QCNDD
      STORE(K,39)=QCNDCN
      STORE(K,40)=TGEXPA
      STORE(K,41)=TGCMPA
      STORE(K,42)=QSHTL
      STORE(K,43)=QINB
      STORE(K,44)=WRKBAS
      DO 93 L=1,13
      IF(I.EQ.13)  GO TO 91
      M=L+48
      STORE(K,M)=TGCYC(L)
   91 M=L+60
      STORE(K,M)=TGACYC(L)
      M=L+73
   90 STORE(K,M)=TMCYC(L)
  100 CONTINUE
      IF (JIP.GT.0.AND.JIP1.NE.NOCYC) GO TO 301
      IF (JIP.GT.0) WRITE (6,202)
  202 FORMAT (' LAST CYCLE')
      WRITE (6,200) QIN,QOUT,WRKEXP,WRKCMP,WRKTOT,EFFTOT,REFF1,REFF2,
     *QREGEN,PWRHP,FREQ,WRKLT,     ENTH,UTOTAL,
     *EN3PH,AVGWSP,        WDISP,WPIST,WTPIST,WRKLP,
     *QEXPN,QEXPP,QHEATN,QHEATP,QCOOLN,QCOOLP,QCOMPN,QCOMPP,
     *QREGN,QREGP,WDISPP,WDISPN,WPISTP,WPISTN,QCNDRI,QCNDRO,
     *QCNDCL,QCNDD,QCNDCN,TGEXPA,TGCMPA,QSHTL,QINB,WRKBAS
```

```
 200 FORMAT (/' QIN=',F8.3,1X,'QOUT=',F8.3,1X,'WRKEXP=',F8.3,1X,
    1'WRKCMP=',F8.3,1X,'WRKTOT=',F8.3,1X,
    2'EFFTOT=',F8.3,1X,'REFF1=',F8.3,1X,'REFF2=',F8.3,1X/
    3' QREGEN=',F8.3,' PWRNP=',F8.3,' FREQ=',F8.3,
    4' WRKLT=',F8.3,                ' ENTN=',F8.3,' WTOTAL=',
    $F13.3/' ENJPN=',F10.3,' AVGWSP=',F9.3,
    6' WDISP=',F8.3,' WPIST=',F8.3,' WTPIST=',F8.3,' WRKLP=',F8.3/,
    7' QEXPN=',F8.3,' QEXPP=',F8.3,' QHEATN=',F8.3,' QHEATP=',F8.3,
    8' QCOOLN=',F8.3,' QCOOLP=',F8.3,' QCOMPN=',F8.3,' QCOMPP=',F8.3/,
    9' QREGN=',F9.3,' QREGP=',F8.3,' WDISPP=',F8.3,' WDISPN=',F8.3,
    1' WPISTP=',F8.3,' WPISTN=',F8.3,' QCNDRI=',F7.3,' QCNDRO=',F7.3,/
    2' QCNDCL=',F8.3,' QCNDD=',F8.3,' QCNDCN=',F8.3,' TGEXPA=',F8.3,
    3' TGCMPA=',F8.3,' QSHTL=',F8.3/,' QINB =',F8.3,' WRKBAS =',F8.3)
 301 CONTINUE
     DO 300 I=1,66
 300 VAR(I)=0.0
     IF(J.EQ.5) GO TO 400
     RETURN
 400 K=0
     J=0
     DO 450 KK=1,86
     STORE(11,KK)=STORE(1,KK)/5.
     DO 450 IK=2,5
 450 STORE(11,KK)=STORE(11,KK)+STORE(IK,KK)/5.
 575 CONTINUE
     IF (JIP.GT.0.AND.JIP1.NE.NOCYC) GO TO 601
     WRITE (6,600)
     WRITE (6,200) (STORE(11,KK),KK=1,66)
     IF (JIP.GT.0) WRITE (6,2300)
 200 FORMAT (' AVERAGE TEMPERATURES OVER LAST CYCLE')
     WRITE(6,201)  TGCYC,TGACYC,TNCYC
 201 FORMAT ('  TGCYC=',4X,12F8.0/,' TGACYC=',13F8.0/,'  TNCYC=',13F8.0
    X/)
 600 FORMAT (1HO,'AVERAGE VALUES OF LAST 5 CYCLES')
 601 RETURN
     END
```

Subroutine CNDCT

```
      SUBROUTINE CNDCT (TNA,QCREG ,QCYL,QCONDD,QCAN,QSHTTL,RWGAS)
      DIMENSION TNA(13),                                  TCYL(3),TCAN(3),
     1          ACAN(2),          DCAN(2)
      COMMON /CYC/ QEXP,QHEATR,QREGEN,QCOOLR,QCOMP,ENFRTN,ENFNTR,
     1ENFCTR,ENFRTC,WRKP,WRKEXP,
     2WRKCMP,WRKLEX,WRKLCM,WRKLP,WRKN,SUMNUM(13),SUMDEN(13),ENTN,
     3WDISP,WPIST,WTPIST,QEXPN,QEXPP,QHEATN,QHEATP,
     4QCOOLN,QCOOLP,QCOMPN,QCOMPP,QREGN,QREGP,WDISPP,WDISPN,WPISTP,
     5WPISTN,QCNDRI,QCNDRO,QCNDCL,QCNDD,QCNDCN, QSHTL,TGEXPA,TGCMPA
      DATA TRD,TR1,TR2,TCYL/1760.,1172.,585.,1760.,1255.,975./,
     1     R12,R2,R3,R4,RL3,RL4/1.38,1.62,1.56,1.53,1.126,0.400/,
     1     R11,R0,R1,RL1,RL2,/0.454,0.521,0.495,0.400,0.470/,
     1       ACONDD,QCONDD/0.5879,1.718/,
     1       TCAN/1400.,1203.,1100./,
     1       ACAN,DCAN/1.154,1.196,0.5,0.75/,
     1       CLEAR,DISPD,STRONE/.010,2.75,1.23/
C ACONDR,ACYL,ACONDD,ACAN---AREA S IN IN2
C DCONDR,DCYL,DCONDD,DCAN---DISTANCE IN IN
```

```
C TCYL,TCAN--- TEMPERATURES IN DEGREES R
C CLEAR--CLEARANCE BETWEEN DISPLACER AND CYLINDER, IN.
C DISPD---DISPLACER DIAMETER, IN
C STROKE---DISPLACER STROKE, IN.

C CALCULATE HEAT CONDUCTED THROUGH CYLINDER,BTU/SEC
      TCAV61=(TCYL(1)+TCYL(2))/2.
      TCAV62=(TCYL(2)+TCYL(3))/2.
      THCND1=(.00387*TCAV61+6.793)/(3600.*12.)
      IF (TCAV61.GT.1060.) THCND1=(.00467*TCAV61+5.932)/(3600.*12.)
      THCND2=(.00387*TCAV62+6.793)/(3600.*12.)
      IF (TCAV62.GT.1060.) THCND2=(.00467*TCAV62+5.932)/(3600.*12.)
      QCYL1=6.283*THCND1*R12*(R3-R2)*(TCYL(1)-TCYL(2))/(XL3*ALOG((R3-
     1R12)*(R2+R12))/((R3+R12)*(R2-R12)))
      QCYL2=6.283*THCND2*R12*(R4-R3)*(TCYL(2)-TCYL(3))/(XL4*ALOG((R4-
     1R12)*(R3+R12))/((R4+R12)*(R3-R12)))
      QCYL=(QCYL1+QCYL2)/2.
C CALCULATE HEAT CONDUCTED THROUGH DISPLACER,BTU/SEC
      TBAV6=(TBEXPA+TBCMPA)/2.
      THCOND=(.00387*TBAV6+6.793)/(3600.*12.)
      IF (TBAV6.GT.1060.) THCOND=(.00467*TBAV6+5.932)/(3600.*12.)
      QCONDD=ACONDD*THCOND*(TBEXPA-TBCMPA)/DCONDD
C CALCULATE HEAT CONDUCTED THROUGH EXTERNAL CAN,BTU/SEC
      QCAN=0.0
      DO 300 I=1,2
      TCAV6=(TCAN(I)+TCAN(I+1))/2.
      THCOND=(.00387*TCAV6+6.793)/(3600.*12.)
      IF (TCAV6.GT.1060.) THCOND=(.00467*TCAV6+5.932)/(3600.*12.)
  300 QCAN=QCAN+ACAN(I)*THCOND*(TCAN(I)-TCAN(I+1))/(DCAN(I)*2.)
C CALCULATE HEAT CONDUCTION THROUGH REGENERATOR,BTU/SEC
      TRAV61=(TRO+TR1)/2.
      TRAV62=(TR1+TR2)/2.
      THCND1=(.00387*TRAV61+6.793)/(3600.*12.)
      IF (TRAV61.GT.1060.) THCND1=(.00467*TRAV61+5.932)/(3600.*12.)
      THCND2=(.00387*TRAV62+6.793)/(3600.*12.)
      IF (TRAV62.GT.1060.) THCND2=(.00467*TRAV62+5.932)/(3600.*12.)
      QCRIN=3.142*(RO**2-R11**2)*THCND1 *(TRO-TR1)/XL1
      QCROUT=6.283*THCND2*R11*(R1-RO)*(TRO-TR1)/(XL2*ALOG((R1-R11)*
     1(RO+R11))/((R1+R11)*(RO-R11))))
      QCRES=(QCRIN+QCROUT)/2.*8.
C CALCULATE SHUTTLE HEAT TRANSFER, BTU/SEC
      THCND6=2.481E-09*(TCYL(1)+TCYL(3))/2.*1...: -06
      IF (NW6AS.EQ.4) THCND6=1.962E-09*( TCYL(1)+TCYL(3))/2.*1.115E-6
      QSHTTL=THCND6*3.1416*DISPD*STROKE**2*(TCYL(1)-TCYL(3))/(8.0*CLEAR*
     1(XL3+XL4          ))
      RETURN
      END
```

Subroutine XDELP

```
      SUBROUTINE  XDELP(K,AREAIN,AREAOT,DHX,XLGTH,ROX,VISX,FLOWIN,PRIN,
     XCOEF,DP,N)
C     IDENTIFICATION OF TYPE OF LOSSES
C     KTYPE=1 CONTRACTION--KTYPE=2 EXPANSION--KTYPE=3 90-TURN --KTYPE=4 1
C     KTYPE=5 OTHER TURN --KTYPE=6 FRICTION-TUBE--KTYPE=7 FRICTION-REGENE
C     KTYPE=8 FRICTION+MOMENTUM FOR TUBE--ISOTHERMAL
C     KTYPE=9 FRICTION+MOMENTUM FOR REGENERATOR--ISOTHERMAL
```

```
      DIMENSION  COEFX(40),DPX(40)
      DATA  GRAV/32.2/,  PSI/0.006945/
      GAMMA=DP
      IF (ABS(FLOWIN).LE.0.0)  RETURN
      PR=0.
      POUT=0.
      DPNORM=0.
      KTYPE=K
      AIN=AREAIN/144.
      AOUT=AREAOT/144.
      DE=DWR/12.
      XLG=XLGTH/12.
      RO=ROX*144.*12.
      VISC=VISX*12.
      FLOW=ABS(FLOWIN)/8.3
      PIN=PXIN
      ROMEAN=RO
      IF(AIN-AOUT)  30,30,31
   30 AMIN=AIN
      A=AIN/AOUT
      GO TO 32
   31 AMIN=AOUT
      A=AOUT/AIN
   32 CONTINUE
      IF(A.LT.0.001)  A=0.0
      VEL=FLOW/AMIN/RO
      VELHD=RO*VEL**2/(2.0*GRAV)
      RE=RO*VEL*DE/VISC
      GO TO (1,2,3,4,5,6,7,6,7),KTYPE
C
    1 CONTINUE
C     KTYPE=1 CONTRACTION
      IF(RE-3000.0)  12,12,11
   11 COEF=-0.44*A+0.5
      GO TO 100
   12 COEF=-0.44*A+1.0
      GO TO 100
C
    2 CONTINUE
C     KTYPE=2 EXPANSION
      IF(RE-3000.0)  21,21,22
   21 COEF=(1.0-2.6*A+1.0)5*A**2)*(-1.0)
      GO TO 100
   22 COEF=(1.0-2.0928*A+0.996*A**2)*(-1.0)
      GO TO 100
C
    3 CONTINUE
      COEF=0.22
      GO TO 102
C
    4 CONTINUE
      COEF=3.0*0.22
      GO TO 102
C
    5 CONTINUE
      COEF=0.11
      GO TO 102
C
    6 CONTINUE
C     KTYPE=6 FRICTION-TUBE
      IF(RE.LT.1500.)  COEF=16.0/RE*(XLG/(DE/4.0))
      IF(RE.GE.1500.)  COEF=0.046/RE**0.2*(XLG/(DE/4.0))
      GO TO 102
C
    7 CONTINUE
C     KTYPE=7 FRICTION-REGENERATOR
```

```
      COEF=0.96*EXP(-0.0190*RE)+0.54
      COEF=COEF*(RLG/(DE/4.0))
      GO TO 102
  100 COEF=1.0-A**2*COEF
  102 DP=COEF*VELHD*PSI
      IF(                KTYPE.LT.8)  GO TO 101
C     (KTYPE=8 FRICTION+MOMENTUM --TUBE          KTYPE=9 SAME FOR REGENERATO
C     KTYPE=10 --TUBE      NON.+FRIC.       KTYPE=11--FOR REGENRATOR      ADI
      IF(KTYPE.GE.10)  GAMMA1=GAMMA
      XMA1=VEL/SQRT(GAMMA*PIN*144.0/RO*GRAV)
      XMA2=1.0/SQRT(1.0/XMA1**2-GAMMA*COEF)
      FMA21=1.0
      IF(ABS((XMA2-XMA1)/XMA1).LE.0.001)  GO TO 52
   51 XMAO=(XMA1+XMA2)*0.5
      FMA21=((GAMMA-1.0)*XMA)**2+2.0)/((GAMMA-1.0)*XMA1**2+2.0)
      IF(KTYPE.LT.10)  FMA21=1.0
      IF(KTYPE.LT.10)  GAMMA1=1.0
      XMA2=1.0/SQRT(1.0/XMA1**2-GAMMA*COEF*GAMMA*((GAMMA1+1.0)/2.0/GAMMA1
     1*ALOG((XMA1/XMAO)**2*FMA21))
      IF(ABS(XMA2-XMAO).GT.0.001)  GO TO 51
   52 TR=1.0/FMA21
      VR=XMA2/XMA1*SQRT(1.0/FMA21)
      PR=XMA1/XMA2*SQRT(1.0/FMA21)
      POUT=PR*PIN
      DP=PIN-POUT
  101 CONTINUE
      IF(FLOWIN.LE.0.0) DP=(-1.)*DP
      COEFR(N)=COEF
      DPR(N)=DP
      RETURN
      END
```

Printed Output of Sample Run

```
$STRLNG
P       =      .85003000E+03
REALGS  =      .13333303E+31
FIXCYC  =      .10000000E+34
IPRINT  =                +530
ITMPS   =                  +3
COEFF   =      .10003000E-03
T3      =      .70003000E+03
P3      =      .87333003E+33
OMEGA   =      .50003000E+02
FACT1   =      .40003000E+00
FACT2   =      .13333303E+32
NOCYC   =                 +58
NSTOT   =                  +5
NOEND   =                 +23
NUBAS   =                  +6
T6      =      ..86033000E+04,   .18600000E+04,   .18633033E+04,   .18600000E+04,
               .16583303E+34,   .14900303E+34,   .13343333E+34,   .10743333E+04,
               .77503003E+03,   .54000000E+03,   .54000000E+03,   .54000000E+03
T6A     =      .19003000E+04,   .18600000E+04,   .18600033E+04,   .18600000E+04,
               .16503003E+34,   .14943333E+34,   .13343333E+34,   .13743333E+04,
               .77503000E+03,   .54000000E+03,   .54033033E+03,   .54000000E+03,
               .54033003E+33
TH      =      .17603003E+04,   .19300000E+04,   .19333033E+04,   .16250000E+04,
               .16503303E+34,   .14943333E+34,   .13343333E+34,   .13743333E+04,
               .77503003E+03,   .54000000E+03,   .54000033E+03,   .54000000E+03,
               .54003000E+03
RHCFAC  =      .10003000E+31
JIP     =                 +1

$END
LAST CYCLE

QIN= 330.056 QOUT= 179.851 WRKEXP= 305.677 WRKCMP=-161.296 WRKTOT= 144.181 EFFTOT=    .436 REFF1=    .997 REFF2=    .994
QREGEN=    .137 PWRMP=  13.197 FREQ=  50.333 WRKLT=  17.515 ENTN=  -1.433 QTOTAL=  1780.693
ENSPN=  3586.449 AVEWSP=  787.240 WDISP= -10.219 WPIST= 154.400 WTPIST= 154.400 WRKLP=   6.443
QEXPN= -53.328 QEXPP=  92.978 QHEATN=-339.904 QHEATP=  30.687 QCOOLN=    .000 QCOOLP= 157.259 QCOMPN=   -.052 QCOMPP=   2.306
QREGN= -931.252 QREGP= 831.390 WDISPP=   8.710 WDISPN= -18.929 WPISTP= 551.515 WPISTN=-397.116 QCNDRI=  8.483 QCNDRO=  8.483
QCNOCL=   9.157 QCNOD=   1.535 QCNOCN=   1.201 T6EXPA=1720.129 T6CMPA= 636.009 QSHTL=   9.962
QINB = 319.267 WRKBAS = 161.696

AVERAGE VALUES OF LAST 5 CYCLES

QIN= 329.957 QOUT= 179.292 WRKEXP= 330.640 WRKCMP=-160.029 WRKTOT= 143.819 EFFTOT=    .436 REFF1=    .997 REFF2=    .995
QREGEN=    .143 PWRMP=  13.079 FREQ=  50.000 WRKLT=  17.481 ENTN=  -1.569 QTOTAL=  1775.684
ENSPN=  3586.449 AVEWSP=  787.987 WDISP= -10.203 WPIST= 154.022 WTPIST= 154.022 WRKLP=   6.427
QEXPN= -52.895 QEXPP=  92.921 QHEATN=-339.368 QHEATP=  30.693 QCOOLN=    .000 QCOOLP= 156.709 QCOMPN=   -.053 QCOMPP=   2.298
QREGN= -829.403 QREGP= 829.543 WDISPP=   8.685 WDISPN= -18.888 WPISTP= 549.970 WPISTN=-395.909 QCNDRI=  8.483 QCNDRO=  8.483
QCNOCL=   9.157 QCNOD=   1.535 QCNOCN=   1.231 T6EXPA=1720.276 T6CMPA= 635.850 QSHTL=   9.962
QINB = 318.353 WRKBAS = 161.390
AVERAGE TEMPERATURES OVER LAST CYCLE
 T6CYC=       1706.   1714.   1655.   1588.   1397.   1209.   1022.    877.    651.    639.    638.    644.
T6ACYC=   1724.   1760.   1743.   1625.   1492.   1332.   1115.    929.    745.    633.    629.    632.    636.
 THCYC=   1760.   1930.   1930.   1625.   1492.   1303.   1115.    929.    745.    540.    540.    540.    540.
```

DEFINITIONS OF NAMELIST INPUT VARIABLES[1]

COEFF	leakage coefficient for flow between buffer and compression spaces
FACT1, FACT2	convergence constants used in regenerator metal temperature convergence scheme
FIPCYC	number of iterations per cycle
IPRINT	number of iterations between printouts (if JIP=0)
ITMPS	1, printout gas and metal control volume temperature at every iteration 0, do not do the above
JIP	>0, short-form printout =0, long-form printout
MWGAS	4, use helium working gas ≠4, use hydrogen working gas
NOCYC	number of engine cycles to be run
NOEND	number of cycle at which convergence scheme is turned off
NSTRT	number of cycle at which regenerator metal temperature convergence scheme is turned on
OMEGA	drive speed, Hz
P	initial pressure, lbf/in.^{2} (N/m^2) (approximately equal to mean pressure for GPU)
P3	initial buffer space pressure, lbf/in. (N/m^2)
REALGS	1, use real-gas equation of state 0, use ideal-gas equation of state

[1]Although both U.S. customary and SI units are given here, U.S. customary units are used in the program.

RHCFAC	regenerator heat-transfer coefficient multiplication factor
TG	12 control volume interface gas temperatures, ^{o}R (K)
TGA	13 control volume gas temperatures, ^{o}R (K)
TM	13 metal boundary temperatures, ^{o}R (K)
T3	buffer space temperature (assumed constant), ^{o}R (K)

Definitions of Output Variables

AVGWSP	mean working-space pressure, lbf/in.^{2} (N/m^2)
EFFTOT	efficiency, WRKTOT/QIN
ENTH	net enthalpy flow from working space to buffer space over one cycle, ft-lbf (J)
EN3PM	rate of displacement of working-space gas, in.^{3}/min (cm^3/min)
FREQ	rotational frequency of crankshaft, Hz
PWRHP	indicated power - WRKTOT/cycle period, hp (kW)
QCNDCL	heat conduction through cylinder, ft-lbf/cycle (J/cycle)
QCNDCN	heat conduction through insulation container, ft-lbf/cycle (J/cycle)
QCNDD	heat conduction through displacer, ft-lbf/cycle (J/cycle)
QCNDRI	heat conduction through regenerator casing, ft-lbf/cycle (J/cycle)
QCNDRO	heat conduction through regenerator casing, ft-lbf/cycle (J/cycle)
QCOMPN	heat from compression-space wall to gas, ft-lbf/cycle (J/cycle)
QCOMPP	heat from gas to compression-space wall, ft-lbf/cycle (J/cycle)

QCOOLN	heat from cooler to gas, ft-lbf/cycle (J/cycle)
QCOOLP	heat from gas to cooler, ft-lbf/cycle (J/cycle)
QEXPN	heat from metal wall to gas in expansion space, ft-lbf/cycle (J/cycle)
QEXPP	heat from gas to metal wall in expansion space, ft-lbf/cycle (J/cycle)
QHEATN	heat from heater to gas, ft-lbf/cycle (J/cycle)
QHEATP	heat from gas to heater, ft-lbf/cycle (J/cycle)
QIN	heat into gas in expansion space and heater tubes over one cycle, ft-lbf (J)
QOUT	heat out of gas in cooler tubes and compression space over one cycle, ft-lbf (J)
QREGEN	net heat flow from gas to regenerator metal over one cycle, ft-lbf (J)
QREGN	heat from regenerator metal to gas, ft-lbf/cycle (J/cycle)
QREGP	heat from gas to regenerator metal, ft-lbf/cycle (J/cycle)
QSHTL	shuttle heat loss, ft-lbf/cycle (J/cycle)
REFF1	a measure of regenerator effectiveness
REFF2	another measure of regenerator effectiveness
TG	gas temperature at interface of two adjacent control volumes, ^{o}R (K)
TGA	working bulk gas temperature of a control volume, ^{o}R (K)
TGACYC	cycle-time average temperature of TGA, ^{o}R (K)
TGCMPA	as TGACYC in compression space
TGCYC	cycle-time average temperature of TG, ^{o}R (K)
TGEXPA	as TGCYC in expansion space
TM	metal temperature of a metal control volume, ^{o}R (K)

TMCYC	cycle-time average temperature of TM, ^{o}R (K)
UTOTAL	internal energy content of working-space gas, ft-lbf (J)
WLASP	net work done on displacer piston by working-space gas, ft-lbf (J)
WDISPN	work done on gas by displacer, ft-lbf/cycle (J/cycle)
WDISPP	work done on displacer by gas, ft-lbf/cycle (J/cycle)
WPISTP	work done on piston by gas, ft-lbf/cycle (J/cycle)
WPIST	work done on power piston by working-space gas, ft-lbf (J)
WPISTN	work done on gas by piston, ft-lbf/cycle (J/cycle)
WRKCMP	work done by the gas in compression space over one cycle, ft-lbf (J)
WRKEXP	work done by the gas in expansion space over one cycle, ft-lbf (J)
WRKLP	power-piston work lost due to pressure drop from regenerator to compression space, ft-lbf/cycle (J/cycle)
WRKLT	work lost due to pressure drop over one cycle, ft-lbf (J)
WRKTOT	net work done by gas in working space over one cycle, WRKEXP + WRKCMP, ft-lbf (J)

REFERENCES

1. Walker, Graham: Stirling Cycle Machines. Clarendon Press, Oxford, 1973.

2. Martini, W. R.: Stirling Engine Design Manual. (Washington Univ., Wash.; NASA Grant NSG-3152.) NASA CR-135382, 1978.

3. Finegold, Joseph G.; and Vanderbrug, Tom G.: Stirling Engines for Undersea Vehicles. JPL Report 5030-63, Jet Propulsion Lab., 1977.

4. Rios, Pedro Agustin: An Analytical and Experimental Investigation of the Stirling Cycle. D. Sci. Thesis, Mass. Inst. Technol., 1969.

5. Qvale, Einar Bjorn: An Analytical Model of Stirling-Type Engines. Ph. D. Thesis, Mass. Inst. Technol., 1967.

6. Urieli, Israel; Rallis, Costa J.; and Berchowitz, David M.: Computer Simulation of Stirling Cycle Machines. Twelfth Intersociety Energy Conversion Engineering Conference Proceedings, Vol. 2. American Nuclear Society, Inc., La Grange Park, Ill., 1977, pp. 1512-1521.

7. Urieli, Israel: A Computer Simulation of Stirling Cycle Machines. Ph. D. Thesis, Univ. Witwatersrand, Johannesburg, South Africa, 1977.

8. Finkelstein, T.: Computer Analysis of Stirling Engines. Tenth Intersociety Energy Conversion Engineering Conference Proceedings, IEEE, Inc., 1975, pp. 933-941.

9. Shock, A.: Nodal Analysis of Stirling Cycle Devices. To be presented at the 13th Intersociety Energy Conversion Engineering Conference (San Diego, Calif.), Aug. 20-25, 1978.

10. Cairelli, J. E.; Thieme, L. G.; and Walter, [illegible] J.: Initial Test Results with a Single Cylinder Rhombic Drive Stirling Engine. NASA Lewis Research Center. (Work performed for Energy Research and Development Administration under Interagency Agreement EC-77-A-31-1011.)

11. Vargaftix, N. B.: Tables on the Thermophysical Properties of Liquids and Gases. Second ed., John Wiley & Sons, Inc., 1975.

12. Flow of Fluids Through Valves, Fittings and Pipe. Technical Paper No. 409, Crane Co., Chicago, Ill., 1942.

13. Kays, W. M.; and London, A. L.: Compact Heat Exchangers. The National Press, 1955.

14. McAdams, William H.: Heat Transmission. Third ed., McGraw-Hill Book Co., Inc., 1954.

15. Walker, G.; and Vasishta, V.: Heat-Transfer and Flow-Friction Characteristics of Dense-Mesh Wire-Screen Stirling-Cycle Regenerators. Advances in Cryogenic Engineering, Vol. 16, K. D. Timmerhaus, ed., Plenum Press, 1971.

TABLE I. - CHARACTERISTICS OF STIRLING ENGINE

GROUND-POWER-UNIT SIMULATION RUN

Working fluid	Hydrogen
Frequency, Hz	50
Average working-space pressure, N/m^2 (psi)	5.50×10^6 (800)
Heater temperature (average gas temperature for control volume 2, fig. 2), K ($^{\circ}$R)	976 (1760)
Cooler temperature (cooler metal-wall temperature), K ($^{\circ}$R)	300 (540)
Leakage flow coefficient (used in eq. (27))	0.0001

TABLE II. - PERFORMANCE PREDICTIONS FOR STIRLING ENGINE

GROUND-POWER-UNIT SIMULATION RUN

Indicated power, kW (hp)	11.0 (14.8)
Indicated efficiency	0.49
Indicated work per cycle, J (ft-lbf)	220.4 (162.5)
Work loss per cycle, due to pressure drop, J (ft-lbf)	11.7 (8.6)
Conduction heat loss per cycle, J (ft-lbf)	20.9 (15.4)
Shuttle heat loss per cycle, J (ft-lbf)	8.3 (6.1)

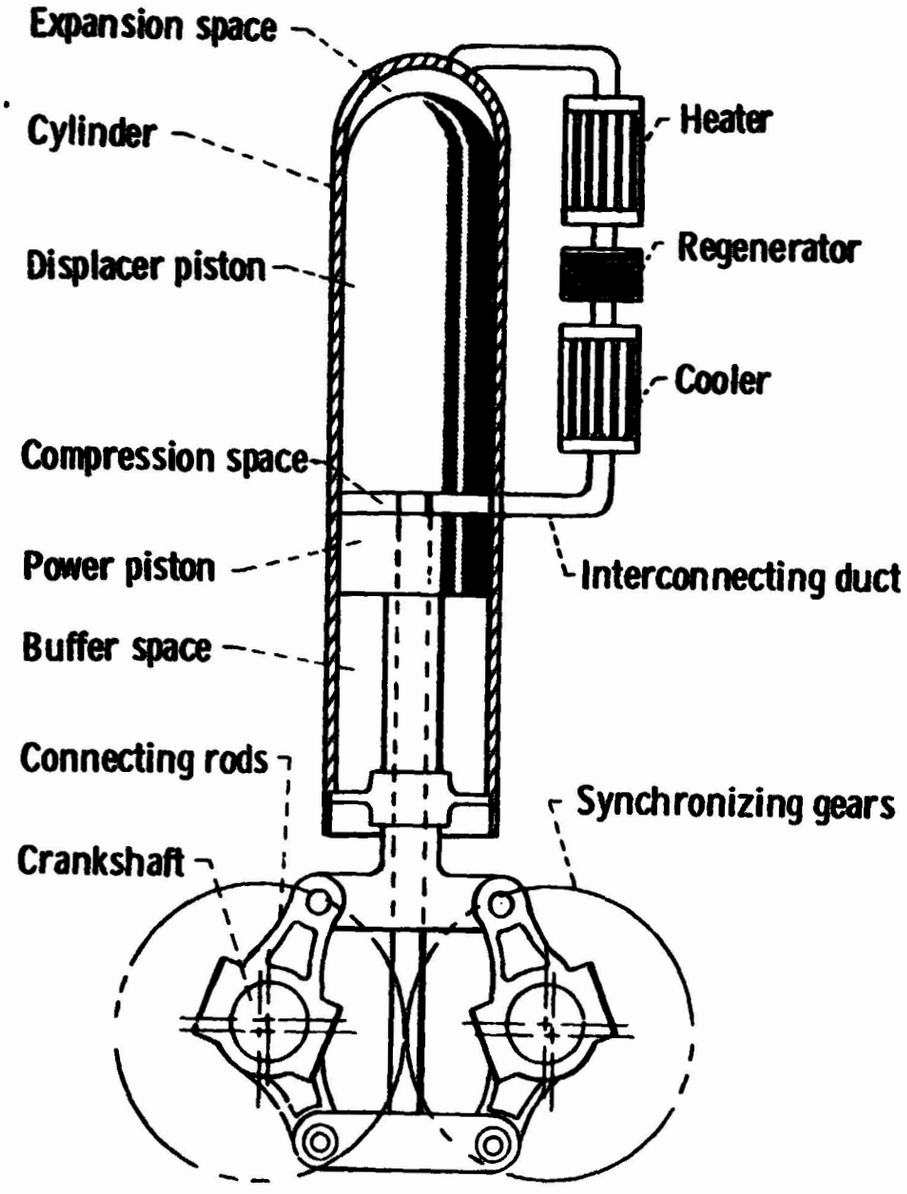

Figure 1. - Schematic of a single-cylinder Stirling engine with rhombic drive.

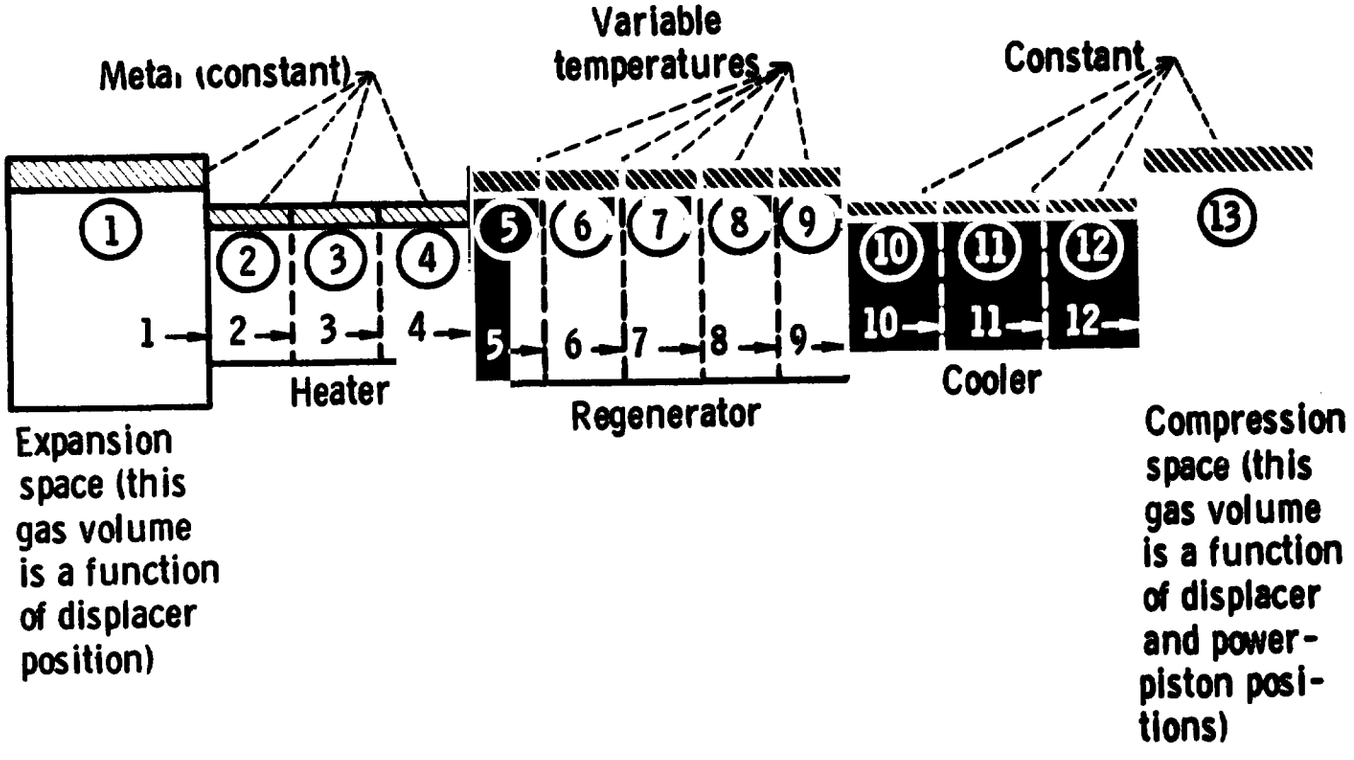

Figure 2. - Heat- and mass-transfer control volumes.

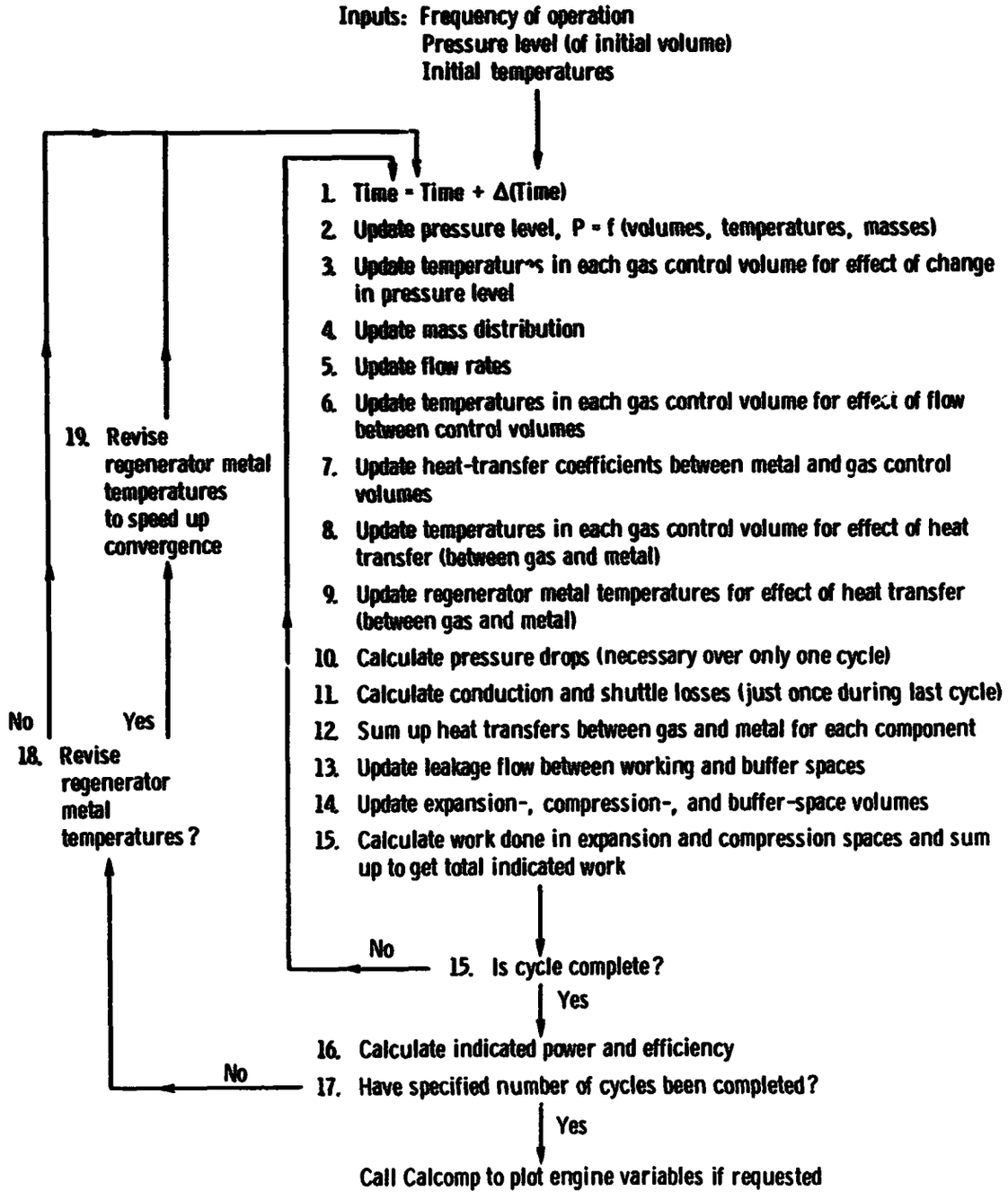

Figure 3. - Outline of calculation procedure.

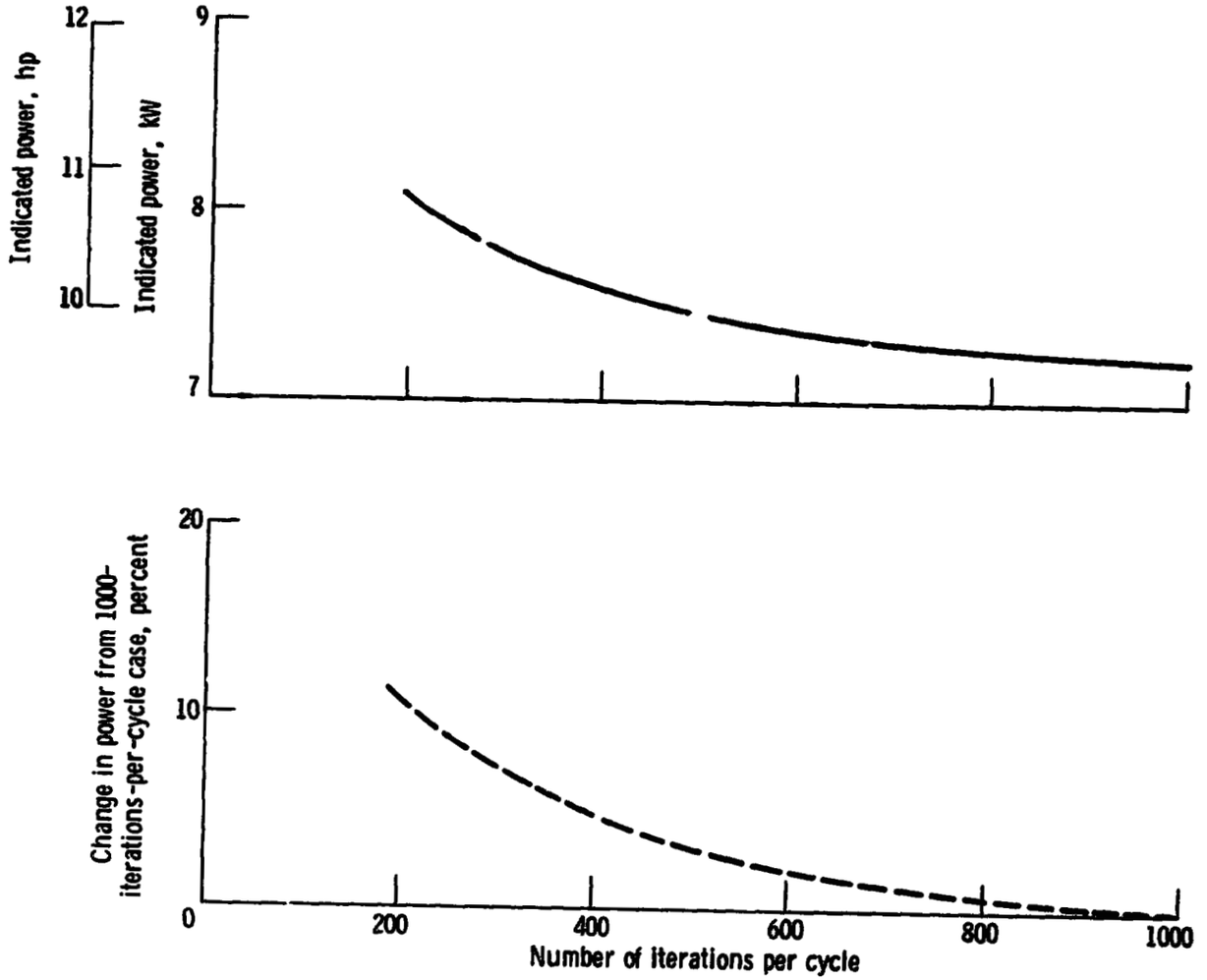

Figure 4. - Indicated power and change in indicated power as function of number of iterations per cycle. Working fluid, helium; frequency, 50 hertz; heater-tube temperature, 978 K (1760 ^{o}R); cooler-tube temperature, 325 K (585 ^{o}R); mean pressure, 4.43x10^{6} N/m^{2} (643 psi).

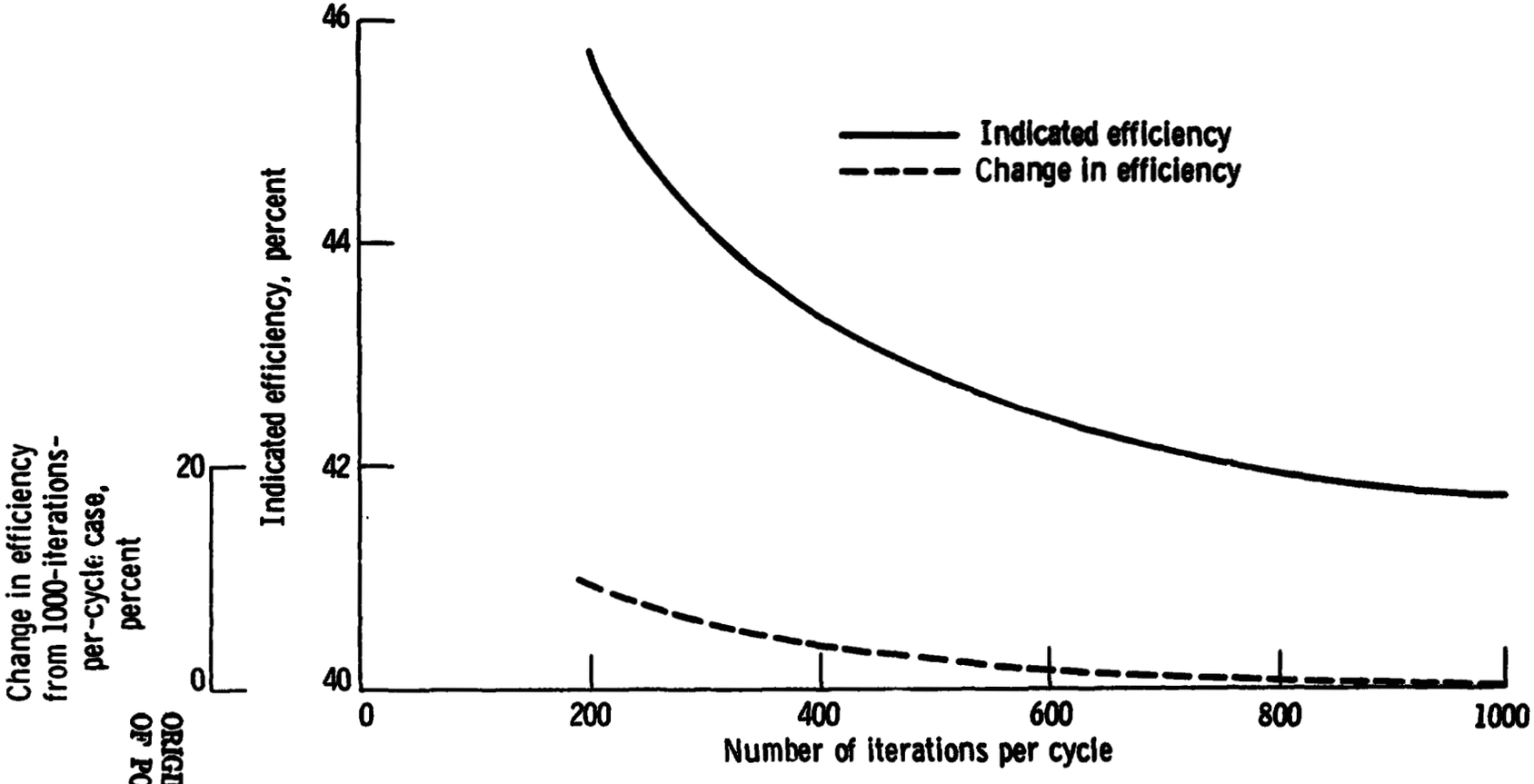

Figure 5. - Indicated efficiency and change in indicated efficiency as a function of number of iterations per cycle.

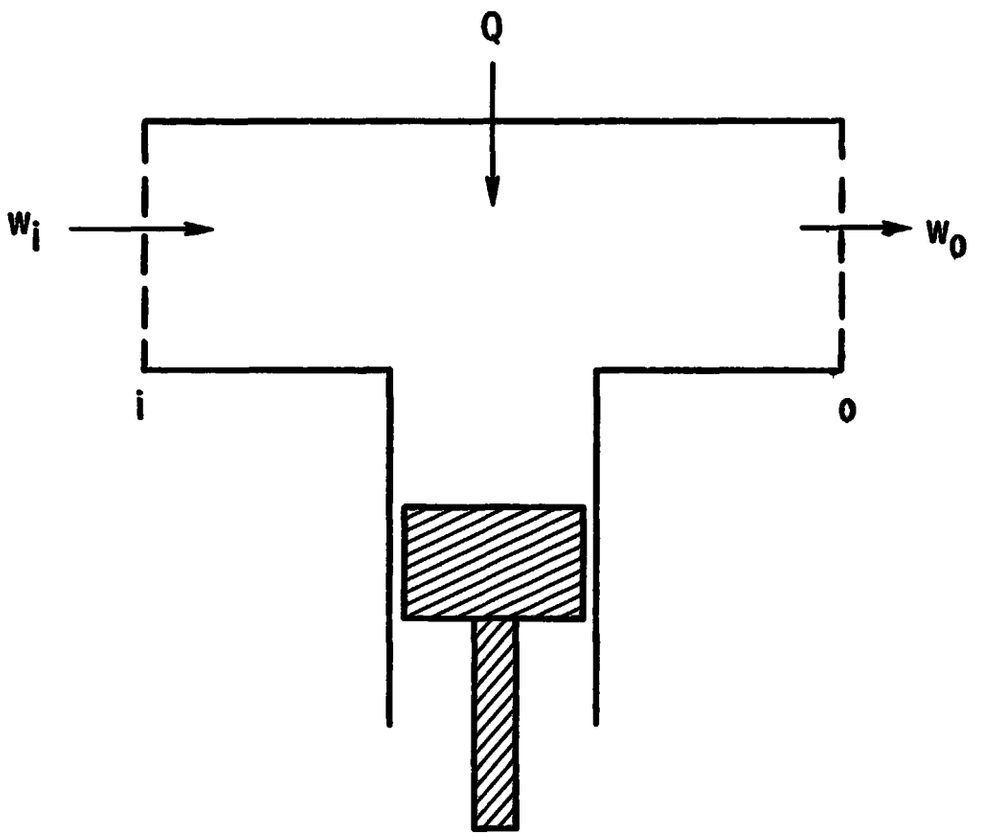

Figure 6. - Generalized control volume.

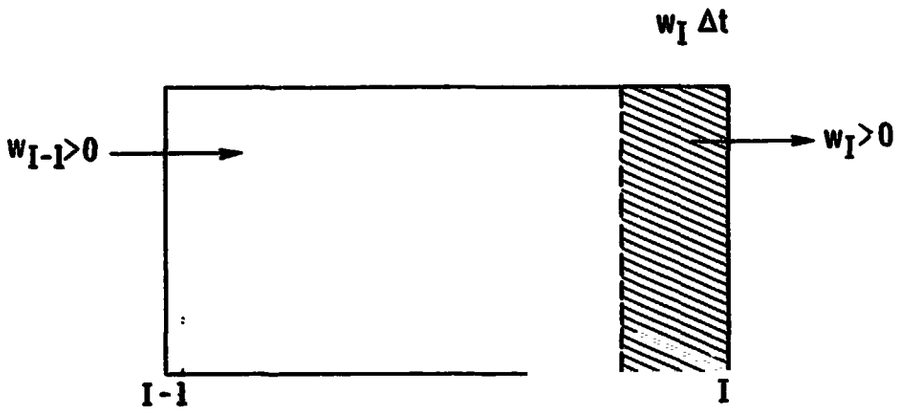

(a) Sample regenerator control volume.

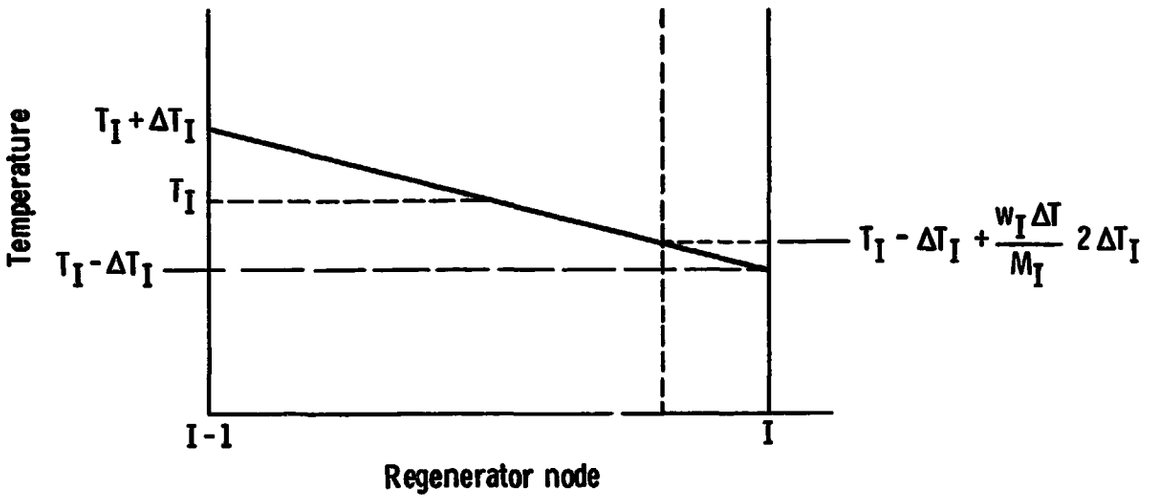

(b) Control-volume temperature profile.

Figure 7. - Sample regenerator control volume and temperature profile.

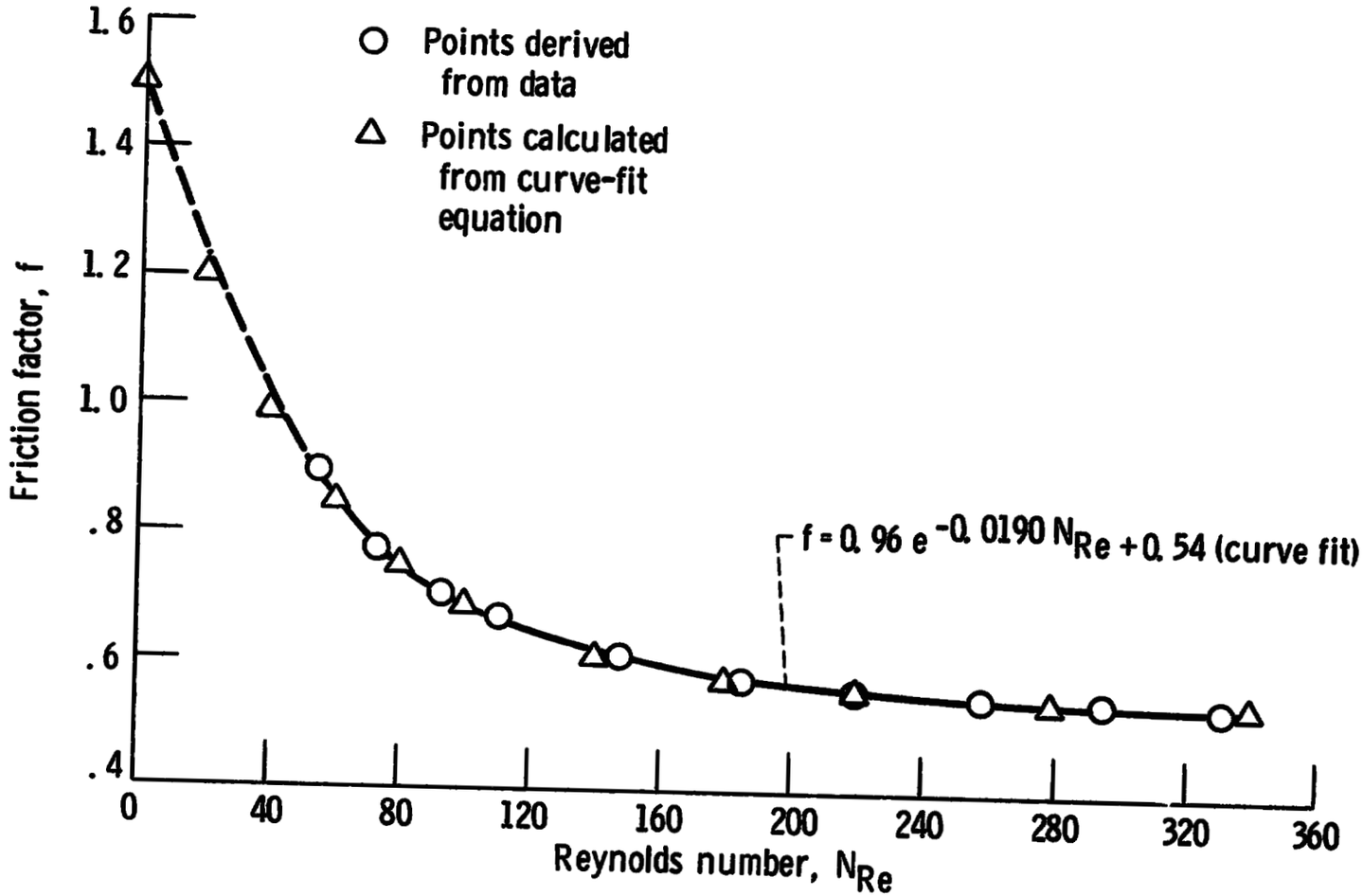

Figure 8. - Regenerator friction factor data and curve fit.

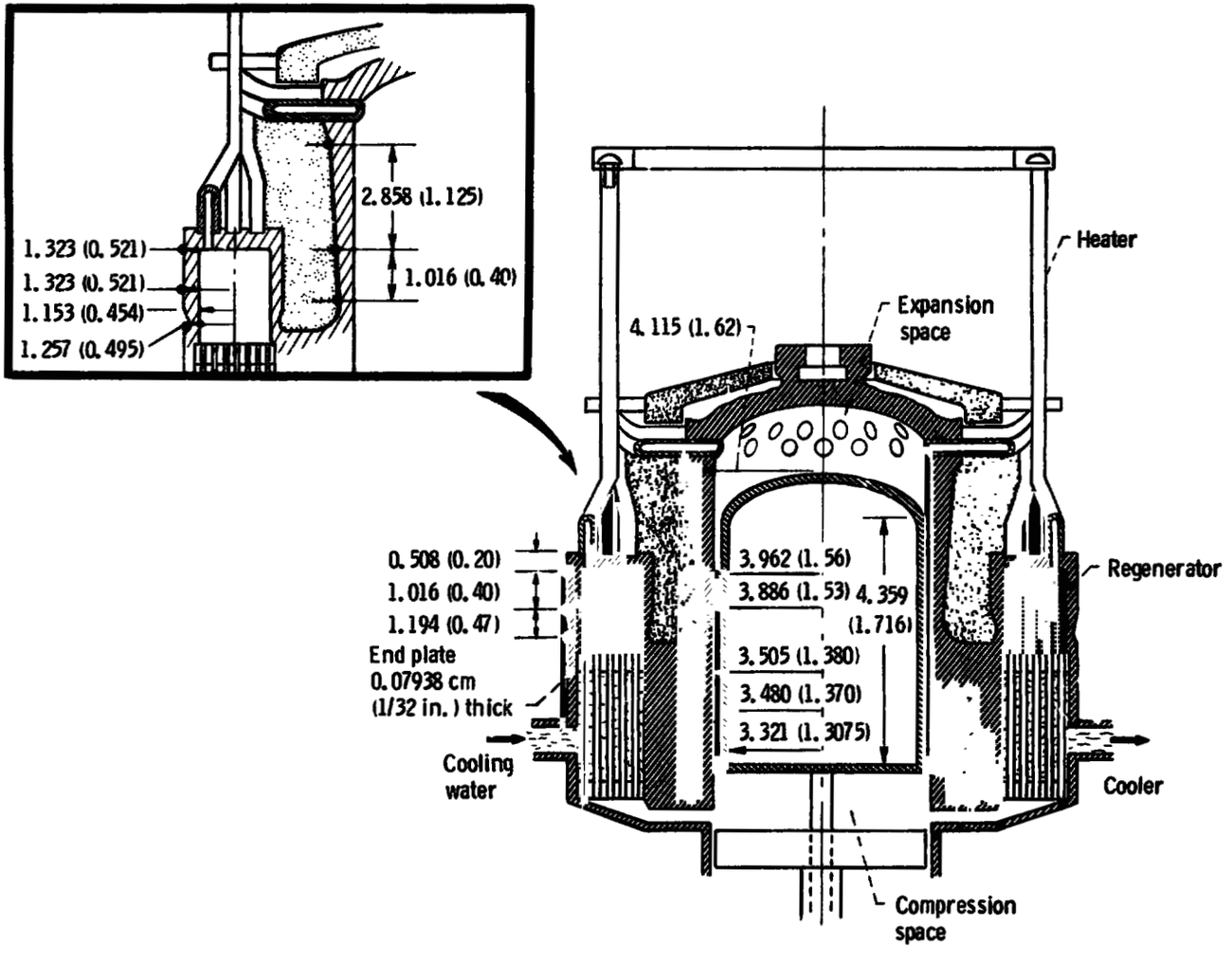

Figure 9. - Schematic showing dimensions needed for calculating heat conduction. (Regenerator, housing, cylinder, and displacer are 310 stainless steel. Dimensions are in cm (in.).)

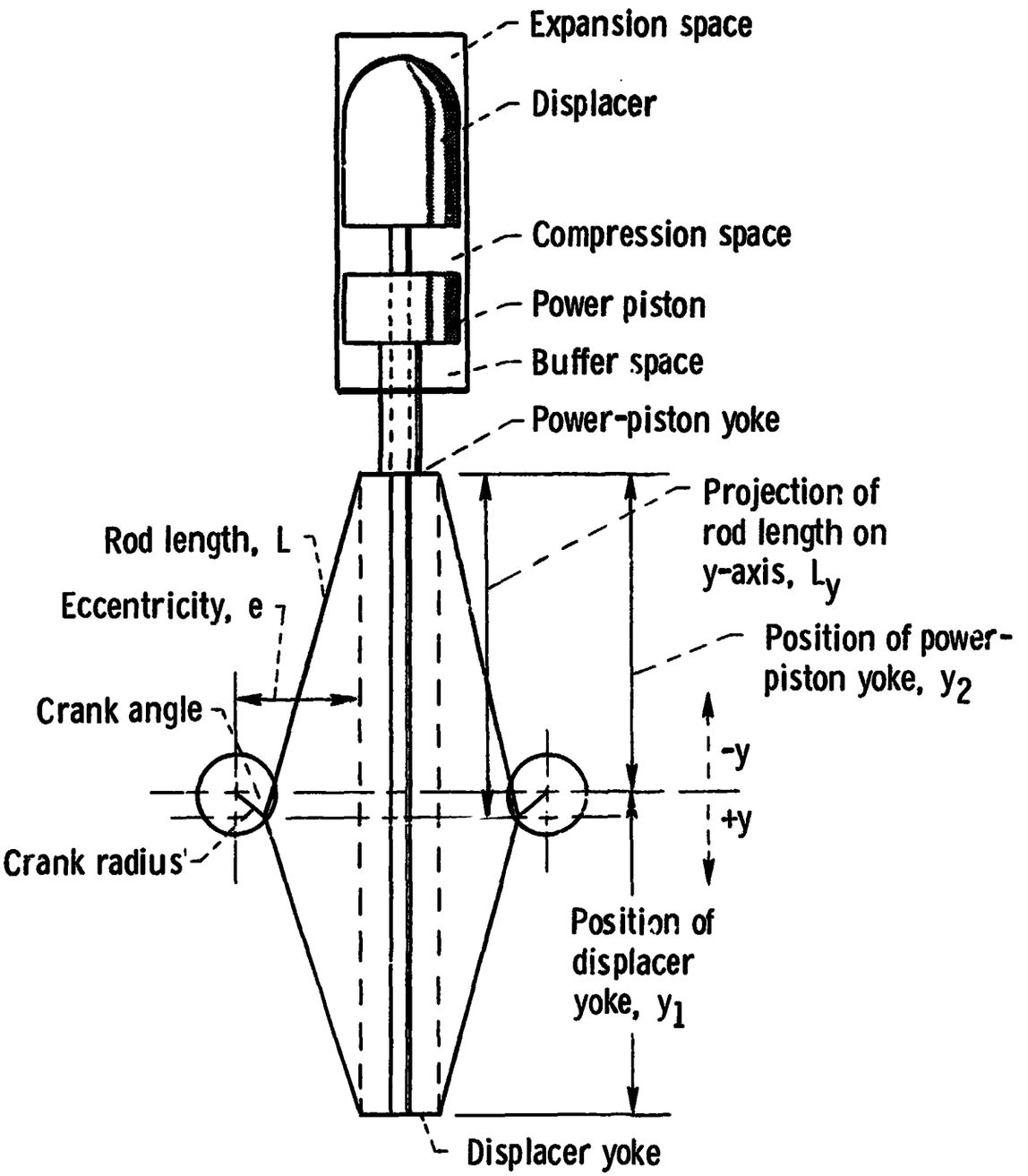

Figure 10. - Schematic showing geometric relations between piston positions and crankshaft angle.

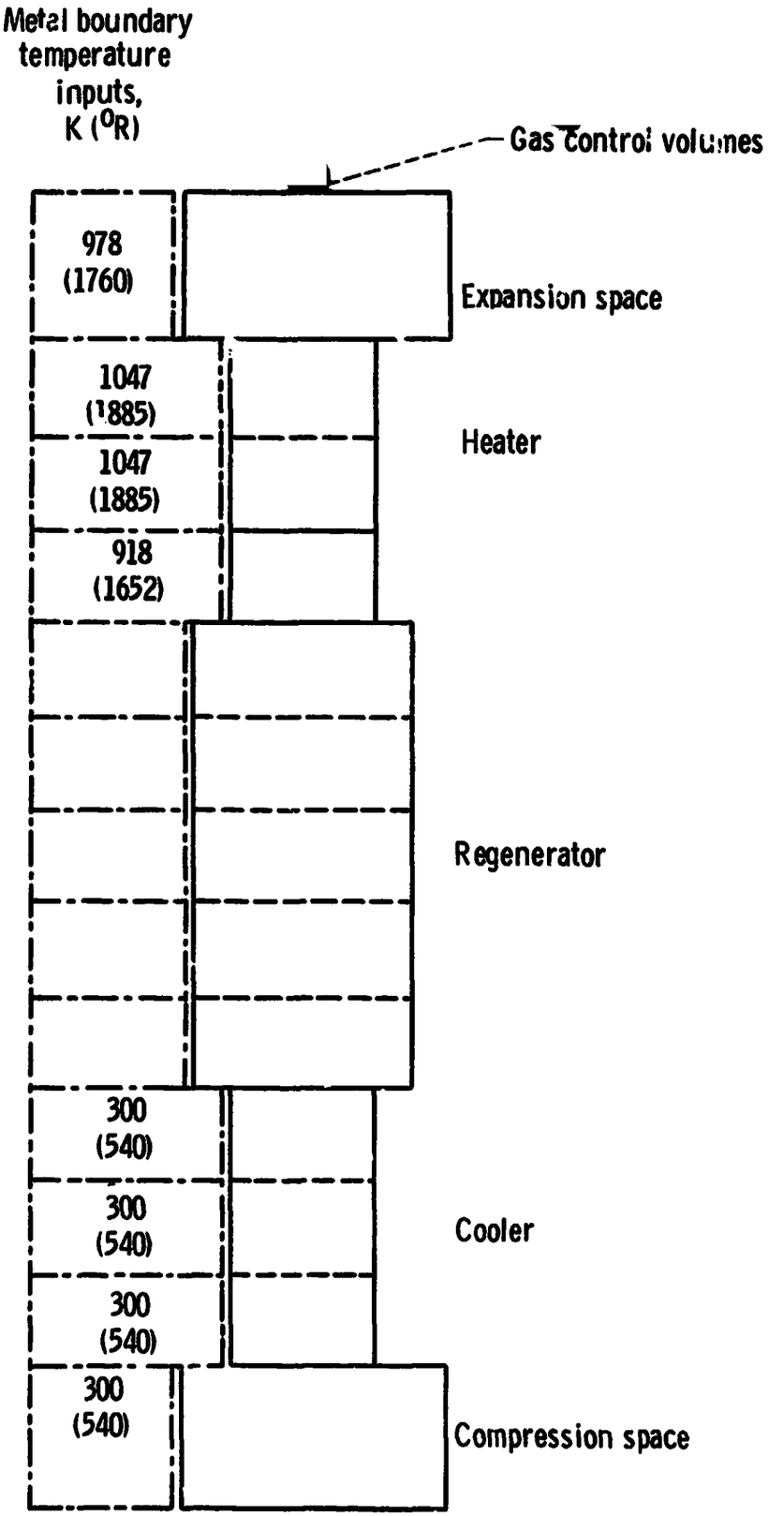

Figure 11. - Assumed metal boundary temperatures for sample run.

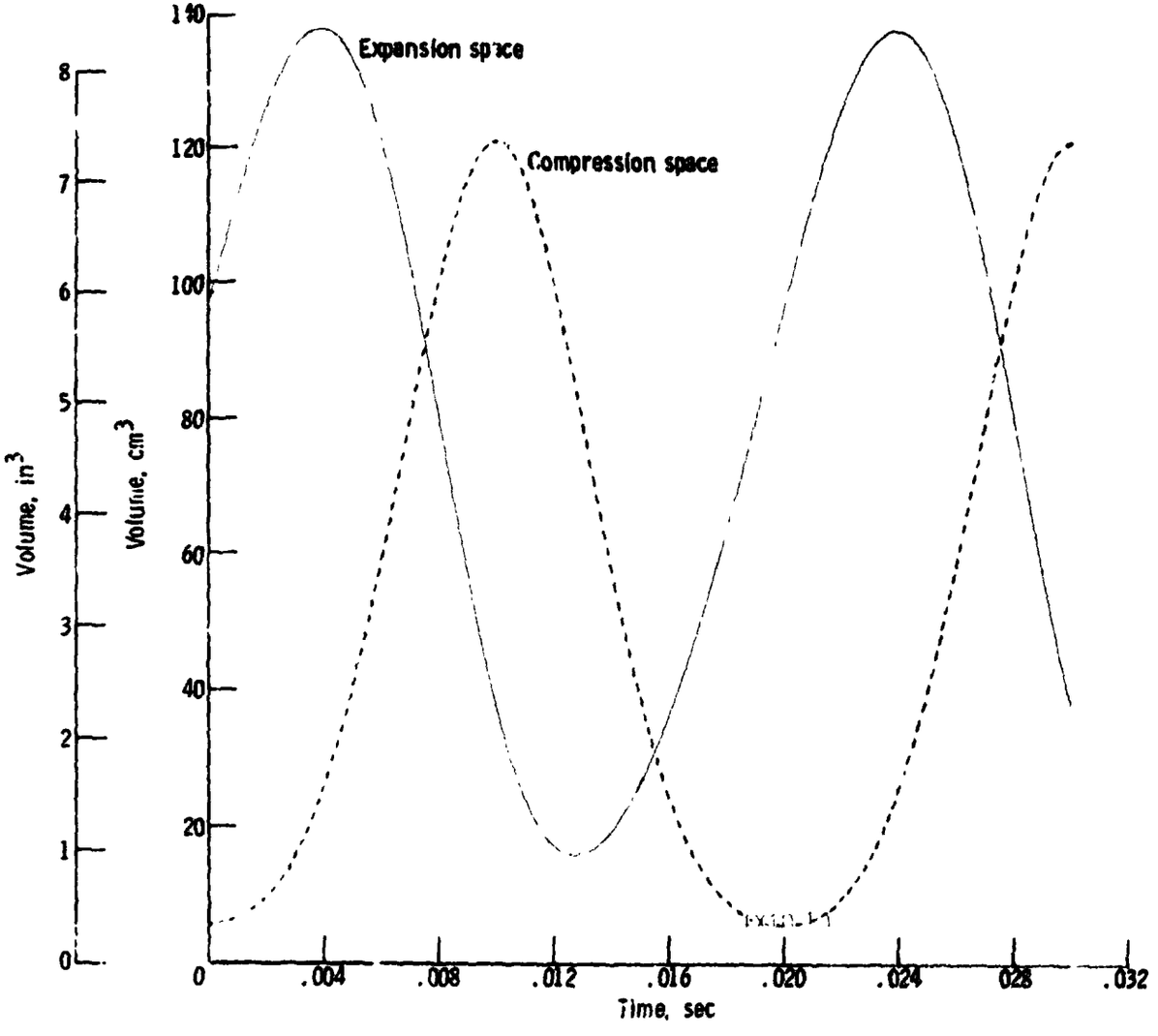

Figure 12. - Expansion- and compression-space volumes as functions of time.

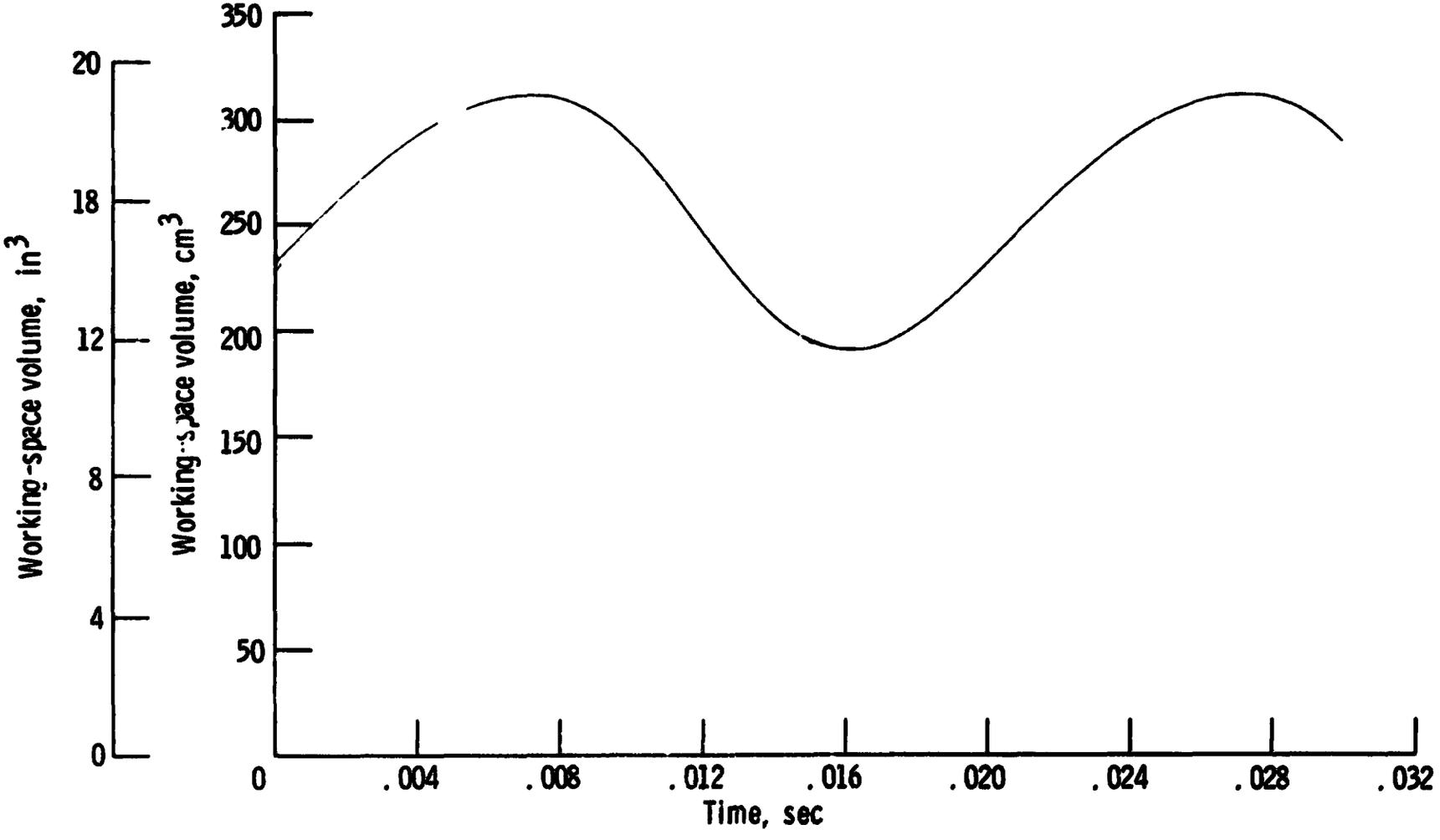

Figure 13. - Working-space volume as function of time.

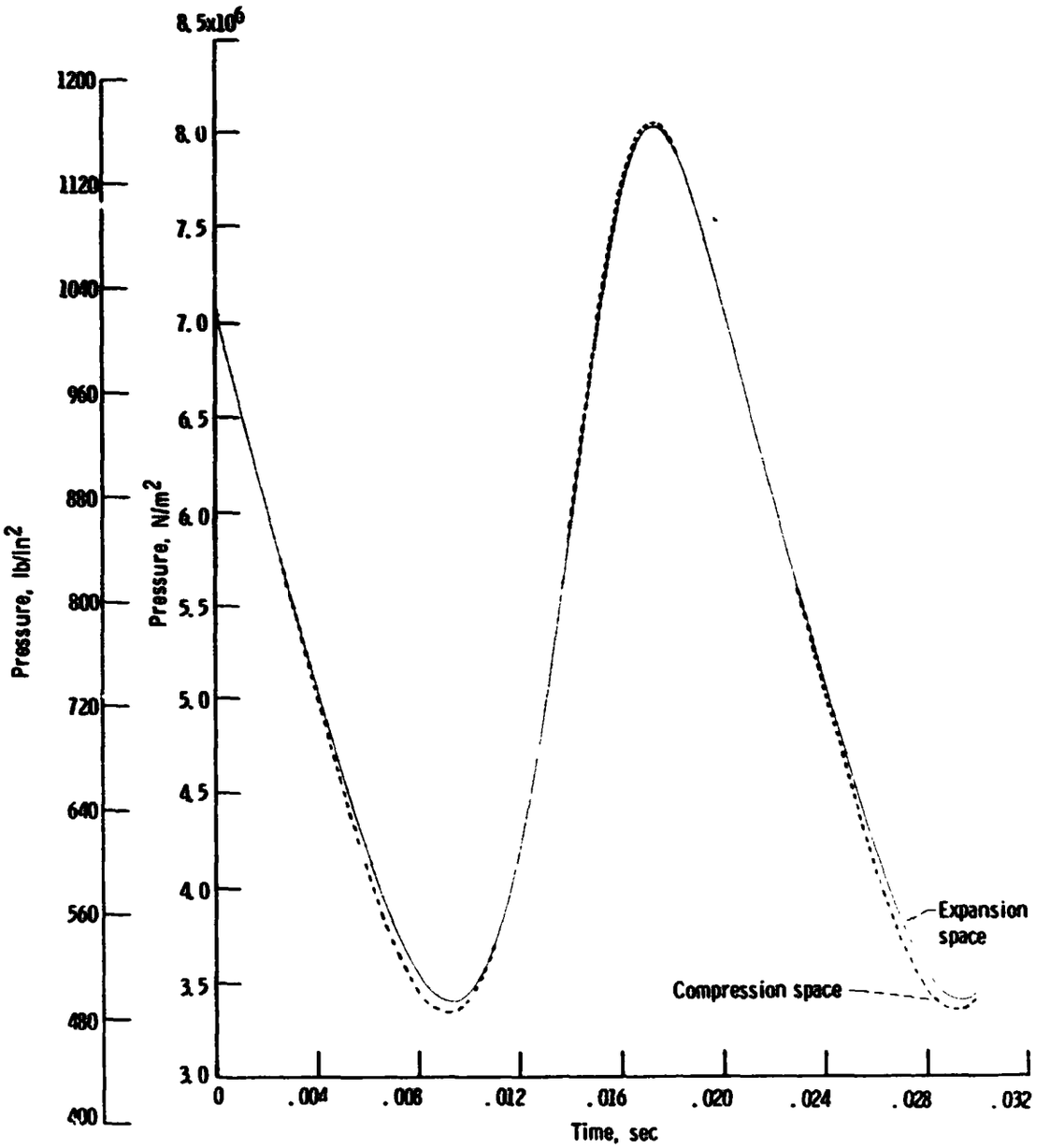

Figure 14. - Expansion- and compression-space pressures as functions of time.

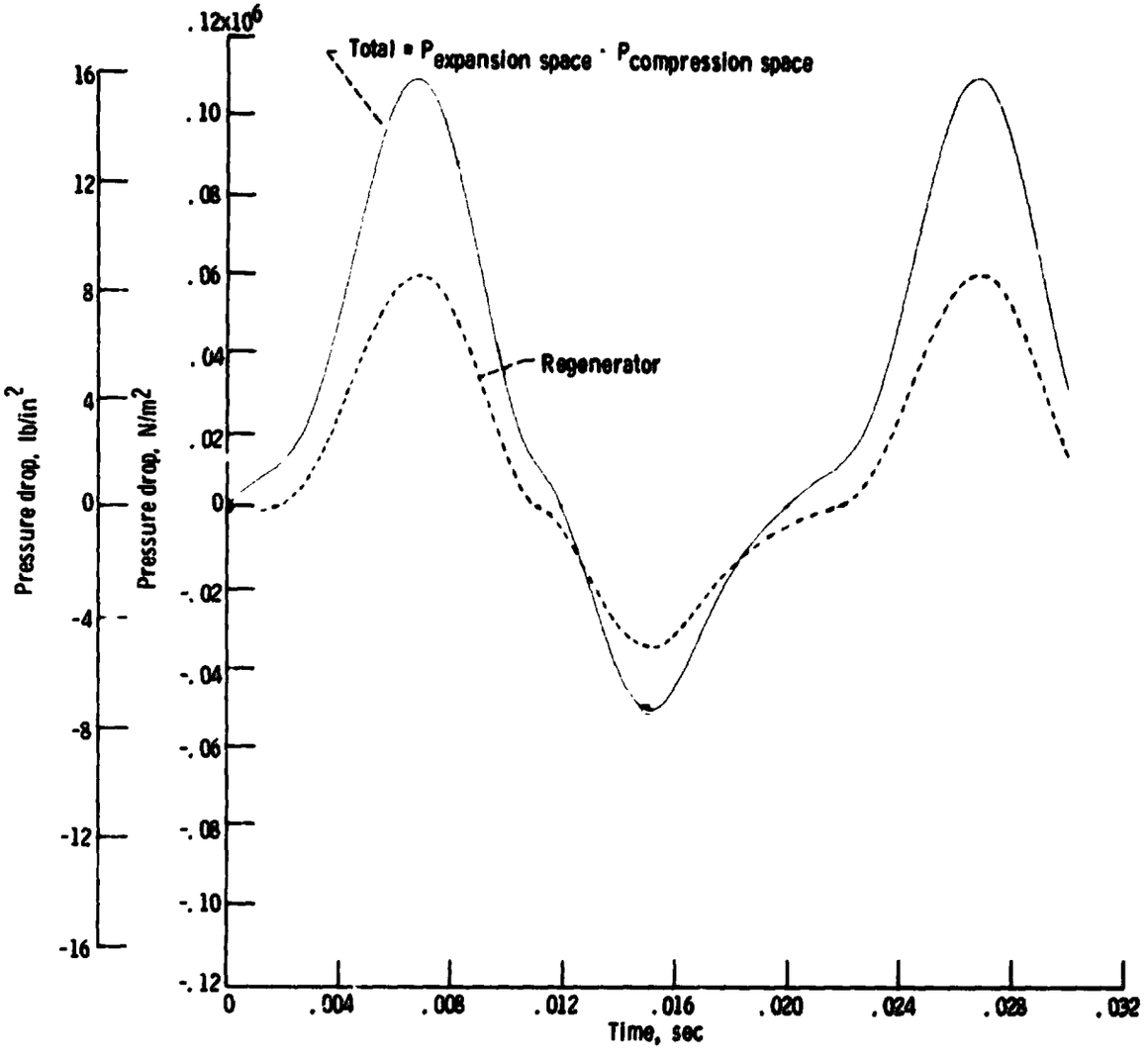

Figure 15. - Pressure drop as a function of time.

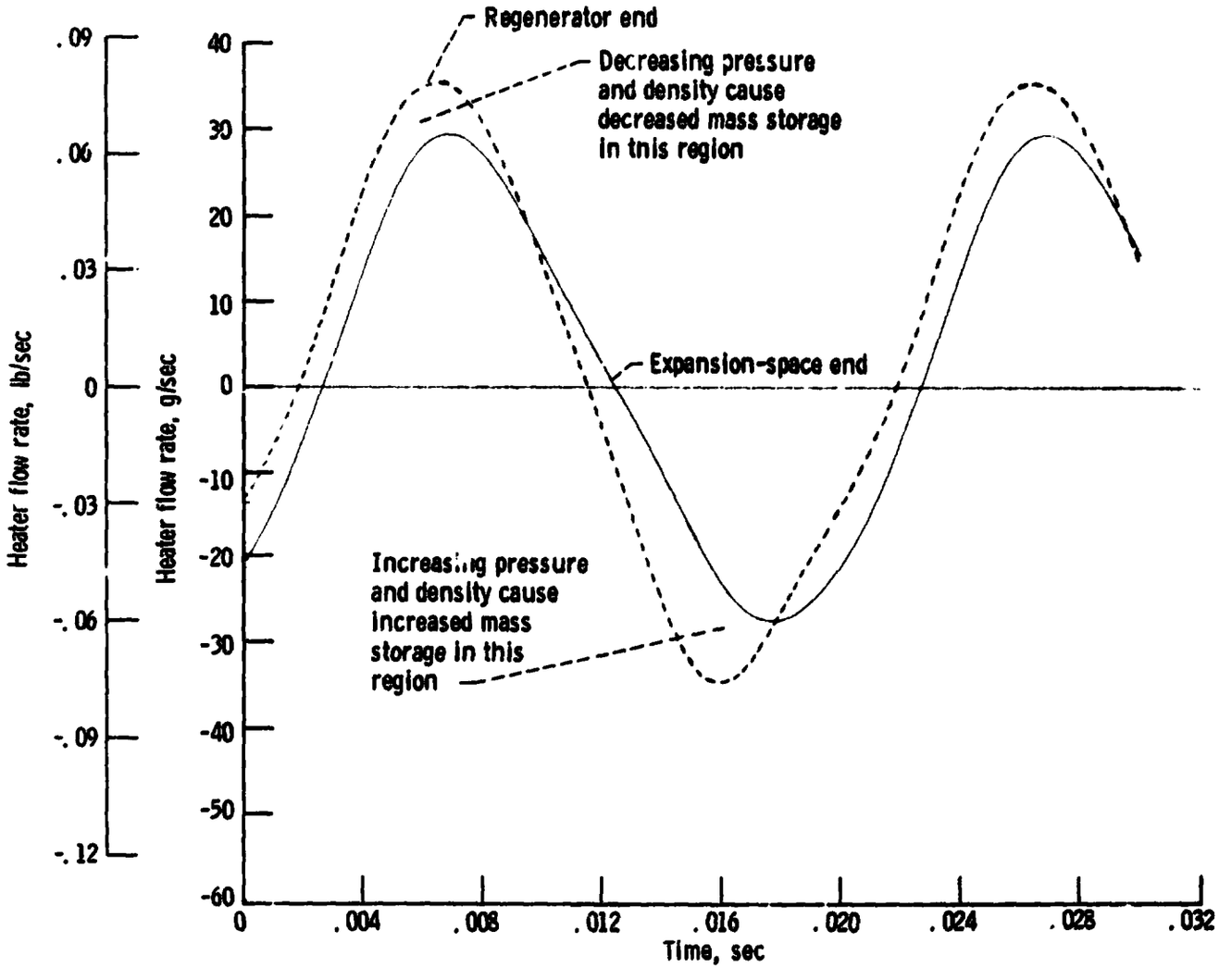

Figure 16. - Heater flow rates as functions of time.

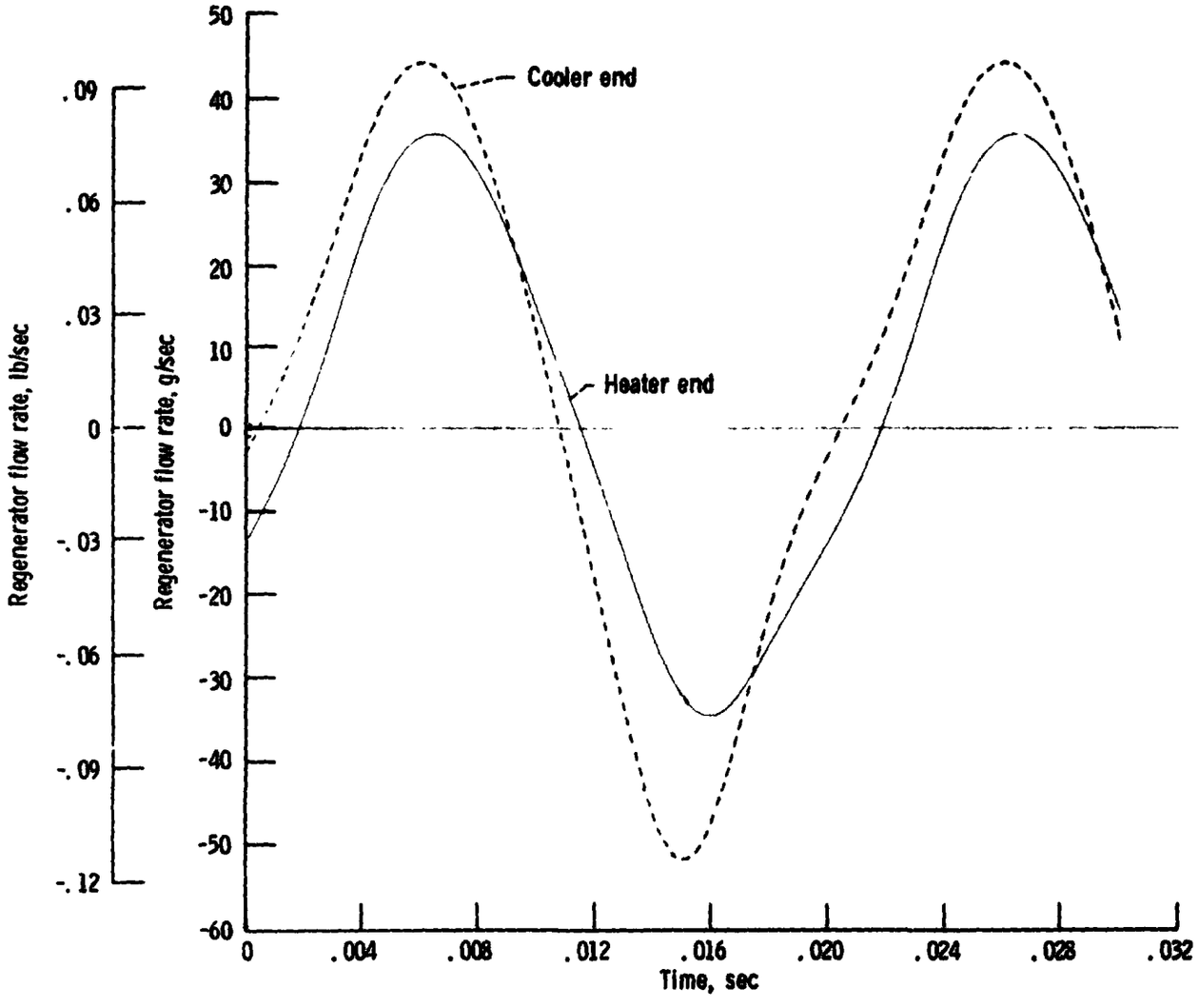

Figure 17. - Regenerator flow rates as functions of time.

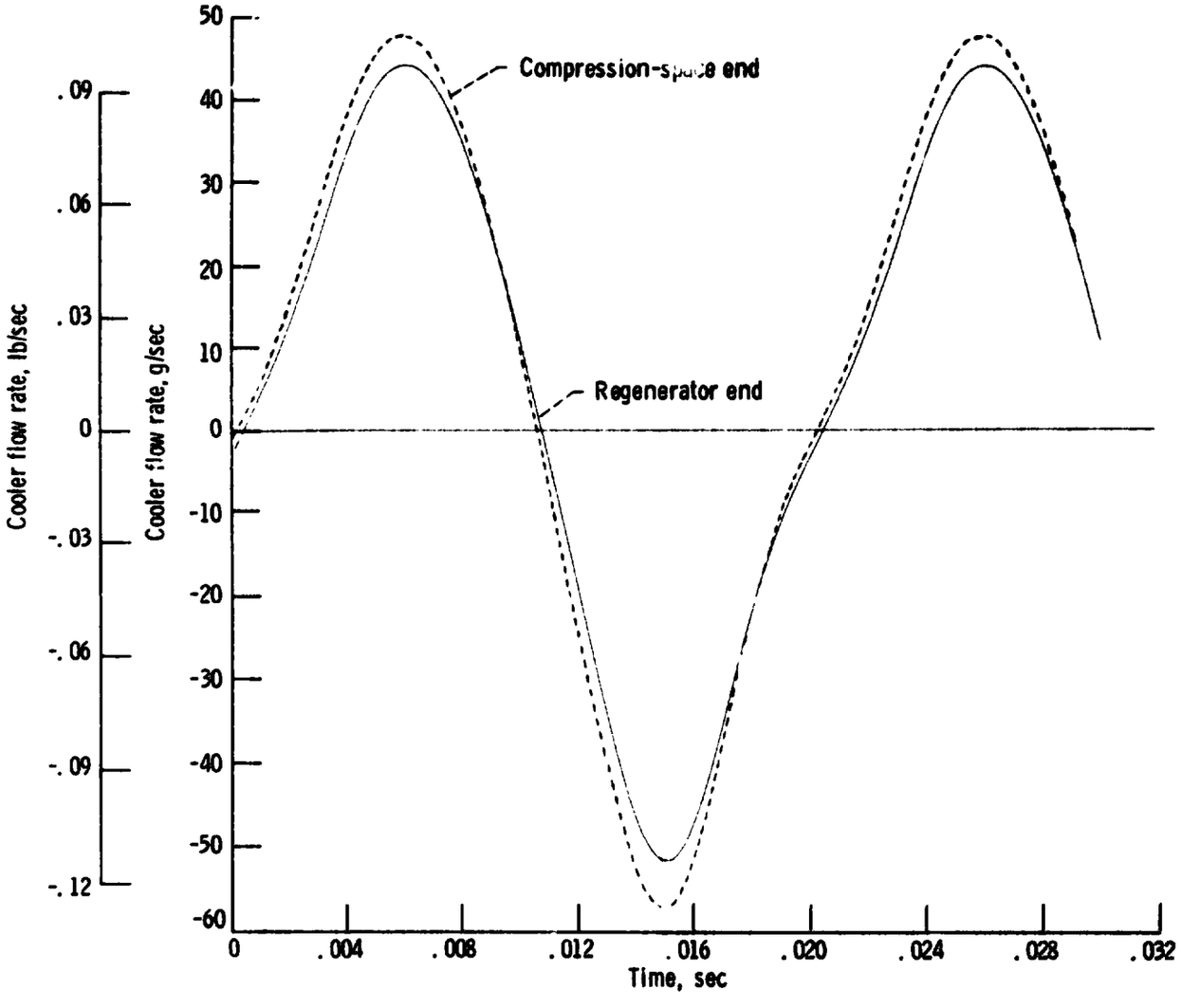

Figure 18. - Cooler flow rates as functions of time.

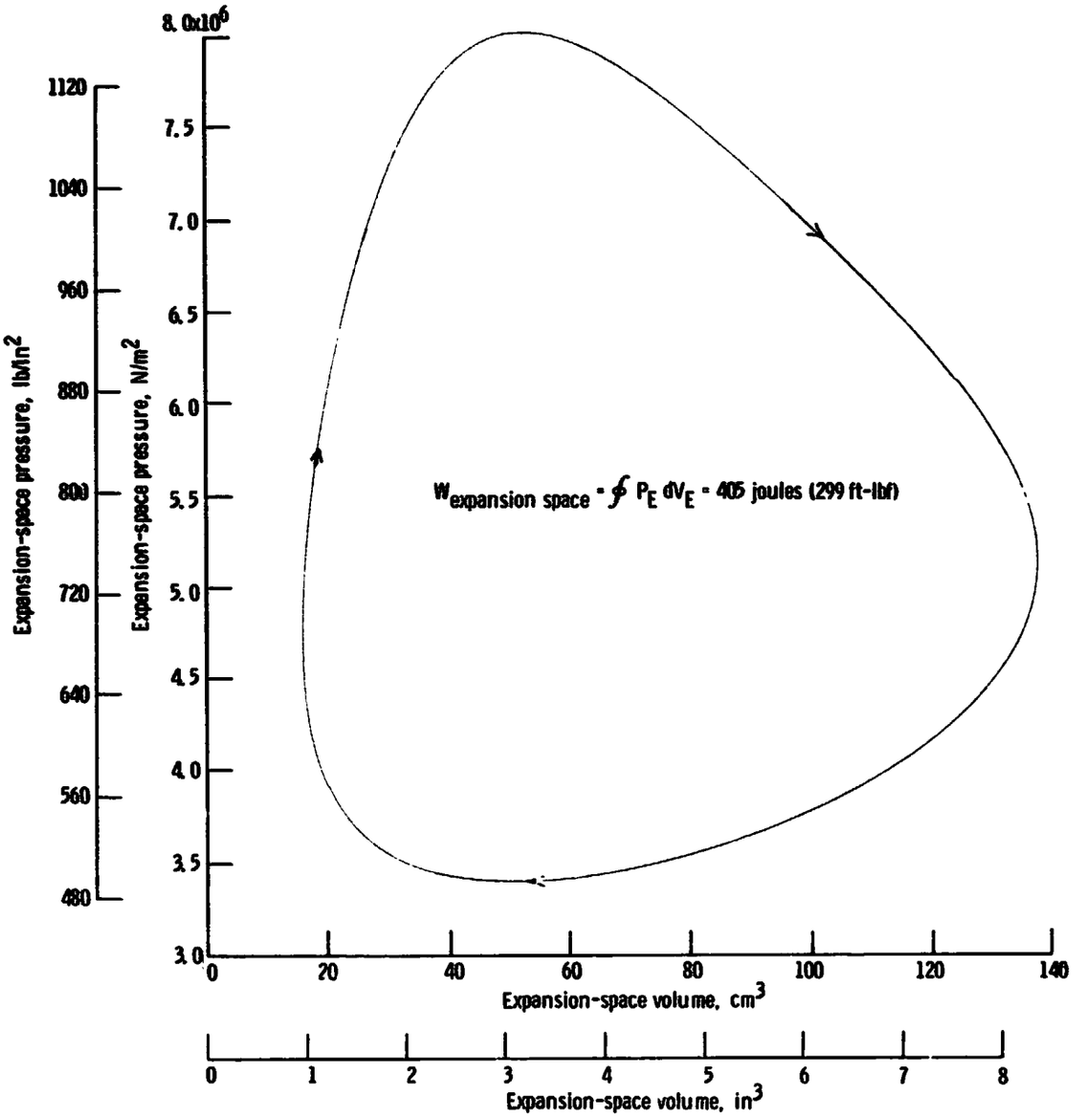

Figure 19. - Expansion-space pressure-volume diagram.

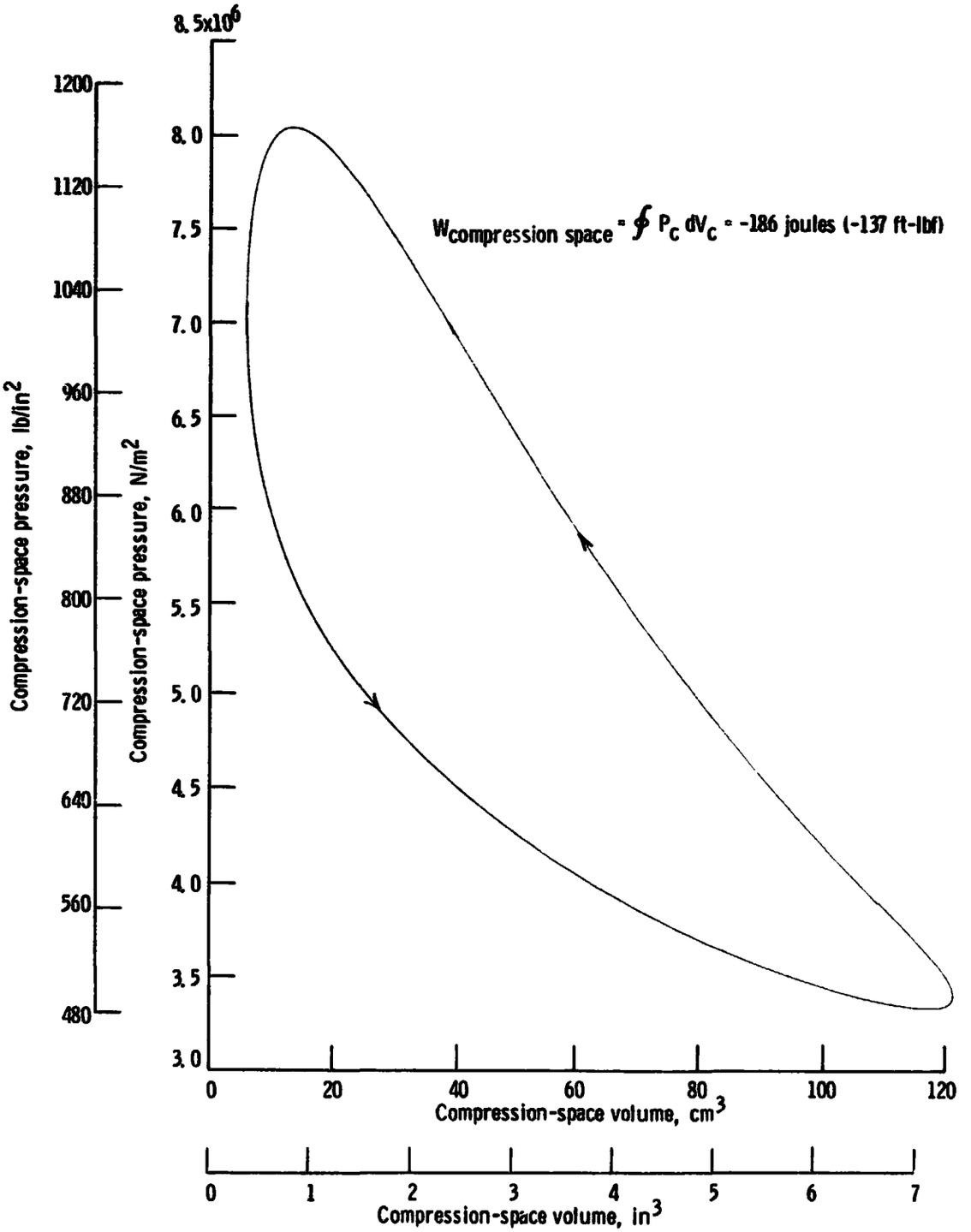

Figure 20. - Compression-space pressure-volume diagram.

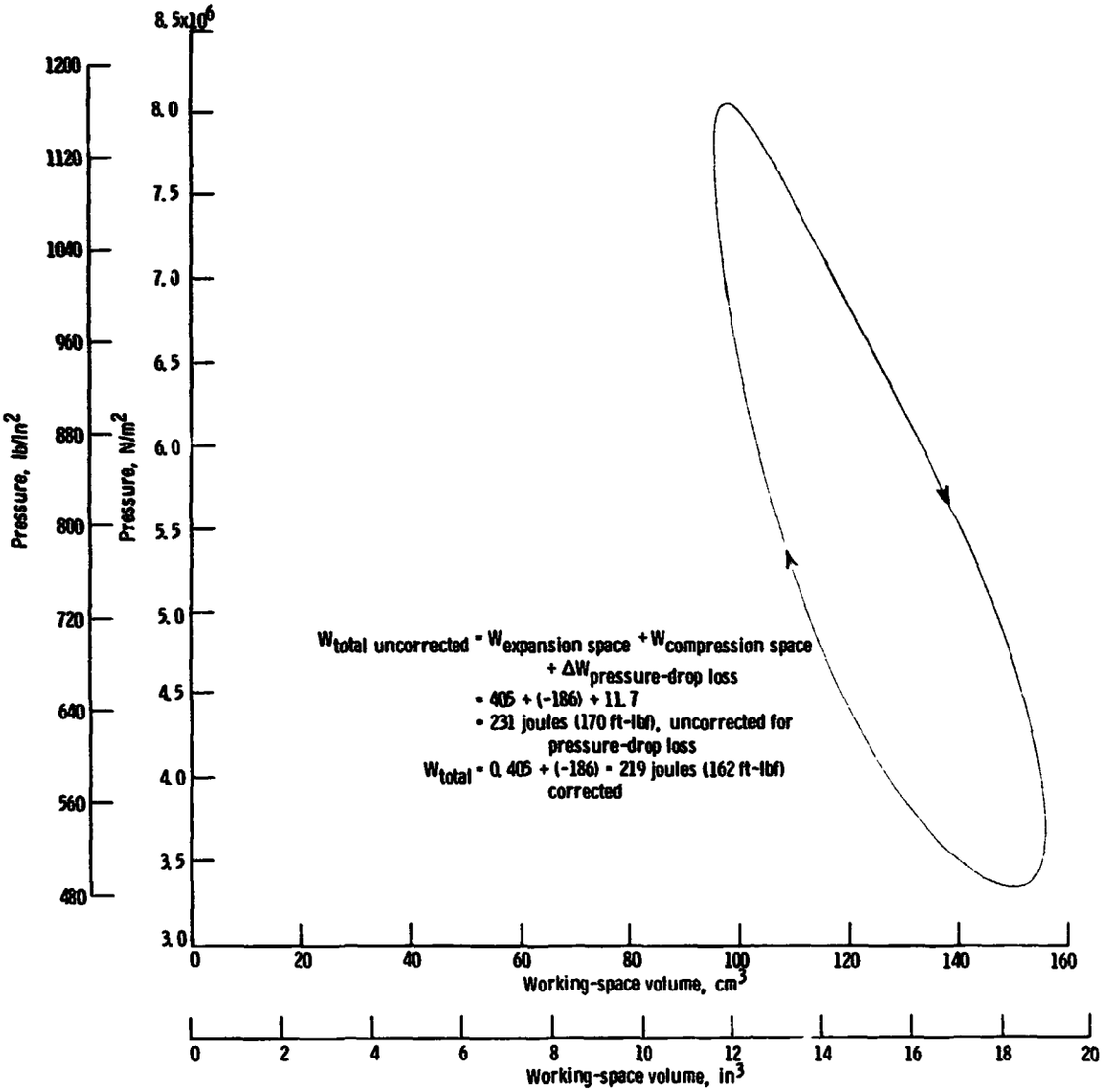

Figure 21. - Total-working-space pressure-volume diagram (neglects pressure drop).

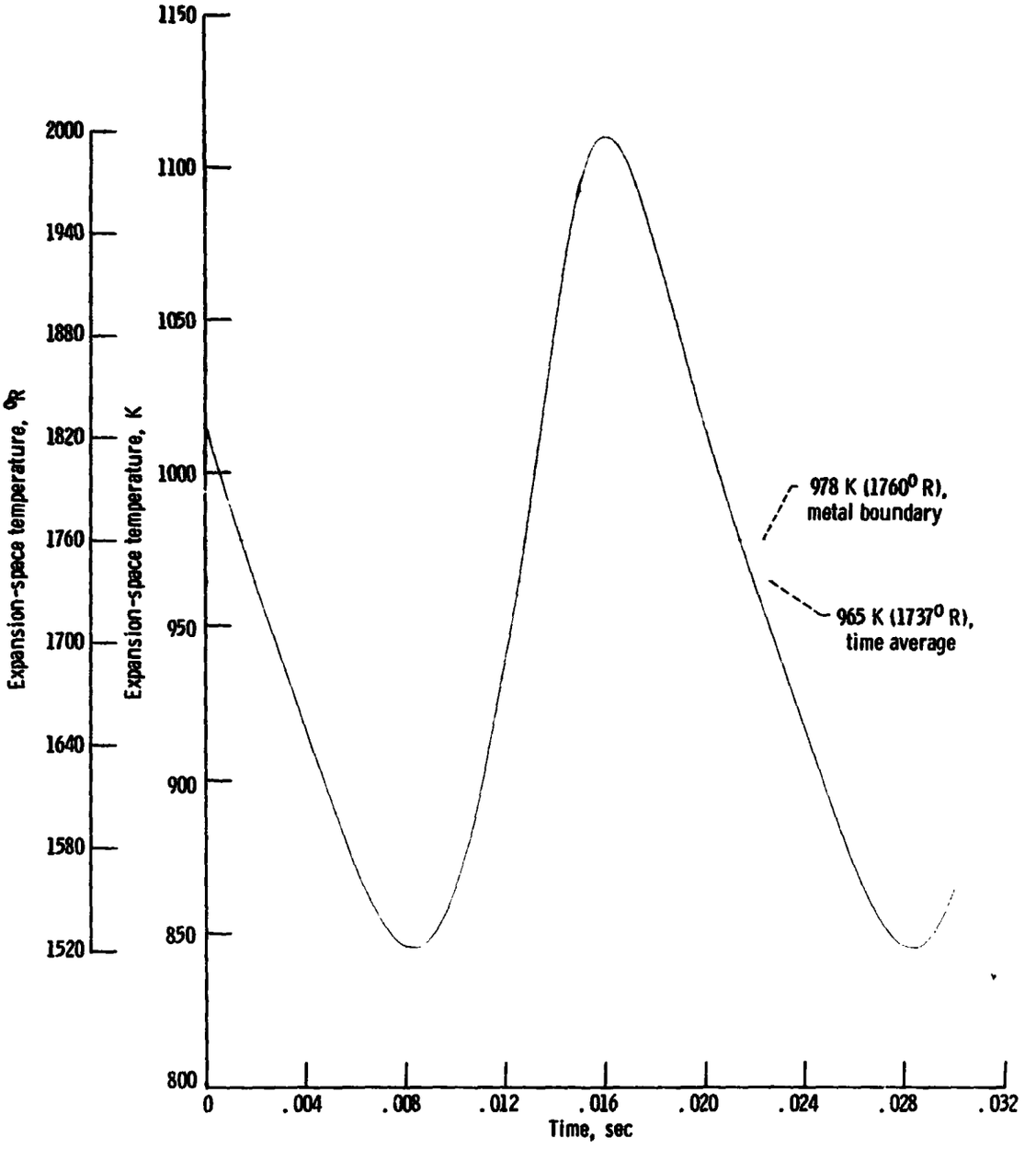

Figure 22. - Expansion-space temperature as a function of time.

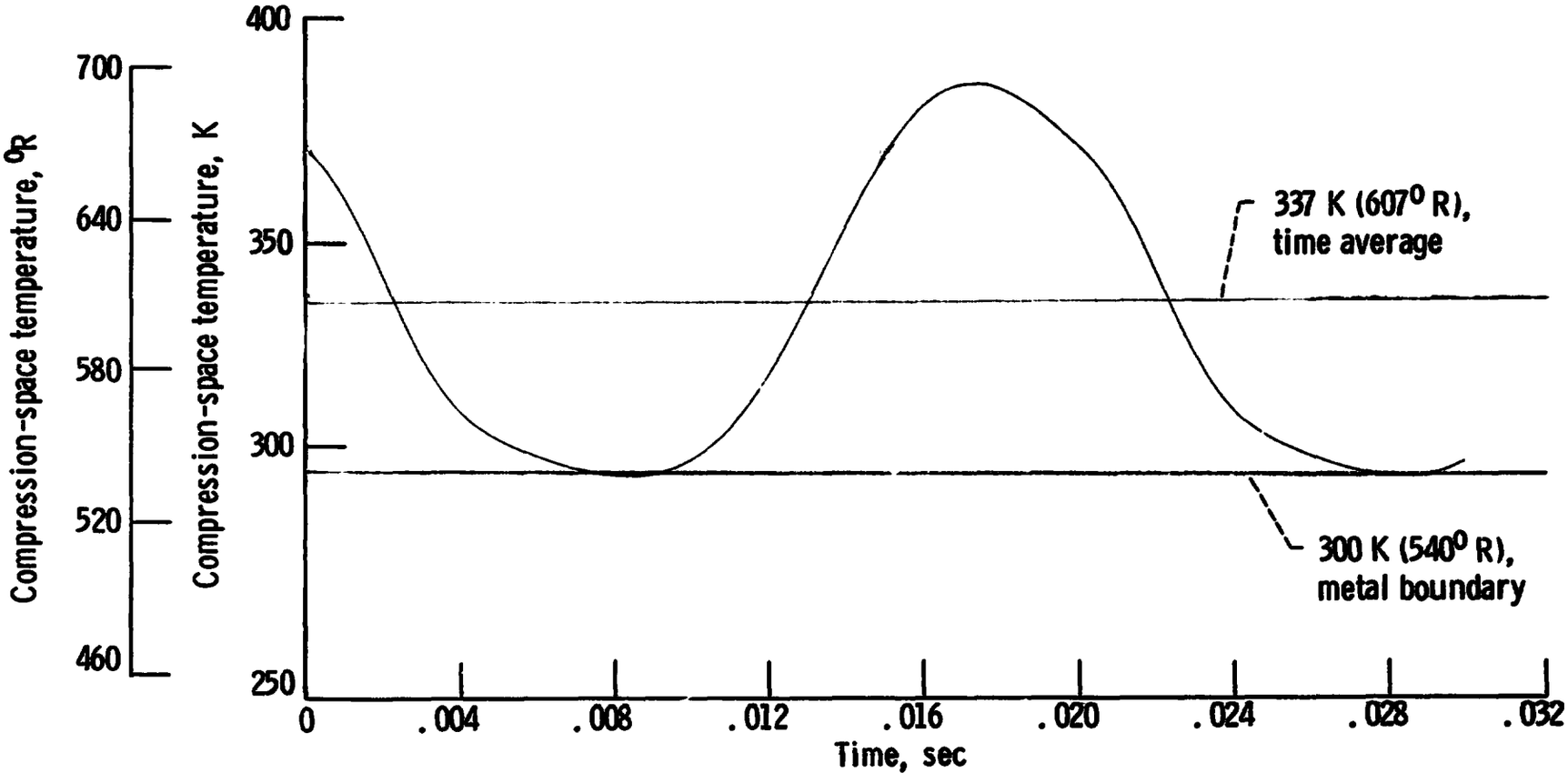

Figure 23. - Compression-space temperature as a function of time.

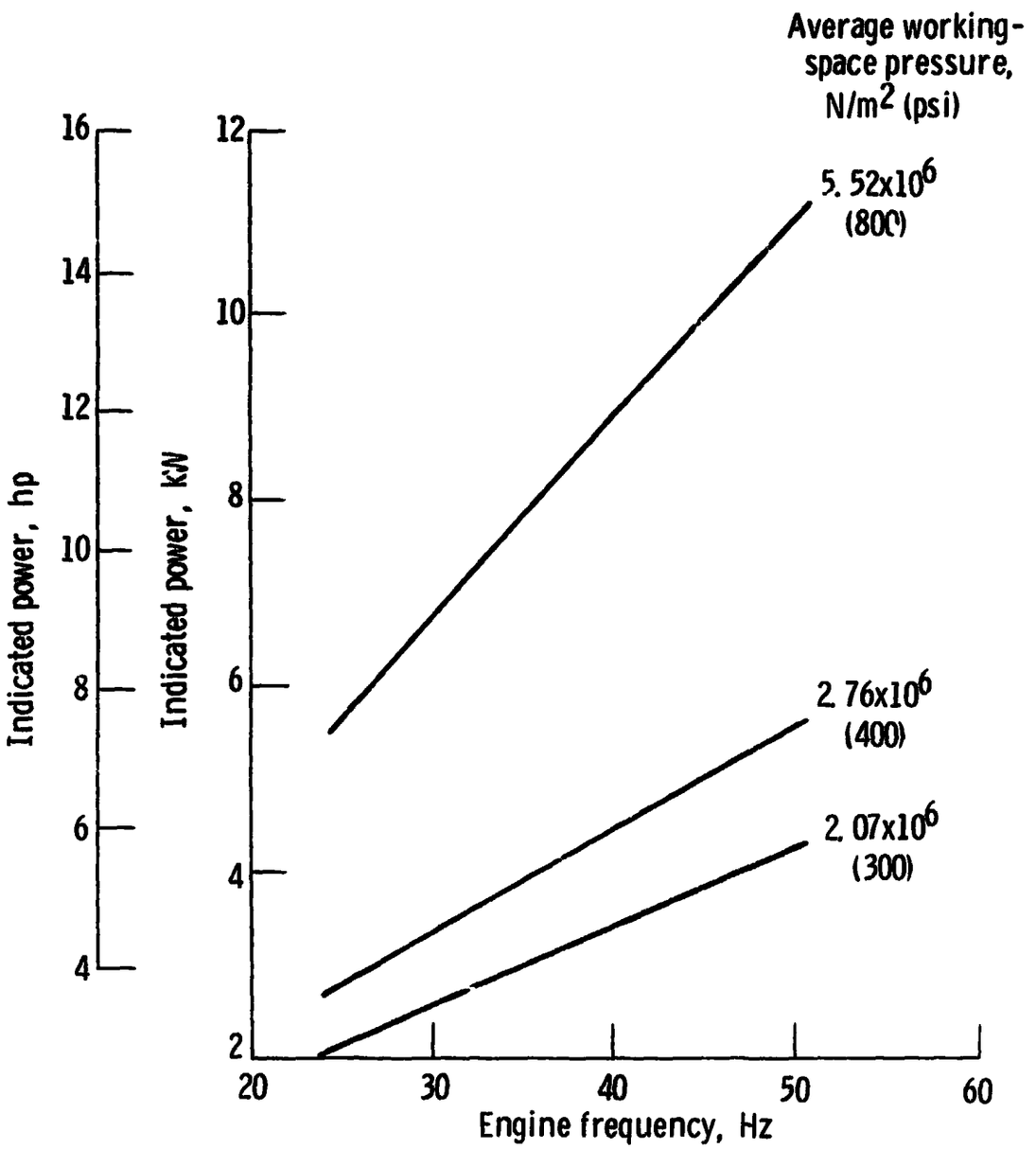

Figure 24. - Indicated power as a function of engine frequency for several average working-space pressures.

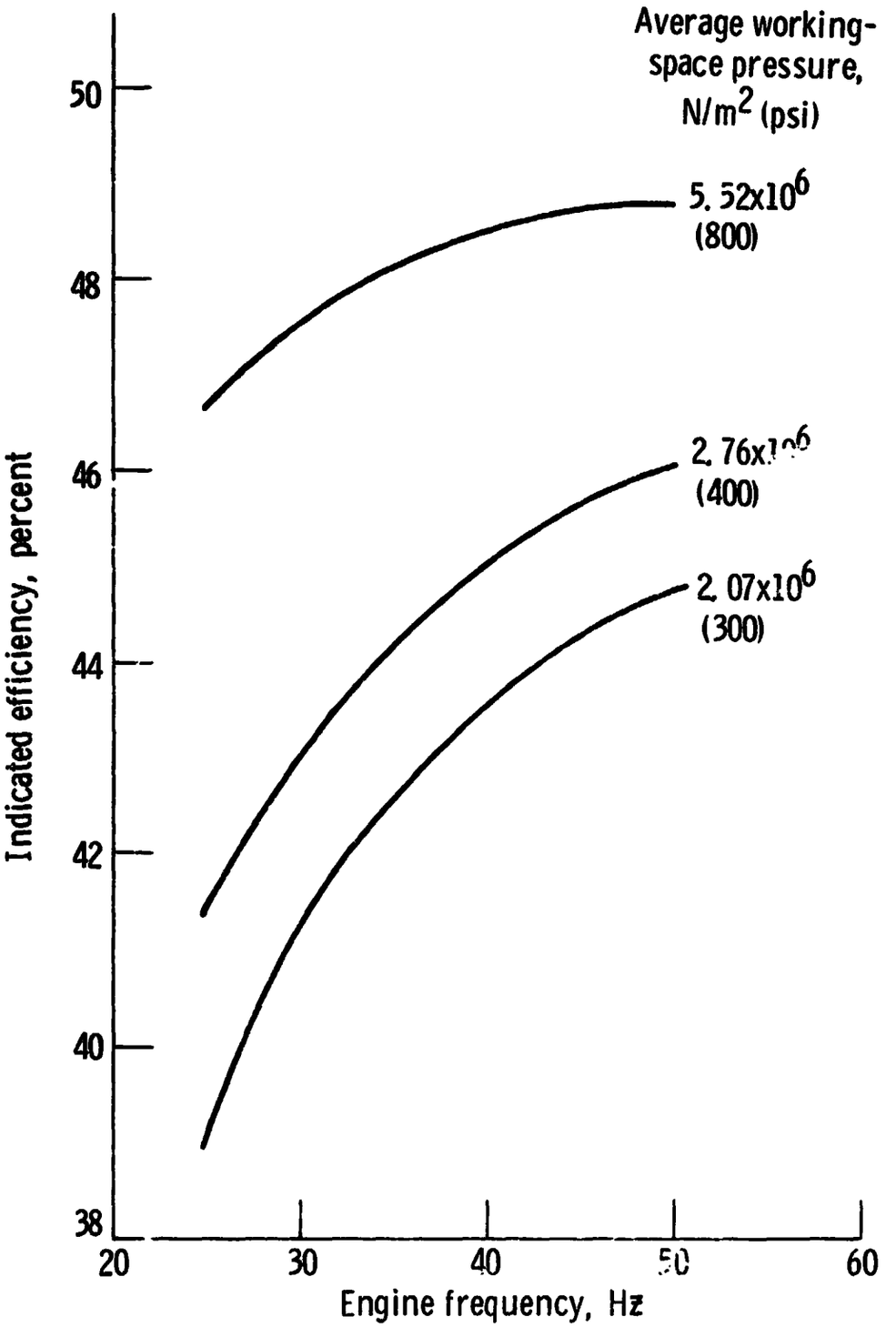

Figure 7. - Indicated efficiency as a function of engine frequency for several average working-space pressures.

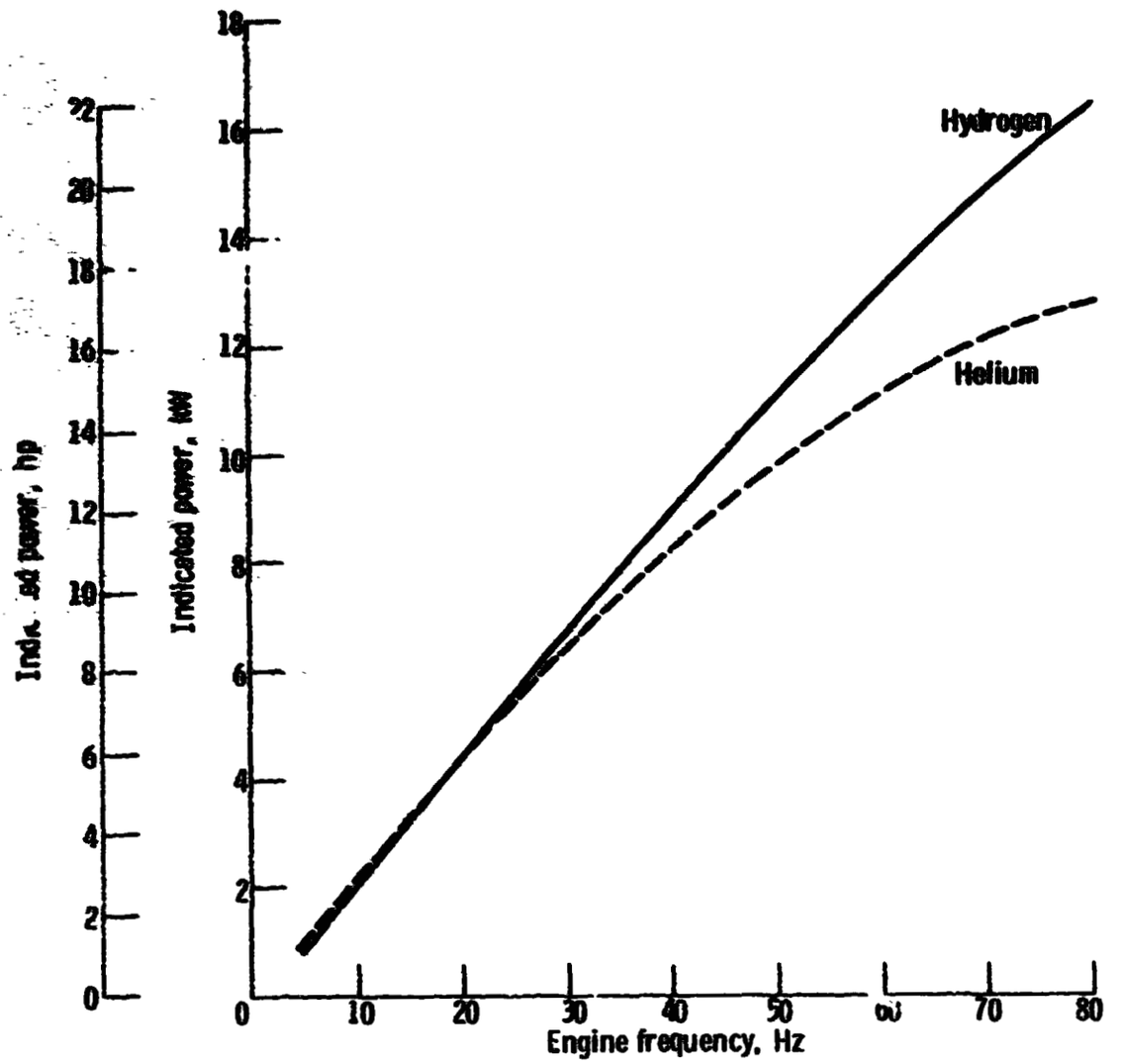

Figure 26. - Indicated power as a function of engine frequency for hydrogen and helium.

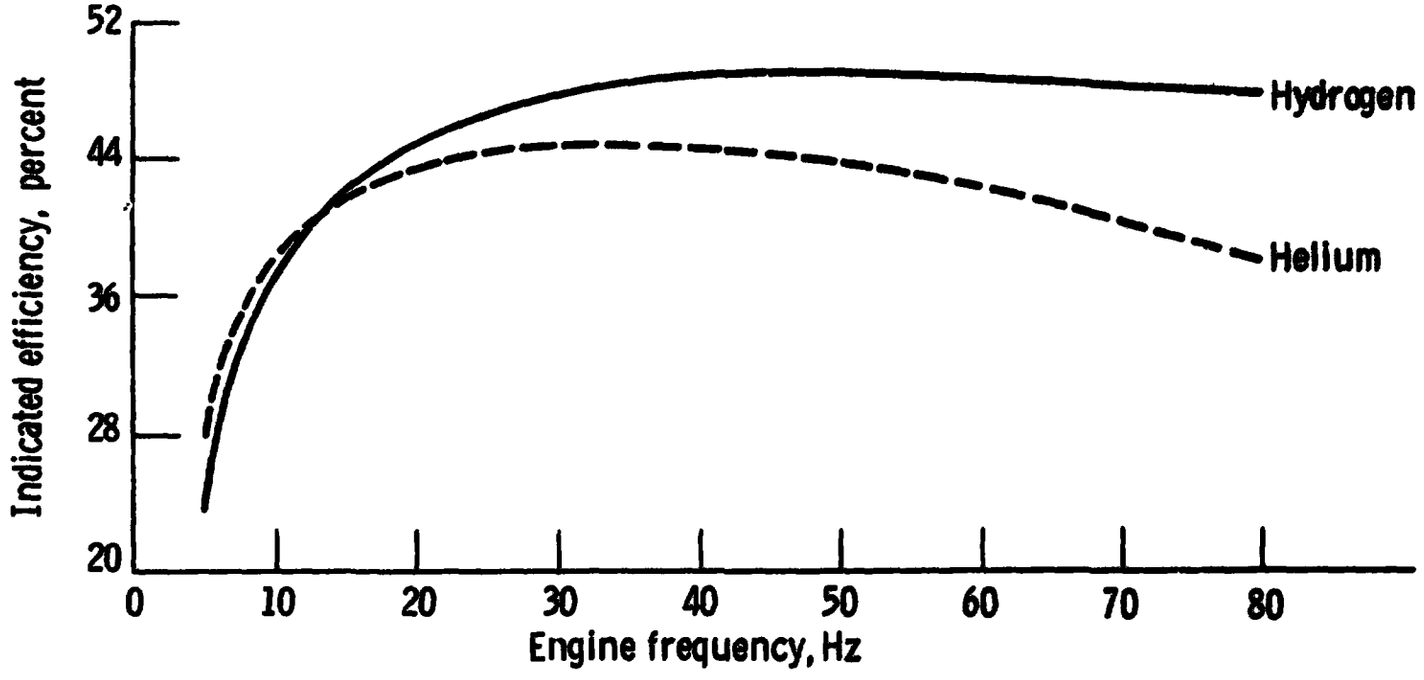

Figure 27. - Indicated efficiency as a function of engine frequency for hydrogen and helium.

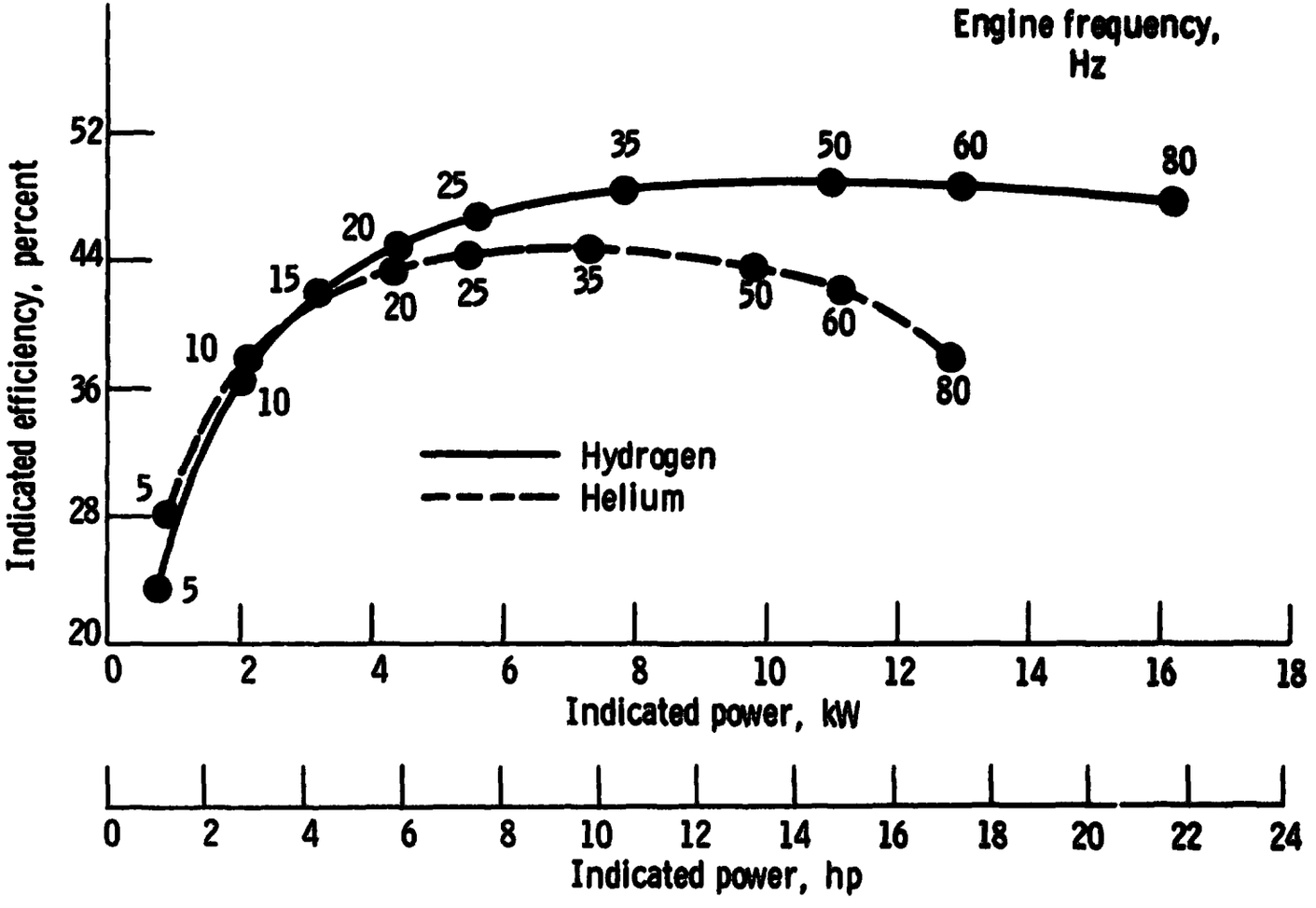

Figure 28. - Indicated efficiency as a function of indicated power (with engine frequency shown on curves).

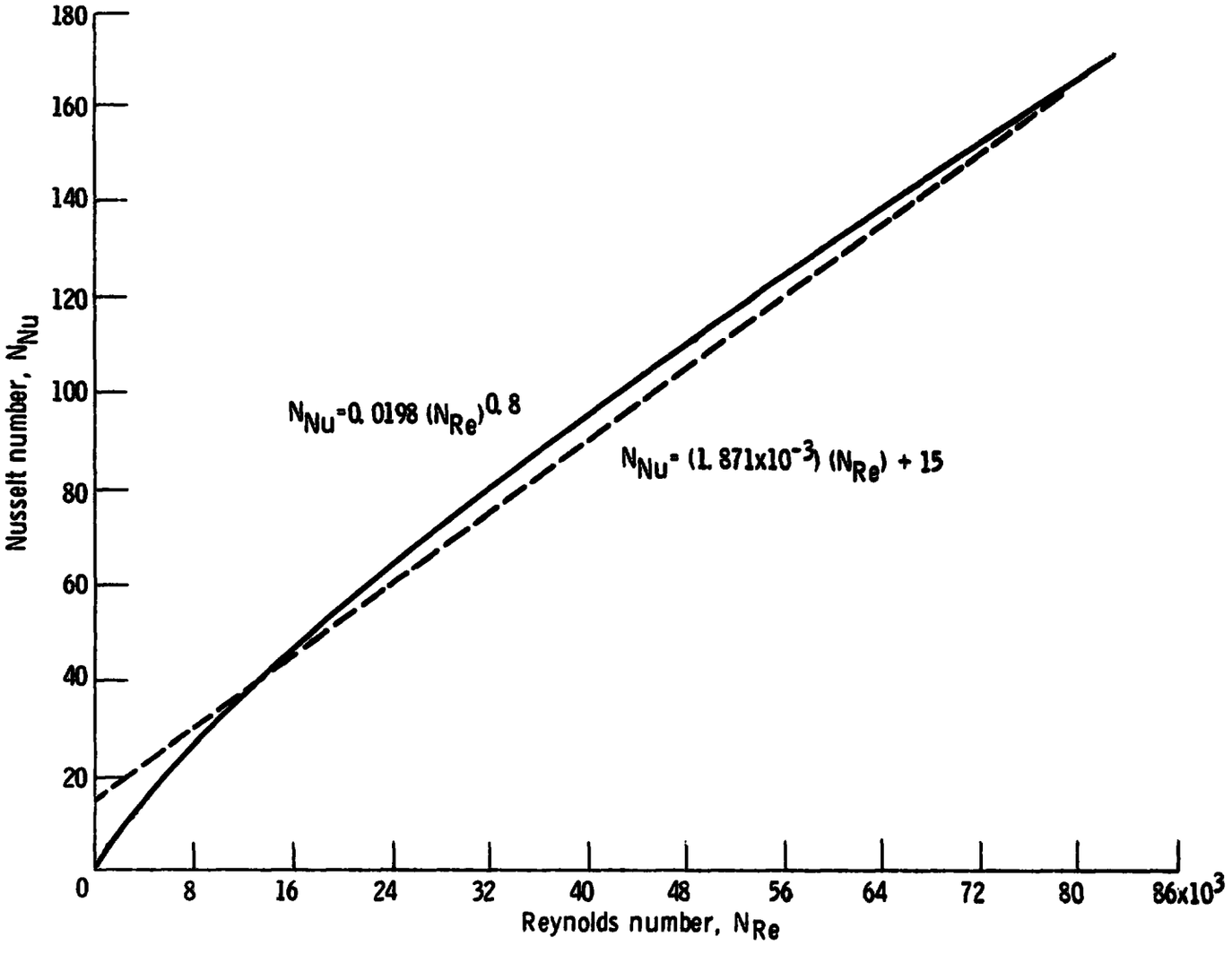

Figure 29. - Comparison of equations (C3) and (C4).

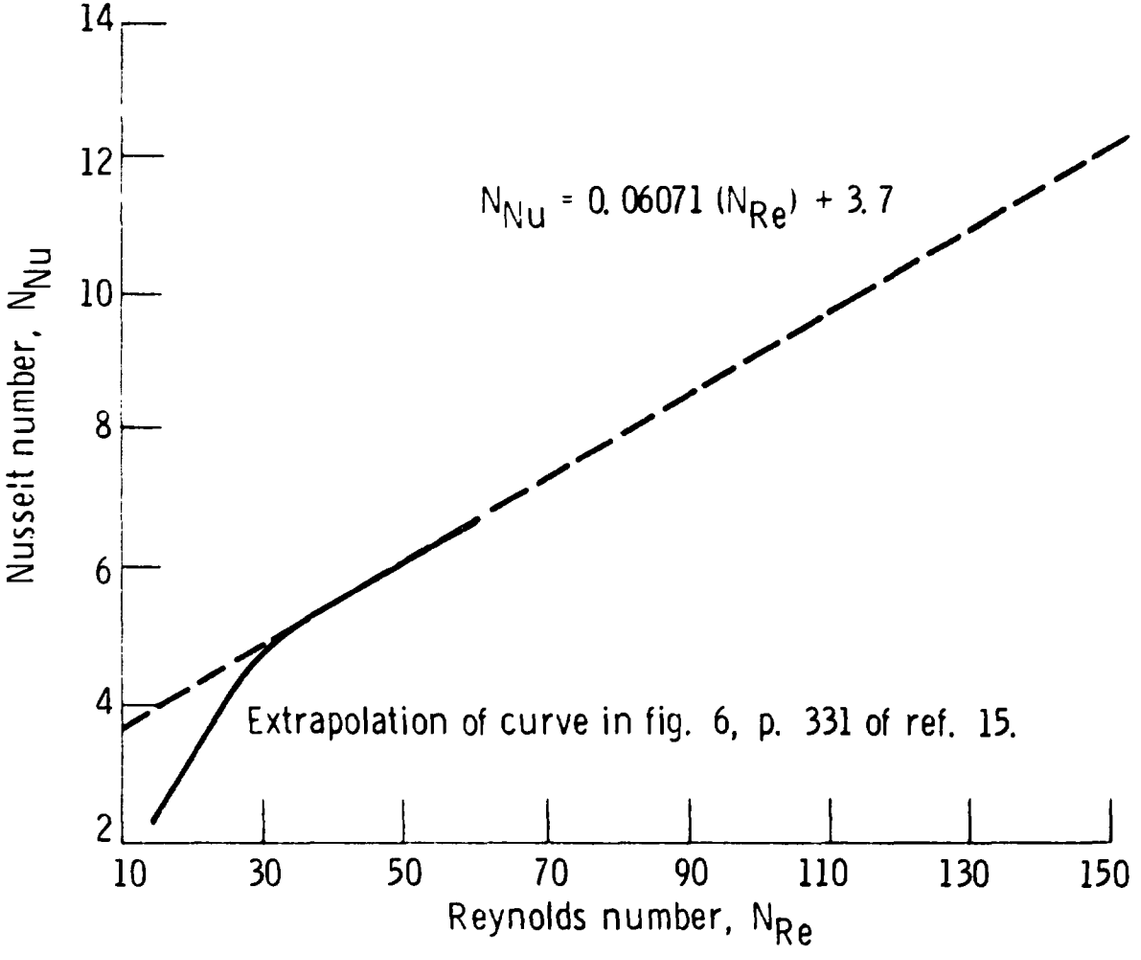

Figure 30. - Regenerator heat-transfer data used for ground-power-unit model.

1 Report No.	2 Government Accession No.	3 Recipient's Catalog No.
NASA TM-78884		

4. Title and Subtitle	5 Report Date
A STIRLING ENGINE COMPUTER MODEL FOR PERFORMANCE CALCULATIONS	July 1978
	6 Performing Organization Code
7. Author(s)	8 Performing Organization Report No.
Roy Tew, Kent Jefferies, and David Miao	E-9613
	10 Work Unit No.
9. Performing Organization Name and Address	
National Aeronautics and Space Administration Lewis Research Center Cleveland, Ohio 44135	11 Contract or Grant No.
	13 Type of Report and Period Covered
12. Sponsoring Agency Name and Address	Technical Memorandum
U.S. Department of Energy Division of Transportation Energy Conservation Washington, D.C. 20545	14 Sponsoring Agency Code Report No. DOE/NASA/1011-78/24

15 Supplementary Notes

Final report. Prepared under Interagency Agreement EC-77-A-31-1011.

16. Abstract

To support the development of the Stirling engine as a possible alternative to the automobile spark-ignition engine, the thermodynamic characteristics of the Stirling engine were analyzed and modeled on a computer. The modeling techniques used are presented. The performance of an existing rhombic-drive Stirling engine was simulated by use of this computer program, and some typical results are presented. Engine tests are planned in order to evaluate this theoretical model.

17. Key Words (Suggested by Author(s))	18 Distribution Statement
Stirling engine Computer model Stirling cycle	Unclassified - unlimited STAR Category 85 DOE Category UC-96

19 Security Classif. (of this report)	20 Security Classif. (of this page)	21 No. of Pages	22 Price*
Unclassified	Unclassified		

* For sale by the National Technical Information Service, Springfield, Virginia 22161